Drug Research Program
Division of Pharmaceutical Bioscience
Faculty of Pharmacy
University of Helsinki
Dissertationes Universitatis Helsingiensis 297/2026

Nanofibrillated cellulose hydrogel as a reservoir for NIR light-activated liposomes

Puja Gangurde

ACADEMIC DISSERTATION

To be presented, with the permission of the Faculty of Pharmacy of the University of Helsinki, for public examination in Athena, room 302, Siltavuorenpenger 3 A, on the 26th of June 2026, at 12 noon.

Helsinki 2026

Publisher: University of Helsinki
Series: Dissertationes Universitatis Helsingiensis 297/2026

ISBN 978-952-84-2470-3 (paperback)
ISBN 978-952-84-2469-7 (PDF)
ISSN 2954-2898 (print)
ISSN 2954-2952 (online)
PunaMusta, Joensuu 2026

Supervisors: Professor Timo Laaksonen
Division of Pharmaceutical Biosciences
Faculty of Pharmacy
University of Helsinki
Finland

Dr. Tatu Lajunen
Department of Pharmacy
Faculty of Health Sciences
University of Eastern Finland
Finland

Dr. Patrick Laurén
Division of Pharmaceutical Biosciences
Faculty of Pharmacy
University of Helsinki
Finland

Pre-examiners: Assistant Professor Luís M. Bimbo
Pharmaceutical Technology
University of Coimbra
Portugal

Associate Professor Hang Zhang
Department of Chemical and Biomolecular Engineering
Eastern Institute of Technology
China

Opponent: Assistant Professor Luís M. Bimbo
Pharmaceutical Technology
University of Coimbra
Portugal

Custos: Professor Timo Laaksonen

Abstract

Cellulose nanofibril (CNF) hydrogels are water-rich, biocompatible, and mechanically tunable biomaterials that are increasingly explored for biomedical applications, including localized drug delivery and wound healing. Their TEMPO-oxidized form (aCNF) carries anionic carboxylate groups, which can strongly retain cationic components via electrostatic interactions. These features make aCNF a promising matrix for forming local drug depots. However, many depot systems still rely on preprogrammed release profiles that cannot be easily adjusted after administration. Stimuli-responsive delivery aims to address this limitation by enabling release to be triggered when needed. For example, light is an especially attractive trigger because it is non-invasive and can be easily controlled and focused on the target site. This thesis investigates aCNF as a carrier matrix for light-activatable liposomes, combining hydrogel-based localization with externally controlled release.

In the first publication, a stable cationic near-infrared (NIR) light-activated liposomal formulation was developed through systematic lipid optimization. The results show that lipid structure, transition temperature, and additive lipids strongly influence stability and release behavior. Based on these results, a formulation was optimized to enable rapid release under NIR exposure with minimal passive leakage. In the second study, these optimized liposomes were embedded into aCNF hydrogel to create a depot-like system. Cationic liposomes were effectively retained in the anionic network, and cargo release could be externally tuned by light dose and hydrogel thickness, showing that both matrix geometry and irradiation conditions shape release performance. To address the need for surgical removal of such cellulose-based hydrogel depot systems from the application site, the third study was extended to enable on-demand biocatalysis of cellulose-based hydrogels by encapsulating cellulase enzymes in light-responsive liposomes. Enzyme stability was evaluated under formulation- and light activation-relevant conditions, and light-triggered release of cellulase from ROS-sensitive liposomal hydrogels was demonstrated in cellulose-based systems. Release was light dose-dependent, with measurable increases in the amount of reducing sugars produced, indicating enzyme activity and hydrogel degradation.

In conclusion, this thesis presents a modular approach in which aCNF provides localized retention and serves as a stable reservoir, while light-activatable liposomes act as a controllable release mechanism. The research also emphasizes key considerations in designing such systems, including trade-offs in lipid composition, optical delivery limitations, system stability, and the preservation of enzyme activity in responsive formulations. Overall, the findings highlight the versatility of CNF-based hydrogels and provide practical guidance for designing more controllable and application-relevant delivery systems in biomedical contexts.

Acknowledgements

The work in this thesis was carried out at the Division of Pharmaceutical Biosciences, Faculty of Pharmacy, University of Helsinki. This work was financially supported by the European Research Council Consolidator Grant Project. I would also like to acknowledge the Doctoral Program in Drug Research and all the brilliant people I have had the opportunity to learn from and work with during my doctoral studies.

I would like to begin by expressing my deepest gratitude to the supervisors who guided me throughout this PhD journey. In the Indian tradition, a teacher is not only someone who shares knowledge, but also someone who gives direction, confidence, and courage during the process of learning. The Sanskrit expression **"तस्मै श्री गुरवे नमः" (Tasmai shri gurave namaḥ)** beautifully reflects this feeling: my deep respect and gratitude to the teacher who guides the way.

My deepest gratitude goes to my supervisor, Professor Timo Laaksonen, for giving me the opportunity to pursue this PhD and for trusting me with a project that allowed me to grow both scientifically and personally. Timo, thank you for your kindness, patience, and support throughout these years. I have always appreciated that you were available for discussions, whether about experimental challenges, manuscripts, or simply finding the next step when things felt unclear. Thank you for giving me the freedom to explore my ideas, learn through the process, and become more confident as a researcher. Your guidance has been an important part of my growth, and I will always be grateful for it.

I would also like to express my heartfelt gratitude to Dr. Tatu Lajunen and Dr. Patrick Laurén, who have both been an important part of my PhD supervision. Tatu, thank you for your practical guidance, valuable suggestions, and support during different stages of my PhD. I especially appreciated your clear advice when I needed to think through experimental problems and next steps. Patrick, thank you for your thoughtful scientific input, discussions, and for helping me look at my work from different perspectives. I truly appreciate the time and generous support you both gave to my research, manuscripts, and overall progress. I feel fortunate to have been guided by supervisors who supported me not only as a doctoral researcher but also as a person learning to navigate the challenges and growth that come with a PhD.

I am sincerely grateful to Professor Luís Bimbo and Professor Hang Zhang for serving as the preliminary examiners of this thesis and for their careful evaluation, constructive feedback, and insightful suggestions. I also warmly thank Professor Luís Bimbo for agreeing to serve as the opponent of my doctoral thesis and for making time to attend my defence. My sincere thanks go to Dr. Jukka Saarinen for

accepting to be the faculty representative. I would also like to thank my thesis committee members, Professor Tomi Rantamäki and Professor Mauri Kostiainen, for their time, valuable discussions, and support throughout my doctoral studies.

In addition to my supervisors, I have received support, knowledge, and encouragement from many people during my PhD. Thank you, Dr. Zahra Gounani, for your support during the experiments, for all the fun chats we had over the years, and for believing in me. I also warmly thank Dr. Ali Eftekhari for his encouraging words and for boosting my confidence. I am grateful to Dr. Kaisa Marjamaa and Dr. Suvi Arola for the great collaboration through the BIOBLOCKS project, I learned a lot during this experience. Special thanks to Suvi for teaching and supporting me during our research visit to Nagoya University. You have been truly an inspiration to me. I have always admired your confidence and the way you carry yourself as a researcher, and I hope to grow into a confident woman in research like you.

I am also very grateful to all my colleagues for making this journey memorable: Anton, Anna, Deborah, Eija, Elena, Irem, Kelsey, Olga, Paria, Roosa, Riikka, Sari, Sergei, Shihab, Shirin, Sina, Suvi H., and Yu. It has been a pleasure to share this journey with all of you. Thank you for the laughter, interesting discussions, help, and everyday moments that made these years much lighter and happier. Special thanks to Anna and Eija for your wonderful friendship, constant support, new experiences, and the best company during conference trips. I am so glad we shared this journey together.

Having hobbies outside the laboratory was also important during my PhD, and I would like to thank all the members of the PCS cricket club for exciting matches, loud cheers, and great team spirit. To my Unihome friends, Anna, Athisha, Jéssica, Shuddhodana, Soham, and baby Druta, thank you for being such a special part of my life in Finland. I feel lucky to have you around for game nights, dinners, conversations, and all the fun moments that helped me unwind.

My family has been my strongest support throughout this journey. This thesis would not have been possible without your love, constant encouragement, and belief in me. Thank you, Moma and Papa, for the long calls that helped me through hard times, and for the reassurance of “mana bap na kade gan paisa she…” which always reminded me that, no matter what, you always have my back. Huge thanks to my brother Pratik for being my anchor, your resilience has been a constant inspiration to me. Thank you to my sister Vipula and my brother-in-law Anup for your guidance and encouragement; it means a lot. Special thanks to my niece, Aarnu baby, whose smile and joyful nature kept me going through this journey. *To my family:* your love has been my strength, and I carry this achievement with all of you in my heart.

Puja Gangurde
Helsinki, June 1st, 2026

Index

Abstract iv

Acknowledgements v

List of original publications ix

Abbreviations xi

1 Introduction 1

2 Review of the literature 4

2.1 Controlled drug delivery 4

2.1.1 Need for controlled drug delivery 4

2.2 On-demand drug delivery 6

2.2.1 Stimuli-responsive systems 7

2.2.1.1 Endogenous triggers 8

2.2.1.2 Exogenous triggers 11

2.3 Why light-triggered systems are attractive and what limits them 14

2.4 Light-triggered liposomal release: design strategies 16

2.4.1 Liposomes for drug delivery 16

2.4.2 Designing light-activated liposomes 19

2.4.2.1 Engineering thermosensitive light-activated liposomes 19

2.4.2.2 Engineering ROS-activated liposomes 22

2.5 Cellulose nanofiber hydrogels as a drug reservoir for nanoscale carriers 24

2.5.1 Cellulose nanofiber hydrogel 24

2.5.2 Cellulose nanofiber as drug reservoir 25

2.5.3 Liposome loading into hydrogels as nanodepots 27

2.6 On-demand biocatalysis of cellulose hydrogel with encapsulated enzymes 29

3 Aims of the study 31

4 Materials and methods 32

4.1 Preparation of Light-Activated Liposomes (I, II, III) 32

4.2 Preparation of liposomal hydrogel system 33

4.3 Characterization of Liposomes 33

4.4 Stability of liposomes and liposomal hydrogel systems (I, II) 34

4.5 Light-activated release from liposomes and liposomal hydrogel systems (I, II, III) 35

4.6 Degradation of liposomal hydrogel system after enzyme release upon light-activation 36

4.7 High Speed-Atomic Force Microscopy 37

4.8 Other characterizations **38**

5 Results and Discussion **39**

5.1 Release from light-activated liposomes (I) **39**

5.2 Characterization of liposomal hydrogel system (II) **42**

5.2.1 Surface interactions between liposomes and aCNF hydrogel 42

5.2.2 Stability of liposomal hydrogel system 44

5.3 Release from liposomal hydrogel system (II) **46**

5.3.1 Heat and light-activated release from LHS 46

5.3.2 Factors influencing the release from LHS upon light activation (II) 48

5.4 On-demand enzymatic degradation of cellulose hydrogels (III) **49**

5.5 Studying ROS-sensitive lipid film degradation using high-speed atomic force microscopy (III) **52**

6 Future directions **56**

7 Conclusion **58**

References **59**

List of original publications

This thesis is based on the following publications:

I **Gangurde P**, Mahmoudzadeh M, Gounani Z, Koivuniemi A, Laurén P, Lajunen, T., Laaksonen, T. Development of Robust Cationic Light-Activated Thermosensitive Liposomes: Choosing the Right Lipids. Molecular Pharmaceutics. 2023 Oct 24;20(11):5728-5738.

II **Gangurde P**, Gounani Z, Zini J, Polez RT, Österberg M, Lauren P, Lajunen, T., & Laaksonen, T. Harnessing liposomal nanocellulose hydrogel for NIR-light driven on-demand drug delivery, Carbohydrate Polymer Technologies and Applications, 2025 June;10:100787.

III **Gangurde P**, Cheng Y, Arola S, Marjamaa K, Chan F, Efimov A, Laurén P, Lajunen T, Uchihashi T, Gounani Z, Laaksonen T, Light-Responsive Liposomes for On-Demand Degradation of Polysaccharide-Based Hydrogels, *Unpublished draft*

The publications were adapted with the permission of the copyright owners and are referred in the text by their Roman numerals.

Author contribution

I. The author designed all the experiments and analyzed data with the help of supervisors. Performed all the trials to develop light-responsive thermosensitive liposomes. The molecular dynamics simulations were performed by Mohammad Mahmoudzahdeh and Artturi Koivuniemi. Author wrote the first draft of the manuscript and finalized it with the help of all the co-authors.

II. The author designed the experiments together with the supervisors. Author prepared the liposomes and performed the release experiments on developed liposomal hydrogel system. Author supported Zahra Gounani in confocal imaging. Author performed FTIR analysis under the supervision of Jacopo Zini. The author successfully planned and conducted the research, wrote the manuscript and submitted the manuscript for publication after the comments from the co-authors.

III. The author planned and designed the experiments together with the supervisors, and helpful guidance from VTT research collaborators. The author performed and analyzed all the experiments in the publication except the SEM and confocal imaging, which were performed by Yu Cheng and Zahra Gounani respectively. Author conducted HS-AFM analysis of the prepared lipid films under the supervision of Suvi Arola. The author wrote the first draft of the manuscript and revised it according to the suggestions and comments from supervisors and co-authors.

Abbreviations

3D	Three-dimensional
aCNF	Anionic cellulose nanofiber
AMF	alternating magnetic field
CDD	Controlled drug delivery
Chol	Cholesterol
CLTSL	Cationic light-activated thermosensitive liposomes
CMC	Critical micelle concentration
CNF	Cellulose nanofiber
DDS	Drug delivery system
IPN	Interpenetrating polymer network
DSC	Differential scanning calorimetry
FRAP	Fluorescence recovery after photobleaching
FTIR	Fourier transform infrared spectroscopy
HEPES	(4-(2-hydroxyethyl)-1-piperazineethanesulfonic acid)
HS-AFM	Hight speed atomic force microscopy
ICG	Indocyanine green
LHS	Liposomal hydrogel system
LUV	Large unilamellar vesicles
MLV	Multilamellar vesicles
MPP	Matrix metalloproteinases
NIR	Near-infrared
NP	Nanoparticle
PDT	Photodynamic therapy
PEG	Polyethylene glycol
PLGA	Poly(lactic-co-glycolic acid)

PNIPAM	Poly(N-isopropylacrylamide)
PS	Photosensitizer
ROS	Reactive oxygen species
SEC	Size-exclusion chromatography
SEM	Scanning electron microscopy
SLB	Supported lipid bilayers
SPR	Surface plasmon resonance
SUV	Small unilamellar vesicles
TEMPO	(2,2,6,6-Tetramethylpiperidin-1-yl)oxyl
TFF	Tangential flow filtration
T_m	Transition temperature
US	Ultrasound
UV	Ultraviolet light
ZnPc	Zinc phthalocyanine

1 Introduction

Biomaterials have become an important part of modern drug delivery because they can do more than carry drug molecules: they can localize drug delivery, protect sensitive molecules, and shape how a drug is released over time. In many biomedical applications, such as wound healing, post-surgical care, localized disease treatment, and tissue regeneration, the therapeutic goal is not simply systemic delivery but achieving a controlled drug release at the target site (Teixeira do Nascimento et al., 2025). Hydrogels are well suited to this role because they are rich in water, compatible with soft tissues, and their structural and mechanical properties can be adjusted. As a result, hydrogels can be used as wound dressings, injectable depots, or implants that keep therapeutics where they are needed (Hoffman, 2012).

A limitation of many established controlled-release platforms is that they are preprogrammed, and once administered, their release profiles are largely fixed. This can be a limitation in biomedical applications where therapeutic needs vary over time or when dosing should be adjusted to the clinical situation. On-demand drug delivery was developed to address this gap by enabling release to be triggered or modulated after administration, allowing dosing to be timed and, in some cases, tuned to the needs of the patient or the local environment (Antoniou et al., 2021; Ashrafizadeh et al., 2022; El-Husseiny et al., 2022). The first part of the literature review in this thesis discusses different ways to achieve on-demand drug delivery, which can be achieved by internal or external stimuli. Among external triggers, light is particularly attractive for biomedical use because it is non-invasive, can be delivered with spatial precision, controlled temporally, and can be modulated by adjusting wavelength, irradiance, exposure time, and irradiation geometry (Tao et al., 2020; Yang et al., 2024).

In light-responsive delivery, liposomes offer a particularly versatile platform because their membranes can be engineered to respond to light via photothermal heating or photochemical oxidation, thereby releasing encapsulated hydrophilic or hydrophobic agents. (Ashrafizadeh et al., 2022; Chander et al., 2021). The second part of the literature review in this thesis focuses on design strategies for developing thermosensitive and ROS-responsive liposomes for light-triggered release. Despite these advantages, light-activated liposomes face practical limitations that directly motivate this thesis. Since photosensitizers and dyes can aggregate or destabilize bilayers, liposomes can exhibit passive leakage and serum-driven instability. Most importantly, light delivery in tissue is depth- and geometry-dependent, making it difficult to guarantee a uniform trigger dose at the target without careful system

design. These limitations become more critical when localized control is the primary aim.

Cellulose nanofibril (CNF) hydrogels have gained attention in biomedical research as biocompatible, sustainable, water-rich, and mechanically tunable biomaterials, and have been used as biomimetic matrices for tissue regeneration and 3D cell culture (Heise et al., 2021). These properties also make CNF hydrogels attractive as local depots for therapeutic delivery. Cellulose fibers can be chemically modified to introduce new functionality. TEMPO-mediated oxidation introduces C6 carboxylate groups on cellulose microfibril surfaces, producing an anionic CNF (aCNF) hydrogel with a charged interface that supports molecular and colloidal interactions (Isogai et al., 2011; Saito et al., 2007). In practice, this anionic nature can be used to electrostatically retain positively charged components, which is particularly relevant when designing local depots that must hold nanocarriers in place.

These considerations motivate the central idea of this thesis, using aCNF as a carrier matrix for light-activated liposomes, with the hydrogel acting as a depot providing localization and the liposomes providing the triggerable release function. Liposomal hydrogels are increasingly discussed as a practical way to combine the complementary strengths of hydrogels and liposomes, where hydrogels can suppress burst release, improve local retention, and provide mechanical integrity, while liposomes can protect cargo and deliver controlled release upon activation.

The experimental part of this thesis evaluates the suitability of a liposome-hydrogel platform for biomedical use. In addition to studying light-triggered cargo release, we investigated a strategy for light-activated enzymatic degradation of the aCNF hydrogel matrix. This is relevant for potential in vivo applications because aCNF is not naturally degraded under physiological conditions, as humans lack cellulase enzymes, and a persistent depot could otherwise require surgical removal. We also propose an implant-oriented approach to address the practical penetration depth limitation of light as a trigger, by considering how controlled light delivery could be achieved in deeper or less accessible sites.

Overall, the aim was to develop a stable liposomal hydrogel system and determine how formulation and system parameters can be used to tune light-activated release. A second objective was to assess the feasibility of encapsulating cellulase enzymes in light-responsive liposomes and to determine whether light-triggered enzyme release can drive controlled degradation of aCNF hydrogels. Together, these studies support the development of localized, externally controllable delivery systems that combine the depot function of aCNF hydrogels with the triggerable release

capability of light-activated liposomes. While additional work is needed to define application-specific performance and translational requirements, the studies presented here contribute to the design of more controllable, locally retained, and externally triggerable biomaterial-based drug delivery systems.

2 Review of the literature

2.1 Controlled drug delivery

2.1.1 Need for controlled drug delivery

Controlled drug delivery (CDD) systems were developed to address recurring limitations of conventional dosage forms. Conventional dosage forms such as tablets, capsules, and injections do not maintain a constant drug concentration in the blood. After single-dose administration, there may be an abrupt increase in drug concentration in the blood that declines within a short period, resulting in the 'peak-and-trough' effect. Such fluctuations are not optimal as high drug concentration can be toxic to the patients, whereas low concentrations could make the treatment ineffective. (Lipicky, 1994) To keep the drug plasma level within the therapeutic window, there might be a need to administer multiple doses during the day, which can lead to poor patient compliance and reduced drug efficacy. In parallel, many drugs have poor bioavailability, short half-lives, narrow therapeutic indices, or high off-target toxicity. CDD systems address these concerns by improving drug efficacy through improved drug release kinetics. They maintain consistent drug plasma concentrations by delivering the right dose at predetermined time intervals for a long period of time. (Adepu & Ramakrishna, 2021; Larrañeta & Domínguez-Robles, 2025) CDD influences drug pharmacokinetics with the aim, i) to maintain drug concentrations near a target window, ii) to increase their residence time at the site of action, iii) to reduce off target side effects, and iv) to improve patient adherence by lowering dosing frequency.
These objectives are often emphasized while developing CDD systems. Figure 1 shows the release profile of a drug as a plot of drug plasma concentration in dependence of time. In drug release kinetics, there are two important concentration levels, namely the minimum effective concentration, below which the drug is ineffective, and the minimum safe or toxic concentration, above which the drug causes adverse effects. For maximum drug safety and therapeutic effectiveness, it is crucial to maintain drug concentration between these two concentration levels.

The preliminary objective of the CDD is to develop a drug delivery system that maintains elevated drug concentrations in the bloodstream for an extended period. Controlled release formulations can exhibit a zero-order release profile, characterized by the release of drug molecules from a non-degrading matrix. This release profile indicates consistent drug release over time, independent of concentration fluctuations (Figure 1). This helps reduce the dose and dosing frequency, improving patient compliance.

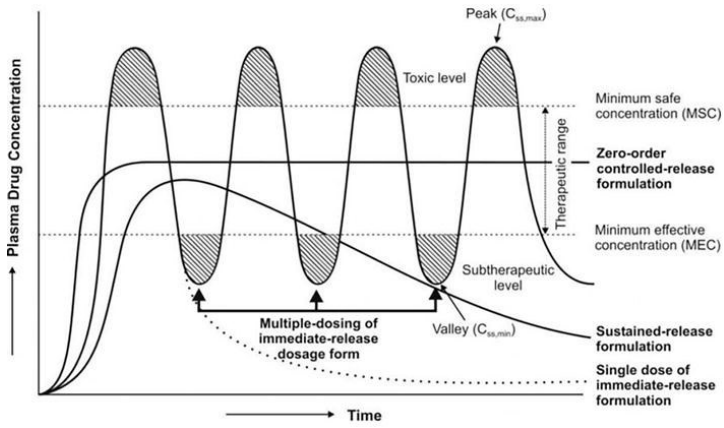

Figure 1 Illustration of drug plasma concentration profile for different formulations. Image is reprinted from (Brahmankar DM, 2009).

Zero-order release kinetics, characteristic of second-generation drug delivery systems, was believed to be the most desirable drug concentration profile. However, after decades of extensive research, the strategy changed: for most drugs, maintaining a constant plasma drug concentration is not essentially required to maintain efficacy, provided the drug concentration remains within the therapeutic window (Figure 1). Moreover, for certain therapeutics, such as nitroglycerin, hormones, and insulin, maintaining a constant blood level may not even be desirable. Hence, strict zero-order release might not be followed by many dosage forms and is not even essential for developing effective sustained-release systems. Understanding these drug delivery needs has shaped the development of third-generation, i.e., modulated drug delivery systems. (Park, 2014) In practice, advanced CDD aims to regulate the rate or location of drug availability to improve therapeutic efficacy and reduce adverse effects. The controlled release is therefore not purely one of slower release, but one of predictable release of the drug molecules, often constrained by biological barriers. Overall, the drug delivery method influences pharmacokinetics, distribution, cellular uptake, metabolism, clearance, and toxicity, meaning that formulation design can be as significant as the drug itself for effective drug action (Q. Chen et al., 2024).

Local drug delivery is viewed as a specialization of CDD where the aim is to keep the drug concentrated where it is needed, while minimizing exposure to other areas. For local delivery applications, factors such as diffusion, total drug concentration, and elimination processes in tissue can strongly shape how far and for how long a drug can penetrate from the application site or around the target area (Brudno & Mooney, 2015; Weiser & Saltzman, 2014). Local drug delivery systems aim to

overcome the limitations of traditional carriers, which provide only monotonic release profiles, irrespective of time, patient needs, or physiological changes. Most local drug delivery applications for CDD rely either on the diffusion of the drug out of the depot or the use of local pH, hydrolysis, and enzymatic cleavage to degrade the drug-containing matrix and release the drug (Alkahtani et al., 2024; Fatima et al., 2023; Weiser & Saltzman, 2014). However, the local disease pathology may significantly affect these processes and vary from patient to patient. Further, the release rate in these systems cannot usually be modified after placement. Many diseases could benefit from regulated drug availability by extrinsic control over drug release. Hence, the use of externally applied signals, such as physical forces or administered signaling molecules, could enable drug release at the ideal time and dose for a specific disease application in a particular patient.

2.2 On-demand drug delivery

On-demand drug delivery is an advanced subset (3rd generation) of controlled delivery systems in which release is not only governed by a predefined material design but is also intentionally triggered by stimuli (Adepu & Ramakrishna, 2021). These systems are designed to release a therapeutic payload only when triggered, either autonomously by an internal physiological signal (i.e., feedback-controlled) or by an externally applied stimulus. Thereby adding temporal control "when" and often spatial control "where" to what conventional immediate-release dosing or passive sustained-release depots can provide (Brudno & Mooney, 2015). This addresses several needs in drug delivery, e.g., i) diseases with fluctuating severity where fixed dosing produces under- or over-treatment (e.g., episodic chronic pain, inflammatory flares, variable insulin demand), ii) narrow therapeutic windows where fluctuations in plasma drug concentrations drive toxicity or loss of efficacy, and iii) treatment adherence, where frequent dosing or parenteral administration reduces patient compliance. The on-demand control of these drug delivery platforms is usually achieved by coupling a drug reservoir (e.g., hydrogels, nanoparticles) to a mechanism that converts a trigger into a change in permeability, matrix degradation, bond cleavage, or phase transition, thereby releasing the drug at the desired time. (Cai, Zhang, et al., 2025; Hu et al., 2024; Lee et al., 2022)

Triggered, on-demand release is particularly relevant for localized diseases, where active targeted release mechanisms are needed to reduce nonspecific toxicity at off-target sites and enhance therapeutic efficacy (Mirvakili & Langer, 2021). The field of on-demand drug delivery is moving towards highly sophisticated, personalized systems that can precisely control drug release based on individual patient needs and real-time physiological conditions. While significant advancements have been made, challenges remain in achieving the full potential of these technologies.

Manufacturing and reproducibility are complex, and in vivo assessment of stimuli-responsive materials, coupled with highly variable patient conditions, can adversely affect standardization and commercialization (Mirvakili & Langer, 2021; Yang et al., 2024). This thesis integrates both concepts by engineering stable carriers and a depot reservoir that remain inert during storage yet respond rapidly to a specific trigger.

2.2.1 Stimuli-responsive systems

Based on the origin of the trigger for drug release, on-demand drug delivery is classified into two main categories: endogenous and exogenous stimulus mediated systems. Endogenous responsive systems use spatially or temporally varying biochemical conditions, such as pH, enzymes, and redox imbalance in the affected area, to facilitate drug release. In contrast, exogenous systems rely on external stimuli such as ultrasound, magnetic fields, and light for drug release, offering better control over release than endogenous systems. (Cook & Decuzzi, 2021; Kost & Langer, 1992) This distinction is useful because it highlights whether control is imposed by the user or clinician (i.e., externally) or emerges from the local microenvironment (i.e., internally) (Figure 2).

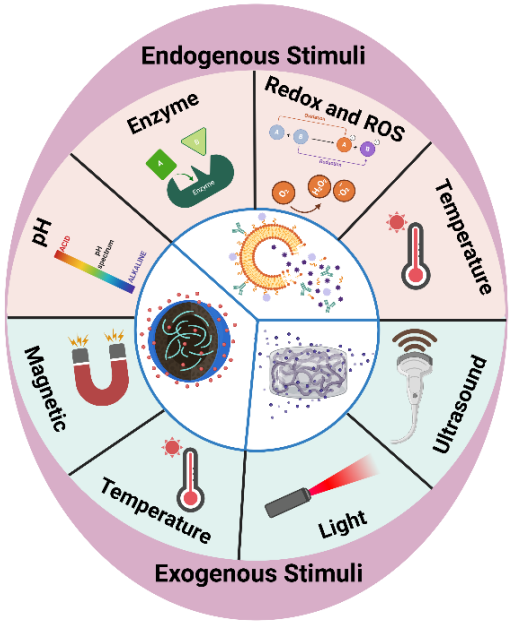

Figure 2 Summary of triggers used for stimuli-responsive drug delivery. Created with Biorender.com

2.2.1.1 Endogenous triggers

The endogenous stimuli-responsive system, also known as the microenvironment responsive system, relies on changes in pathophysiological conditions to trigger drug release. pH-responsive matrices are among the most established examples because pH gradients exist across organs and within cells, and many diseases also generate a local acidic environment. In cancer and inflammatory conditions, the extracellular pH of affected tissues is often lower, typically around 6.0-7.0, than the extracellular pH of healthy tissues, which is approximately 7.2-7.4. (Muhammad et al., 2013) Hence, chemistry associated with pH variations can be used to design drug delivery systems releasing drug molecules at the target site while minimizing exposure to healthy tissues (Ding et al., 2022; Fang et al., 2023). At the cellular stage, the acidic environment of endosomes (pH 5-6) and their fusion with lysosomes (pH 4-5) create another pH gradient that can be used for effective intracellular drug targeting.

Two main strategies exist: polymer networks bearing ionizable groups can swell or collapse as protonation state changes, modulating mesh size and diffusivity. On the other hand, acid sensitive covalent chemistry that remains stable in a neutral pH environment but cleaves in the acidic environment, such as hydrazone linkage in polymers, has been used quite extensively (Yoshida et al., 2013). For instance, Deng et al. studied the release of tumor necrosis factor alpha from chitosan-silica nanospheres in breast cancer therapy. In the local acidic environment of tumor tissues, swelling of the chitosan hydrogels was induced by protonation of the amino group (pKa 6.3), thereby releasing encapsulated molecules (Z. Deng et al., 2011). In addition to cancer treatments, pH-responsive systems have also been used in many other applications, such as inflammatory arthritis (M. Zhang et al., 2022), wound healing (Y. Wu et al., 2022), and kidney disease (Fang et al., 2023), leveraging pH variation in disease conditions. More popular examples are listed in Table 1.

Redox- and Reactive oxygen species (ROS)-responsive designs use the differences in reducing and oxidizing potentials between healthy and diseased states. A common redox strategy relies on the intracellular redox potential generated by different levels of glutathione. Glutathione is found at low concentrations (2-20 μM) in the extracellular environment but at much higher concentrations (2-10 mM) in the intracellular cytosol. This difference is very noticeable in tumor tissues, where intracellular glutathione levels are almost 100 times higher than extracellular levels. Disulfide bonds, which are readily cleaved by glutathione, are commonly incorporated into these systems to facilitate intracellular drug release (Cook & Decuzzi, 2021; X. Guo et al., 2018). Redox-sensitive crosslinking agents in micelles are used for intracellular delivery of hydrophobic drugs (Y. Li et al., 2011). Recent examples are listed in Table 1. In addition to nanoparticles, nucleic acids complexed

with reducible cationic polymers, including disulfide-containing poly(amido amine) (R. Zhang et al., 2022), and histidine-containing polycations (Hooshmand et al., 2022), are often used to achieve better transfection and gene silencing than non-redox-sensitive counterparts. This is due to the high sensitivity of redox-sensitive complexes, which rapidly dissociate under intracellular reducing conditions.

ROS-responsive polymers use enhanced oxidative stress in the inflammatory and cancerous cell microenvironment as a stimulus for drug release. Oxidation-sensitive thioketals containing prodrugs or crosslinked assemblies can remain intact under baseline ROS conditions but undergo cleavage in a ROS-rich cell environment, releasing the drug molecule (Rinaldi et al., 2022). Other cleavage chemistries, such as phenylboronic acid, peroxalate ester, proline oligomer, vinyldithioether, and aminoacrylates, are used for ROS-induced release. (Chi et al., 2024; Jobdeedamrong & Crespy, 2025)

Enzyme-responsive systems use disease-associated enzymatic activity as an on-demand stimuli for drug release. These systems are prepared by embedding enzyme-cleavable peptides as crosslinkers in hydrogels or as coatings on nanoparticles. When the target enzyme is present at sufficient activity, cleavage increases hydrogel permeability, causes coating erosion, facilitating release (Sobczak, 2022; M. Wang et al., 2022). Matrix metalloproteinases (MMPs) are among the most commonly used as enzymatic triggers in many enzyme-responsive applications due to their overexpression in cancerous microenvironments and certain disease conditions (F. Guo et al., 2024). Zhang et al. developed MMP-responsive hydrogel by incorporating an MMP-cleavable peptide into a covalent tetra-armed poly-(ethylene glycol) (PEG) network for on-demand drug release in response to inflammation (M. Zhang et al., 2024). Another popular enzyme responsive system is glucose-responsive insulin delivery. In these systems, hydrogels (X. Li et al., 2017), microgels (Gu et al., 2013), or nanoparticles (X. Li et al., 2016) incorporate glucose-sensing elements, such as glucose oxidase or phenylboronic acid, to couple ambient glucose concentration to insulin release. Glucose oxidase converts glucose to gluconic acid and hydrogen peroxide, lowering local pH and triggering pH-sensitive components, whereas phenylboronic acid binds to glucose in a reversible manner and can drive swelling of the hydrogel matrix (L. Zhao et al., 2017).

Across all endogenous stimuli-responsive systems, the release principle is the same, linking changes in biochemical factors to release. However, these biochemical responses are not very specific to the site of action, making it very challenging to deliver the right amount of drug at the right time and place. Hence, there is a need

to have external control over drug release, which is provided by using stimuli outside of the body.

Table 1 Examples of Endogenous stimuli responsive on-demand drug delivery systems in the literature.

Trigger Mechanism	Cargo /Formulation	Application	References
pH response			
Hydrazone bonds (C=NNHR)	Farnesal/Liposome	Drug release at pH 4.5, treatment of dental caries	(Yi et al., 2020)
Imine bonds d (-C=N-)	Doxorubicin and Curcumin/Prodrug nanoparticle	Drug release at pH 5 and 4.8 Cancer treatment	(Y. Zhang et al., 2016)
ester bond (R-C(O-R)3)	Paclitaxel/ Polymeric nanoparticle	60% at pH 5.5 within 96 h, Cancer treatment	(W. Chen et al., 2023)
amide bond (-CONH)	Paclitaxel and Combretastatin A4/ Polymeric nanoparticle	70.0% at pH 5.5, 24 h Hepatocellular carcinoma	(C. Zhang et al., 2016)
Metal ion coordination bonds	Iron ions/Protocatechualdehyde/ Hydrogel; Zinc oxide/Quercetin/ Nanoparticles	Wound healing; breast cancer therapy	(Liang et al., 2021; Sadhukhan et al., 2019)
pH sensitive polymers	Doxorubicin / Chitosan hydrogel	65% at pH 6.5 and 5.0, Cancer treatment	(Gao et al., 2019)
Redox			
Dual responsive Glutathione depletion and ROS generation	Paclitaxel/ Cinnamaldehyde-based, disulfide-containing polymer nanoparticles	Disrupts intracellular redox homeostasis in tumor cells	(Zeng et al., 2026)
Disulfide bonds cleavage by glutathione	Curcumin / Thiolated Mussel Adhesive Protein (MAP)-based nanoparticles	Pulmonary targeting for lung cancer treatment	(Jeong et al., 2025)
Reactive oxygene spcies (ROS)			
Phenylboronic Acid	Doxorubicin, Epirubicin and Irinotecan /Polymeric micelles	Cancer treatment	(Lv et al., 2018)
Diselenide	Doxorubicin /Diselenide block copolymer anoperticles	Cancer treatment	(L. Zhang et al., 2020)
Thioketal	Cytokine-targeted siRNAs /Thioketal nanoparticles	Anti-inflammatory and inhibits gene expression in the intestines	(Wilson et al., 2010)
Peroxalate Ester	Polymeric nanoparticles /Poly(vanillin oxalate)	Anti-inflammatory	(Kwon et al., 2013)
ProlineOligomer	plasmid DNA/ polymeric nanoparticles	Gene therapy for atherosclerotic lesions	(Gupta et al., 2015)
Enzyme			
Matrix metalloproteinases	Phosphatidylserine/Hydrogel	Bone Regeneration Through Immunomodulation	(M. Zhang et al., 2024)
Thrombin	Plasmin/ thrombin-responsive nanoparticles	Thrombo-occlusive vascular diseases	(Sun et al., 2023)

2.2.1.2 Exogenous triggers

Exogenously triggered on-demand drug delivery systems use externally applied physical stimuli, such as temperature, ultrasound, magnetic fields, or light, to induce the release of drug molecules. By enabling non-invasive control over both dose and release duration, on-demand drug delivery can be tailored as per the patient's needs. Additionally, externally controlled triggers can confine drug release to the exposed site, reducing systemic toxicity to healthy cells, thereby enhancing efficacy while minimizing adverse effects. Owing to these advantages, externally triggered drug delivery strategies show strong potential in personalized drug therapy. This thesis covered only the main exogenous stimuli (Table 2) and did not include radiofrequency and electro-responsive systems.

Temperature regulated systems harness the thermally driven phase transition in either polymers or lipid bilayers. Thermo-responsive polymers like poly(N-isopropylacrylamide) (PNIPAm), remain swollen under their lower critical solution temperature (32-33 °C), and above this temperature, they collapse resulting in heat responsive drug diffusion (Yoo et al., 2000). Additionally, copolymerization with different polymers is used to tune the responsiveness and mechanical properties of PNIPAm polymers (Ansari et al., 2022). Recently developed PLGA-PEG-PLGA based injectable thermosensitive hydrogels are used for tissue regeneration. This thermosensitive hydrogel is liquid at room temperature and solidifies after injection in the tissues at body temperature, causing sustained release of encapsulated vascular endothelial growth factor, supporting long-lasting bone regeneration (Han et al., 2023). In the lipid systems, the thermosensitive lipids are used to prepare thermosensitive liposomes for drug release (discussed in a later section of this thesis). This is the only system that can leverage both internal physiological stimulus (increased temperature in tumor cells) and the external stimuli (Davoodi et al., 2018).

In addition, Ultrasound (US) waves with frequencies ranging from 25 kHz to several MHz are used as stimuli for on-demand drug delivery. US provides deep tissue penetration with a high safety profile and has been widely used in several biomedical applications (Carovac et al., 2011; Piech et al., 2020). A major benefit of the US is that it not only acts as an external trigger for release but also serves as an imaging platform for non-invasive image-guided drug release (Thanou & Gedroyc, 2013; T.-Y. Wang et al., 2014). The mechanisms of release include i) acoustic cavitation, which can induce mechanical disruption or permeabilization of drug carriers, ii) local heating resulting in tissue damage or inducing release from thermosensitive nanoparticles, and iii) microbubble-mediated effects that can destabilize carriers or increase local permeability. Achieving consistent dosing in US DDS depends on acoustic field control and on the stability of ultrasound

sensitive nanocarriers (Kubota et al., 2021; Yeingst et al., 2022; Yudina & Moonen, 2012).

Table 2 Examples of exogenous stimuli responsive on-demand drug delivery systems in the literature.

Trigger Mechanism	Cargo /Formulation	Application	References
Temperature			
Thermosensitive hydrogel	Curcumin and rifampicin/ Micelles-hydrogel platform	Chronic wound treatment, sol-to-gel transition at 33 °C	(Q. Zhao et al., 2022)
Photothermal	Imipenem, IR780 photosensitizer/ Lipid nanoparticle	Bacterial infection	(Qing et al., 2019)
Ultrasound			
Sono-Thermal	Bone morphogenetic protein 2/ Alginate hydrogel	Bone regeneration, 25% amplitude, 9.6 mW/cm^2	(Levingstone et al., 2021)
Sono-Mechanical	ROS/ Azo-based mechanophores PEG Hydrogel	Melanoma, breast cancer, 550 kHz, 115 W/cm^2	(G. Kim et al., 2022)
Magnetic field			
Magneto thermal	RVG29 peptide/ Fe3O4-chitosan-ZIF-8 nanocomposites	Glioblastoma, 2400 rpm,5.3 mN/m Torque, 50–60 Hz	(Savari, 2024)
Light			
Photocleavage	Doxorubicin/Self-assembly organic NP	Treatment of retinoblastoma, 505 nm, 50 mW/cm^2	(Long et al., 2021)
Photoisomerization	Guaiacol and metronidazole /ZIF-90-Azo azobenzen photoswitch	Antibacterial infections, 365 nm, 50 mW/cm^2, and 460 nm, 20 mW/cm^2	(J. Wu et al., 2026)
Photothermal	Doxorubicin, ICG/ PLGA-Fe/FeO nanocrystals	Subcutaneous tumor, 808 nm, 0.3 W/cm^2	(Z. Wang et al., 2019)
ROS-Mediated	siRNA/ Porphyrin-lipid nanoparticle	Enhanced siRNA endosomal release, 660 nm 1.5 J/cm^2	(Mo et al., 2023)

The first use of US for therapeutic drug release from depot in vivo was reported by Huebsch et al., where the ionic crosslinking in the alginate gel was disturbed upon US application, releasing mitoxantrone in a tumor model (Huebsch et al., 2014). There are a wide range of hydrogels used in the drug delivery application for US activated on demand release, some of them listed in Table 2. Despite its popularity and the advantages of US-mediated on-demand drug delivery, some constraints need to be addressed for long-term applications. Polymer disruption by US mainly depends on cavitation generated by dissolved gases or on the encapsulation of microbubbles in hydrogels (Pulsipher et al., 2018). Progressive loss of gases in the systems can potentially reduce the cavitation effect, leading to a decrease in drug release in the long term (Angilè et al., 2014). Hence, designing long lasting US-sensitive on demand drug delivery system is quite challenging.

Magnetic targeting in on-demand release systems uses static field gradients to concentrate drug-loaded magnetic carriers near a magnet and to trigger release. Superparamagnetic nanoparticles, such as iron oxide beads embedded in the lipid bilayer or incorporated into the aqueous core of liposomes, serve as responsive elements to the magnetic field, thereby disrupting the lipid structure and releasing the drug. Such magneto liposomes also allow for image-guided therapies via magnetic resonance imaging (Le-Deygen et al., 2019). Another mechanism uses heat generation by exposing iron oxide nanoparticles to high frequency alternating magnetic fields (AMFs) to induce release from thermosensitive nanoparticles or hydrogels (Y. Chen et al., 2025; J. F. Liu et al., 2019). Wang et al. used this strategy to achieve controlled release from a fully biodegradable membrane composed of silk fibroin and magnetic nanoparticles for the controlled delivery of rhodamine. The magnetic thermal effect of nanoparticles in AMF causes thermal degradation of the silk fibroin protein and the formation of nanopores, thereby releasing the drug solution. The release can be controlled by altering the duration of AFM exposure (Y. Wang et al., 2022). In another interesting example, Zheng et al. developed an implantable, magnetically actuated capsule for on-demand drug delivery. The implant contains two magnetic spheres, an elastic membrane, and a drug reservoir. In an external magnetic field, repulsion between magnetic balls causes the drug solution to be actuated from the reservoir. The implant showed promising results during the course of 15 day insulin treatment in vivo. The diabetic rats treated with the implant showed very similar pharmacokinetic and pharmacodynamic profiles to those administered via subcutaneous injection, showcasing the implant's robust and on-demand drug release performance (Zheng et al., 2023). The key disadvantage of the magnetic field system is that achieving targeted heat generation with AMF is very difficult, potentially leading to unwanted tissue damage. Additionally, magnetic fields have limited depth penetration as the field gets weaker rapidly with distance (Shapiro et al., 2015).

Among all exogenous stimuli used for on-demand drug delivery, light provides excellent temporal precision. As an electromagnetic wave, light can transfer energy to a target area, inducing effects such as localized heating, phase transitions, and cleavage of chemical bonds. Owing to these properties, light has emerged as a powerful tool for achieving on-demand drug release, leading to the development of several photosensitive drug delivery systems to improve precision. Additionally, light-triggered systems offer considerable flexibility, as they can be modified to specific applications by selecting photolinkers and photosensitizers that are responsive to a wide range of wavelengths (100 to 1700 nm). (Yang et al., 2024) This thesis primarily focuses on the use of near-infrared (NIR) light to develop on-demand drug delivery systems. The rationale and limitations of light as a stimulus

for drug release are discussed in detail in the next section. Overall, developing on-demand drug delivery systems is not a single component optimization. There is a multicomponent optimization involved, spanning materials chemistry, transport kinetics, trigger physics, and human factors. Hence, the ideal on-demand drug delivery platform is dictated by the therapeutic context, such as required dose, target depth, permissible trigger exposure, disease conditions, and most importantly, biocompatibility.

2.3 Why light-triggered systems are attractive and what limits them

Light-triggered drug delivery offers exceptional spatiotemporal control; light can be focused on a specific target area and applied at a chosen time, enabling on-demand release with minimal effect on other body tissues (Rapp & DeForest, 2021). Mechanically, light activation provides multiple options for achieving control over drug release: i) photothermal pathways, convert absorbed light to heat, which then activates thermo-responsive matrix or membrane to accelerate diffusion or induce structural transitions. ii) photodynamic pathways, in which the effect is generated by photosensitizers after absorbing photons and being excited to the triplet state, generating ROS. ROS may directly harm tumor cells or induce the breakdown of ROS-sensitive nanoparticles, thereby triggering the release of drug molecules. iii) photochemical pathways, where photocleavable linkers, or photo-uncaging, convert photons into bond cleavage and irreversible cargo release. (Hu et al., 2024; Tao et al., 2020) Examples are listed in Table 2.

The same features that make optical triggering powerful also define core constraints of light as on-demand drug delivery platform, starting with penetration depth compromises. UV or blue (200-500 nm) light provides high photochemical reactivity that is useful for high-energy photochemical reactions, which are strongly attenuated in tissue and carry higher phototoxicity risks (Alvarez-Lorenzo et al., 2009). In contrast, visible red light penetrates tissues more effectively than UV and NIR light (Figure 3) and is often considered optimal for therapeutic applications. The wavelength around ~650-900 nm tends to provide deeper penetration with lower background absorption and reduced phototoxicity relative to UV light (Figure 3) (Raza et al., 2019; Timko & Kohane, 2014). Barbora et. al. have studied that only a small fraction of incident power may reach centimeter-scale depths of tissue, with light penetration depending on tissue composition, thickness, and beam parameters (Barbora et al., 2021; Salehpour et al., 2019).
These optical realities drive a second limitation, which is trigger reliability under tissue attenuation. Because tissue scattering and absorption affect photon distribution, the delivered dose rate inside tissue can differ substantially from the

incident irradiance at the surface and can vary across patients and tissue types (Salehpour et al., 2019). In the clinical applications, photodynamic therapy (PDT) dosimetry guidance clearly notes that scattering or absorption can cause large deviations between incident and delivered light doses, hence the guidance suggests having in situ dosimetry, calibrated fiber geometries, and treatment planning rather than relying on device output alone (M. M. Kim & Darafsheh, 2020; Zhu et al., 2025).

Phototoxicity is the third major constraint in the use of light for on-demand drug delivery applications. UV exposure can directly damage biomolecules, meanwhile ROS-generating photodynamic pathways can cause off-target oxidative injury and inflammation if the photosensitizer accumulates outside the target region (Correia et al., 2021). In case of the photothermal pathway, safety constraints are caused by unintended temperature rise and heat diffusion beyond the illuminated target. The photothermal release mechanism can be robust but requires careful control of irradiance, spot size, and proper cycles to keep tissue temperatures within an acceptable range (X. Deng et al., 2021). Finally, the practicality of light-triggered delivery is also one of the critical factor for reproducibility and comparability across studies. Optical dosing is commonly reported as irradiance (power density, W/cm^2) and radiant exposure (dose, J/cm^2), but the biologically relevant dose is frequently the local irradiance within tissue, which depends on laser power, whether irradiation is continuous or pulsed, and on the mechanism of release. Among the available strategies for light-activated drug release, this thesis focuses on thermosensitive and ROS-sensitive mechanisms.

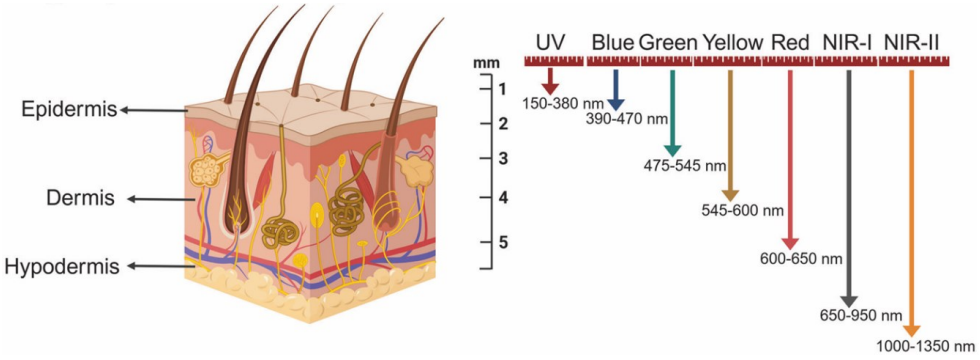

Figure 3 Illustration of approximate penetration depths of light into skin. Reprinted from (Cai, Chai, et al., 2025), with permission from Springer Nature.

2.4 Light-triggered liposomal release: design strategies

2.4.1 Liposomes for drug delivery

Liposomes are self-assembled vesicles made up of phospholipids that organize into one or more circular bilayers surrounding an aqueous core (Bangham et al., 1965). The lipids used to form the liposomes have a dual chemical nature, with a hydrophilic head group and hydrophobic tails. Liposome formation from these lipids depends on the critical micelle concentration (CMC) in water. The CMC is the concentration (moles per liter) of the lipid in the water above which the lipid monomers form a bilayer structure. Above the CMC, lipids arrange themselves to form a stable bilayer structure, excluding water molecules from the hydrophobic regions. Water is an essential component to drive lipid molecules to form stable bilayer structures. (R. M. Shah et al., 2025) Obtaining high CMC alone is not enough to form liposomes; the lipid arrangement, which depends on the surface area of the polar head group relative to that of the hydrophobic chain upon hydration, also plays an important part. For instance, lysophospholipids form micellar structures upon hydration due to the higher proportional surface area of their head groups. In contrast, negatively charged phospholipids (phosphatidylethanolamines) at low pH and in the presence of divalent cations form a hexagonal structure (inverted micelles) due to the increased surface area of the hydrocarbon chains. Whereas normal lipids, PC, DSPC, DSPE, form a perfect bilayer structure due to the similar surface area of both heads and hydrophobic chains. Choosing the right lipids for the right application is very important, as lipid arrangement may vary depending on lipid properties and buffer characteristics. (Weiner et al., 1989)

In liposomes, phospholipids are arranged in a way that they form a bilayer by arranging hydrophilic head groups outward in contact with aqueous layers and hydrophobic chains inward, keeping the hydrophobic region in the bilayer (Figure 4). This structural assembly of the liposomes enables the encapsulation of hydrophilic molecules in the aqueous core and hydrophobic molecules in the bilayer. In addition to carrying drug molecules, liposomes serve an important function by protecting the encapsulated cargo from the external environment, thereby increasing their half-life and biocompatibility. Liposomes span a wide size range from 40 nm to a few micrometers, and the bilayer thickness ranges from 4-6 nm (Regan et al., 2019; Weiner et al., 1989). Liposomes are classified according to their size, small unilamellar vesicles (SUVs) consist of a single lipid bilayer and typically have diameters below 100 nm. Large unilamellar vesicles (LUVs) have a single bilayer and are larger, typically 100–1000 nm. Multilamellar vesicles (MLVs) comprise multiple concentric bilayers within a larger vesicle; their diameters

commonly span from approximately 500 nm to several micrometers, and they are often characterized by a high polydispersity index in size measurement analysis. MLVs are highly unstable owing to their large size and multilamellar structure. During liposome preparation, sonication or extrusion is typically used to form LUVs from MLVs, which may result in the loss of some encapsulated drug molecules (Weiner et al., 1989).

Thin-film hydration is the most common method for preparing liposomes. In this method, the required phospholipids are dissolved in chloroform, and a thin film of the lipid mixture is prepared in a round-bottom flask by evaporating the chloroform, then hydrating with a buffer or drug solution at a temperature above the lipids' phase-transition temperature, thereby forming MLVs. Szoka et al. found that the thickness of the lipid film and the hydration time greatly affect liposome encapsulation, despite similar lipid concentrations, compositions, and volumes of the suspending aqueous phase. A thinner lipid film and more hydration time increase the encapsulation efficiency of the liposomes. (Szoka & Papahadjopoulos, 1978) To obtain more uniform unilamellar vesicles, the dispersion of MLVs is then processed through one or more size-reduction steps.

Sonication is one approach for reducing liposome size. It can be performed using a bath sonicator, a probe sonicator, or focused ultrasonication, in which ultrasonic energy breaks larger structures into smaller vesicles. High-energy probe sonication rapidly reduces the size of the MLVs but can degrade lipids and cause metal particles to shed from the probe, contaminating the sample. Using bath-type sonicators also introduces variability into the samples, such as the tube's position and the water level in the bath, which can affect liposome quality and introduce batch-to-batch variation. Additionally, using sonication can degrade sensitive biological drug molecules like enzymes, peptides, and proteins (Özbek & Ülgen, 2000). Overall, sonication can be convenient, but it often yields formulations with relatively broad size distributions and may introduce variability depending on energy input, temperature rise, and processing time. (Akbarzadeh et al., 2013)

Membrane extrusion is commonly used when uniform size control is required. In extrusion, a liposome suspension is repeatedly forced through membranes with a defined pore size (chosen as required), typically above the lipid's phase-transition temperature, so that the bilayer remains sufficiently fluid during processing. Repeated passes narrow the size distribution and can produce vesicles with a predictable mean diameter. After extrusion, cooling below the transition region helps to stabilize the structure for storage and downstream use. Extrusion is easy to use, reproducible, and it does not induce phospholipid breakdown. Sterile preparation of liposomes can be easily achieved using extrusion. (Olson et al., 1979)

For large-scale production, high-pressure homogenization or microfluidization is used under strict processing parameters to maintain quality (Akbarzadeh et al., 2013; V. M. Shah et al., 2019).

Due to their flexibility and the ability to modify the liposomal surface, liposomes can be tailored into distinct structural forms for specific applications (Figure 4). i) Conventional liposomes, prepared by varying lipid compositions to serve a purpose. Such as cationic liposomes prepared using positively charged lipids. They are widely used for gene delivery due to their ability to electrostatically react with negatively charged nucleic acids. ii) Stealth liposomes, also known as long-circulating liposomes. These are, for example, PEGylated liposomes made by incorporating PEG-attached lipids into the lipid bilayer. The functions are explained in detail in a further section. iii) Targeted liposomes, Liposomes are surface-functionalized with antibodies or ligands to enable receptor-specific targeting and enhance their therapeutic efficacy. Although this technique has proven promising, chemical coupling used to attach target-specific ligands or antibodies to nanoparticles significantly reduces their activity. In contrast, the physical adsorption of the ligands to the liposomes offers better activity towards the final target (Mirshafiee et al., 2013; Salvati et al., 2013). Li et al. have developed galloylated liposomes by incorporating gallic acid-modified lipids into lipid bilayers, thereby enabling stable, controlled adsorption of targeting ligands onto the liposomes via noncovalent interactions. This approach preserves ligand functionality, ensuring that binding sites remain exposed for active targeting (Li et al., 2025). (Chelliah et al., 2025)

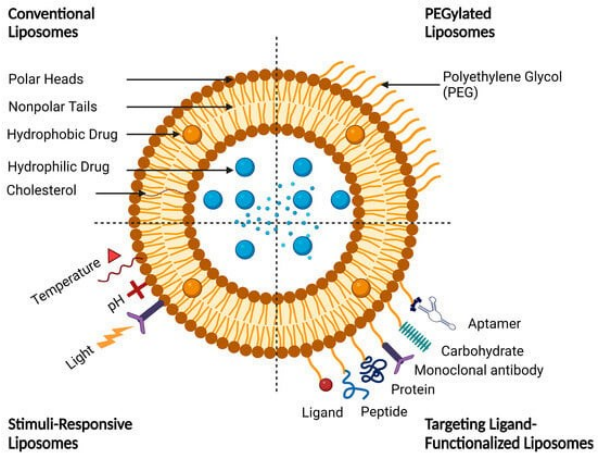

Figure 4 Illustration of liposome classification based on the surface modification. Reproduced from (Agiba et al., 2024), with permission from MDPI.

Most commonly used phospholipids carry zwitterionic headgroups; they contain both positive and negative moieties yet have an overall net neutral charge (e.g.,

phosphatidylcholine and phosphatidylethanolamine). In formulation practice, this neutral charge is often a baseline because it minimizes strong electrostatic interactions. However, liposomes are often tuned by mixing anionic or cationic lipids to modify surface potential, colloidal stability, adsorption to interfaces, and interactions with charged surfaces. For instance, cationic lipids are used as coatings for improved stability and endosomal delivery of nucleic acid drug molecules (siRNA, mRNA, DNA, oligonucleotides) (X. Sun et al., 2024; T. Wang et al., 2024).

2.4.2 Designing light-activated liposomes

Mechanistically, most light-triggered liposomal systems fall into two categories: either reliant on i) photothermal pathways, where absorbed photons are converted to heat that increases bilayer permeability, or on ii) photochemical or photodynamic pathways, where an excited photosensitizer (PS) generates ROS that chemically modify lipids and thereby permeabilize the membrane. Several additional photochemical strategies exist (photoisomerization, photocleavage, photo crosslinking), but for drug delivery, the dominant, best-developed release concepts in liposomes remain photothermal and ROS-mediated permeabilization. (Gangurde et al., 2023; Lajunen et al., 2016; Miranda & Lovell, 2016; Yavlovich et al., 2010)

2.4.2.1 Engineering thermosensitive light-activated liposomes

The hydrophobic region of the lipid bilayer is the dominant factor determining bilayer fluidity. Chain length and degree of unsaturation govern chain packing and order, which in turn modulate membrane rigidity and permeability. Longer saturated chains tend to increase close packing, generally lowering passive solute permeability and increasing bending rigidity. By contrast, unsaturation introduces kinks that disrupt close packing, increase free volume, and reduce chain order, which commonly translates into higher permeability of the lipid bilayer. (Binder & Gawrisch, 2001)

A defining feature of many phospholipid bilayers is a temperature-dependent reverse phase transition. Above the phase transition temperature (T_m), the hydrocarbon chain of the lipids undergoes a change from an ordered, higher-modulus gel-like state to a more disordered, fluid liquid-crystalline state. The T_m of the lipid and its composition can be determined using differential scanning calorimetry (DSC) analysis (Chiu & Prenner, 2011). In practical terms, the T_m is often associated with changes in permeability and mechanical properties of the lipid bilayer. Increasing hydrocarbon chain length usually raises T_m because more thermal energy is required to disrupt ordered packing, whereas unsaturated lipids

lower T_m by destabilizing the ordered state. (Chiu & Prenner, 2011; T. Wu et al., 2022) The headgroup of the lipid can also shift T_m, even when the acyl tails are identical in the lipid, the differences in headgroup packing and intermolecular interactions can alter the enthalpy and consequently the transition temperature. (Schönfeldová et al., 2021). For on-demand drug delivery systems, T_m is therefore not just a material property; it becomes an actionable formulation parameter used to achieve an ideal lipid membrane composition that provides the desired stability at physiological temperatures while retaining responsiveness when conditions change (Figure 5).

In photothermal liposomes, photothermal transducers (photosensitizers) such as chromophores or metallic nanoparticles are used to trigger on-demand release. Each photosensitizer has different absorption wavelengths and is selected based on the application. These molecules are placed in the lipid bilayer or near the liposomes such that they absorb light upon illumination and produce localized heat. This thermal pulse raises membrane temperature and can increase the permeability of the lipid bilayer by disordering acyl chains, thereby increasing the temperature above the lipid bilayer's T_m. Depending on the nature of the photosensitizer, it is either placed in the core (hydrophilic dyes) or in the lipid bilayer (lipophilic dyes) of the liposomes. A key practical point is that photothermal release is not purely a materials property, it depends on heat generation and dissipation under the chosen irradiation geometry and tissue environment. Nonetheless, at the liposome level, the most direct design control is to incorporate the photosensitizer into a bilayer tuned to undergo a sharp increase in permeability within the mild hyperthermia range. (Leung & Romanowski, 2012; Miranda & Lovell, 2016)

For many on-demand drug delivery applications, the pragmatic target is a liposome that is stable at 37 °C yet capable of rapid release upon activation. When the local temperature is raised into a mild hyperthermia window, often between ~40–43 °C, it results in thermosensitive drug release. (Carter et al., 2014; Lajunen et al., 2016) The commonly used saturated phosphatidylcholine DPPC has a transition temperature around 41 °C, whereas DSPC transitions at around 55 °C, illustrating how acyl chain length and saturation set the thermal operating point. In practice, formulations rarely behave like single-component membranes; lipid mixing broadens phase transitions, and the addition of other lipids with different functions can alter the properties of the bilayer. Still, T_m remains the central design parameter because it defines the temperature window where the lipid bilayer becomes permeable.

At the membrane-physics level, the permeability surge near T_m is closely tied to the coexistence of ordered and disordered lipids and the formation of loose patches that

act as transport pathways. Cholesterol is widely used to increase membrane robustness, reduce permeability, and improve stability against serum-induced disruption, but these same effects can suppress thermosensitive or light-triggered release by hindering the cooperative phase transition and reducing the extent of the transition-associated permeability spike (Gangurde et al., 2023; Kaddah et al., 2018). Studies examining cholesterol inclusion in thermosensitive liposomes highlight threshold-dependent effects in which cholesterol can decrease thermoresponsiveness. The mechanism of stability by adding cholesterol is best described as order modulation. Cholesterol places itself among loose areas of lipid tails and can reduce membrane fluidity while smoothing the sharpness of the main transition, typically yielding membranes with reduced permeability to many small solutes and improved mechanical robustness. This stabilization can be advantageous for minimizing passive leakage and preserving cargo during storage and circulation. At the same time, cholesterol can decrease permeability by increasing T_m of lipid bilayers and can shift how membranes respond to external stimuli. In other words, cholesterol is a powerful stabilizer, but its inclusion alters the defect landscape and the coupling between thermal fluctuations and transport, both important considerations in designing thermosensitive liposomes.

PEGylation is a basis of colloidal liposomal stabilization, providing steric repulsion that reduces aggregation and can prolong circulation, but it also changes interfacial chemistry and can interact with photosensitizers. Indocyanine green (ICG) is the most commonly used photosensitizer for near-infrared (NIR)- triggered drug delivery. ICG generates heat upon absorbing light around 808 nm wavelength, most importantly, it is clinically approved as an NIR imaging dye by the Food and Drug Administration and the European Medicines Agency. But it also presents formulation challenges: it degrades rapidly in aqueous media, forms aggregates in water, and is prone to thermal degradation. One strategy is to bind or encapsulate ICG in liposomes to improve its optical properties and to use its photothermal output to trigger release. For instance, ICG-loaded liposomes were reported to be stable from refrigerated storage up to body temperature, and rapid NIR-triggered release was achieved by tuning phospholipid composition and using an optimized ICG-to-lipid molar ratio (1:50); under these conditions, even large molecules like FITC–dextran up to 20 kDa were released completely after short light exposure (15 s). Critically, the presence of PEG in the liposomes plays an important role in ICG encapsulation and promotes ICG stability for long-term applications, whereas certain localization states (ICG in the bilayer plus PEG coating) can destabilize the bilayer at elevated temperatures, underscoring the need to treat PEG-lipids as active participants in the thermosensitive bilayer. (Lajunen et al., 2016; Needham et al., 2013) Overall, PEG-lipids are often indispensable for colloidal stability, but

they can also alter the “release threshold” by changing bilayer packing and photosensitizer localization.

In brief, the lipid composition is tuned according to their functions to achieve an accurate T_m for the thermosensitive liposomes, so that they can release cargo upon light activation while maintaining minimal passive leakage. To achieve this in most formulations, DPPC is used as the base lipid, followed by DSPC and Cholesterol to add stability to the bilayer, with DSPE-PEG serving a dual function of steric stabilization and improving photosensitizer encapsulation.

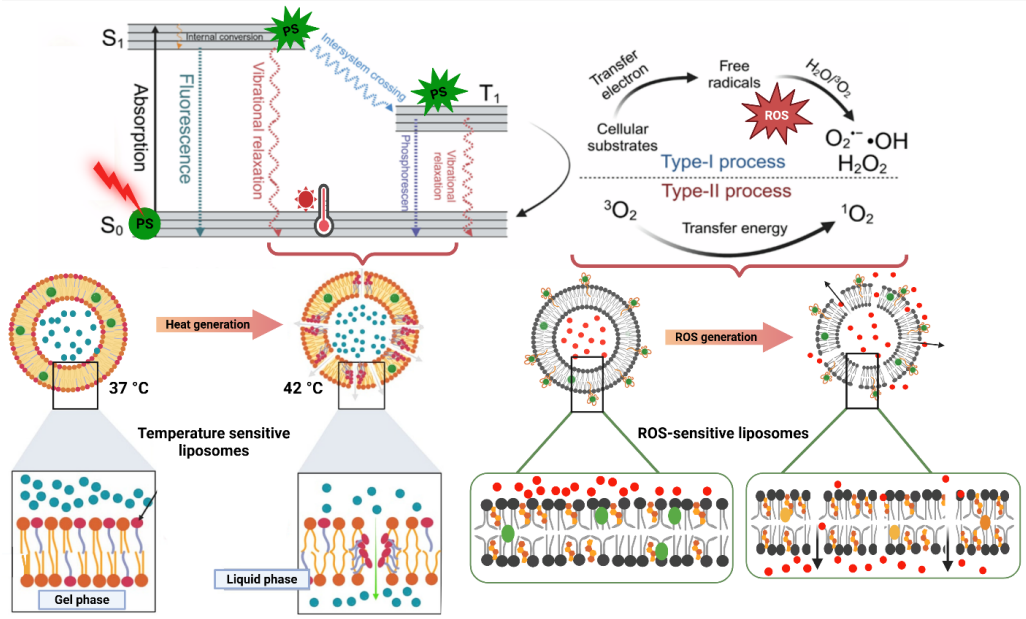

Figure 5 Illustration of a simplified Jablonski diagram showing the excitation of photosensitizer (PS) from its ground state (S0) to the singlet excited state (S1) after light absorption, followed by intersystem crossing to the triplet state (T1) and ROS generation. The bottom part shows the release mechanism from thermosensitive and ROS-sensitive liposomes. Created with Biorender.com

2.4.2.2 Engineering ROS-activated liposomes

In ROS-triggered liposomes, the release of encapsulated cargo molecules happens because of the photo-oxidation of phospholipids, where different unsaturated lipids, such as DOTAP, DOPC, DOPE, and POPC, are responsible for the ROS-sensitivity (Figure 5). The ROS generated by light activation of photosensitizer (PS) reacts with the double bonds in these lipids, destabilizing the lipid bilayer. Mechanistically, a photosensitizer undergoes either Type I (contact-dependent) or Type II (contact-independent) photochemical changes after light absorption. Type I involves electron transfer from a longer-lived triplet state PS to nearby substrate,

generating free radical species, whereas Type II involves energy transfer from the triplet excited state of PS directly to ground-state molecular oxygen to generate singlet oxygen, $^1O_2$ (Figure 5).

The literature on photosensitized lipid oxidation shows that oxidized lipids (e.g., hydroperoxides and other oxidation products) can increase the area per lipid, alter bilayer thickness or curvature stress, and create packing defects that cause leakage. (Miranda & Lovell, 2016; Pashkovskaya et al., 2010) A defining spatial constraint of photodynamic triggering is the short lifetime and diffusion range of reactive intermediates, particularly singlet oxygen, hence, the localization of PS relative to the bilayer is important. Experimental analysis of singlet oxygen behavior in membranes emphasizes rapid quenching and short effective action ranges in cellular environments. This supports the design rule that PS should be embedded in or tightly associated with the liposomal membrane to ensure that ROS chemistry occurs where it can open transport pathways (Sokolov et al., 2018). This is beneficial for controlled release from liposomes. If the photosensitizer remains largely confined to the lipid bilayer, ROS reactions can be concentrated on the liposome itself, enabling membrane permeabilization as a delivery tool (Bacellar & Baptista, 2019).

The permeability of the ROS- sensitive lipid membrane can be influenced by the molar percentage of unsaturated lipid in the bilayer. Luo et al. studied the effect of increased amounts of DOPC in the liposome prepared from DSPC, Cholesterol, and porphyrin–phospholipid. Here, porphyrin–phospholipid acts as a photosensitizer, generating ROS upon exposure to 665 nm light. The researchers found that increasing the amount of DOPC gradually up to 10% leads to more ROS-responsive oxidation of the double bond, resulting in membrane permeabilization, increasing the release of doxorubicin upon light exposure (Luo et al., 2016). Lem et al. use a phthalocyanine photosensitizer to generate ROS upon light activation and study the effect of lipid oxidation on the release of cargo molecules of different sizes. Liposomes prepared by a combination of DOTAP: Cholesterol: DSPE-PEG lipids were used to study the release and found that almost 90 % of small-sized cargo molecules were released within short light exposure due to the formation of hydroperoxides, epoxides, and vic-alcohols. In contrast, 30% of large dextrans (10 and 70 kDa) were released upon longer illumination (9 min) due to the formation of aldehydes, which form large pores or disturb the bilayer, causing the release of large molecules (Lem, Kekki, et al., 2024).

ROS-triggered liposomes must balance photo-reactivity with liposome stability. PS molecules are often hydrophobic or amphiphilic and can disturb bilayer packing, excessive loading can increase baseline permeability at 37 °C. Conversely,

insufficient PS loading or poor oxygen access can limit ROS generation and weaken triggering. The lipid oxidation reaction pathways depend on the proximity of PS to target lipids, and the chemical diversity of oxidized products is strongly influenced by lipid unsaturation and illumination time. Considering these, selecting lipids with appropriate oxidation capacity to improve the ROS response could be beneficial, but this must be weighed against shelf stability and in vivo leakage.

2.5 Cellulose nanofiber hydrogels as a drug reservoir for nanoscale carriers

2.5.1 Cellulose nanofiber hydrogel

Cellulose is the most abundant polymeric raw material found on Earth. It is a fundamental structural component of plant cell walls. In addition to plants, cellulose can be produced from other sources, such as tunicates, bacteria, and algae (Poulose et al., 2022). Cellulose is a linear polysaccharide polymer made from thousands of D-glucose units connected by β (1→4) glycosidic bonds (Figure 6) (Khandelwal & Windle, 2013). Nanocellulose is prepared by breaking down cellulose fibers, usually from wood pulp, into a nanoscale material using chemical, mechanical, or enzymatic methods. Based on the preparation method, nanocellulose is classified as i) cellulose nanocrystals (CNC), which have a short, rod-shaped structure with lengths of 100–500 nm and diameters of 2–20 nm, ii) bacterial cellulose has a fiber diameter of 10-50 nm and a length of 100-1000 nm and iii) cellulose nanofiber (CNF), with diameter of 5-50 nm and length in micrometres (Figure 6). (Phanthong et al., 2018; Poulose et al., 2022; Trache et al., 2020) CNF is composed of both crystalline and amorphous regions, which makes it a more flexible material than other forms of cellulose. CNF can be extracted from plants, bacteria, and algae by mechanical treatments (high-pressure homogenization, microfluidization, micro-grinding, steam explosion, cryo-crushing, and high-intensity ultrasonication) (Abdul Khalil et al., 2014).

Although mechanical treatment is widely used to prepare CNF hydrogels, it consumes a lot of energy, leading to high production costs. Hence, various pretreatments are applied before the mechanical processing of the pulp to minimize the energy consumption. For instance, chemistry-assisted nanofibrillation of cellulose is used to introduce anionically charged functional groups on the cellulose microfibril surfaces, thereby creating strong electrostatic repulsion between microfibrils in water and accelerating homogenization. Saito and team developed a method to prepare completely individualized nanofibers with 3-4 nm diameter and a few micrometers long by 2,2,6,6-tetramethylpiperidine-1-oxyl radical (TEMPO)-mediated oxidation under moderate aqueous conditions, also referred to as anionic

cellulose nanofiber (aCNF). (Isogai et al., 2011; Saito et al., 2007) Oxidation targets the C6 hydroxyl groups of cellulose and oxidizes them to carboxylic acid groups, adding a strong negative charge to the fibrils, thereby producing a transparent nanofibrous hydrogel with high surface area and mechanical strength. This thesis uses aCNF as a drug reservoir for release studies.

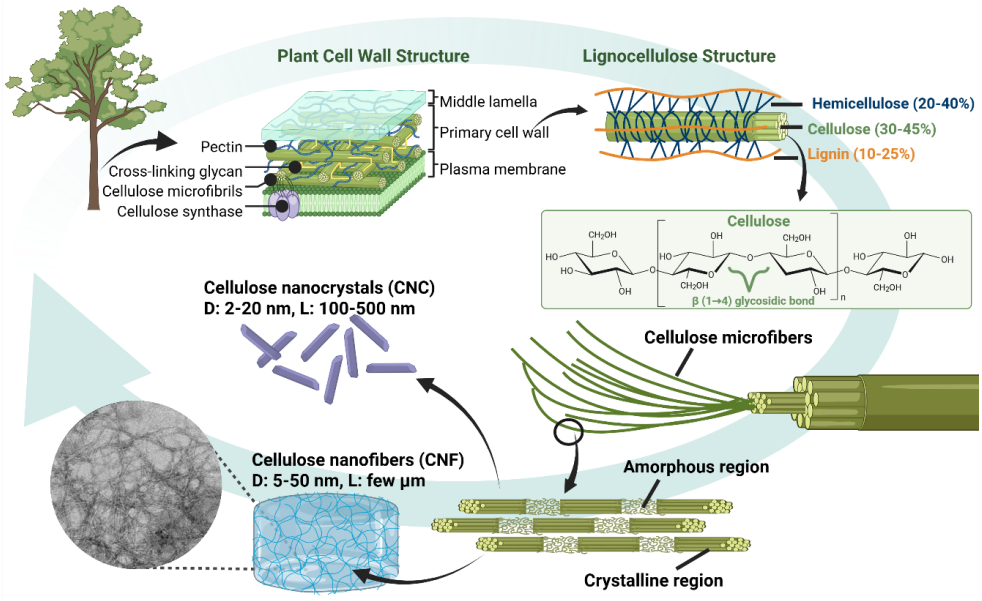

Figure 6 Schematic illustration of types and dimensions of plant based cellulose fiber. Created with Biorender.com

2.5.2 Cellulose nanofiber as drug reservoir

The aCNF hydrogels have gained popularity in the past few years for biomedical applications, such as tissue engineering, 3D cell culture, and wound healing (Ai et al., 2023; Bacakova et al., 2019; Heise et al., 2021). In addition to other biological applications, aCNF are also attractive drug-delivery matrices because they combine three features that are often difficult to reconcile in one material: i) high water content, tissue-like, diffusion-permissive environment, ii) mechanical integrity and shape retention due to 3D fibrillar network, and iii) chemical tunability, which supports affinity-based retention rather than diffusion-only release. The anionic carboxylates of aCNF hydrogels provide a clear chemical basis for electrostatic binding of positively charged species such as small molecules, proteins, dyes, and cationic nanoparticles (Gangurde et al., 2025; Kaya, 2024; Liu et al., 2020). Additionally, CNF hydrogels typically exhibit shear-thinning (pseudoplastic) and thixotropic behavior, meaning their viscosity decreases under shear and the

network can rebuild once the shear is removed. As a result, they can be delivered through a syringe with relatively low force and then quickly regain their gel structure after administration. This combination of injectability and rapid structural recovery makes CNF hydrogels well-suited for localized delivery and other site-specific therapeutic applications (Won et al., 2025).

A key structural parameter connecting release mechanism to drug transport is the mesh size (pore size) of the fibrillar network. The mesh-size analysis of aCNF hydrogels using solute exclusion and PFG-NMR reported that aCNF hydrogels have a nonuniform fiber network, with heterogeneous fiber distributions that can include relatively open regions alongside compact, diffusion-restricting regions (Jowkarderis & van de Ven, 2015). The mesh size of the fibrillar network also depends on the hydrogel concentration, which is directly correlated with the solid content of nanofibrils. From a drug delivery perspective, mesh size matters because aCNF hydrogels can be tuned to operate in regimes where molecular diffusion is allowed but nanoparticle mobility is selectively hindered, thereby enabling the formation of a drug reservoir that stores nanocarriers locally while still allowing them to perform their own release function.

A study by Paukkonen et al. demonstrated the release of model compounds of different sizes from aCNF hydrogel at two concentrations (3% and 6.5%). The release of small molecules was moderately affected by hydrogel concentration, with a minimal difference in diffusion coefficient between the two concentrations, indicating that the release is diffusion-based and depends on the free water present in the hydrogel networks. In contrast, the diffusion of large molecules was notably decreased with increasing aCNF fiber concentration of the hydrogels, providing higher control for release kinetics (Paukkonen et al., 2017). Although the nanocellulose hydrogel is a promising candidate as a drug reservoir, the issue of controlling the drug release kinetics still needs to be addressed in this system. Incorporating nanoparticles into the hydrogel system could minimize burst release while improving sustained release.

To prepare such a system, Auvinen et al. examined the effects of nanoparticle size, shape, and charge on release from aCNF hydrogels at two different concentrations. Smaller particles with a neutral charge were released faster from 1% hydrogels than from 2% hydrogels. Rod-shaped DNA origami was rapidly released from both hydrogel concentrations. Due to the rod shape, the DNA origami does not get entangled in the hydrogel network, facilitating quicker release. Interestingly, small nanoparticles with a cationic surface charge were retained much longer and exhibited sustained/incomplete release from both hydrogels, indicating the effect of electrostatic charge on nanoparticle release. The positively charged nanoparticles

can stay for a longer period in anionically charged CNF, forming a biocompatible depot system for sustained drug release (Auvinen et al., 2022).

Overall, the release from aCNF hydrogels is generally affected by several factors, including pore size, pore size distribution, swelling ability of the hydrogel, and most importantly, the properties of the drug molecule (charge, molecular weight) and nanoparticle (size, shape, and surface charge).

2.5.3 Liposome loading into hydrogels as nanodepots

Using nanocellulose hydrogels as reservoirs for nanoparticles (liposomes, micelles, DNA origami, polymeric nanoparticles) changes the conventional storage and release mechanism. Instead of storing the molecular drug directly in the fibrillar networks and relying mainly on diffusion out of the hydrogel, the hydrogel stores nanocarriers as nanodepots. The therapeutic release from the nanoparticle hydrogel systems is governed by whether the nanoparticles can move through the CNF mesh, sustained release of drug molecules from nanoparticles into the hydrogel, or on-demand release of drug molecules by exposure to external stimuli. Embedding liposomes into a hydrogel is widely pursued as a hybrid strategy that combines the strengths of both components (Atila et al., 2024; Mou et al., 2022; Sanati & Amin Yavari, 2024). In the liposomal hydrogel system (LHS), hydrogels act as a protective matrix that improves liposome stability, reduces premature leakage, and mitigates limitations of either platform alone, particularly for localized therapy.

In practical applications, three rationales dominate, and each maps cleanly onto design choices in nanocellulose systems. First, protect liposomes and prevent burst leakage: Despite their safety and biocompatibility for drug delivery applications, liposomes lack long-term stability. Liposomes suffer from destabilization and elimination due to plasma protein interactions when they reach the blood circulation, which can lead to unwanted leakage. (Comiskey & Heath, 1990; Semple et al., 1998). Incorporating liposomes into the hydrogel can reduce their interaction with destabilizing plasma proteins, as 3D fibrillar networks of the hydrogel hinder protein penetration and can also suppress burst release by imposing an additional diffusion barrier around the liposomes. Second, localized depot and prolonged retention at the target site: hydrogels can be formulated as injectable matrices or implants that remain where placed. When the liposomes are entrapped, they remain concentrated in the target region, improving local bioavailability while reducing systemic escape. In anionic nanocellulose, this can be made particularly strong for cationic liposomes due to electrostatic attraction between carboxylate anions and cationic liposomes, along with the exceptional biocompatibility of

nanocellulose. Also, cationic nanoparticles can cause toxic effects and thus entrapping them into a hydrogel can reduce this problem. (Atila et al., 2024; Correa et al., 2022)

Third, leveraging liposomes' ability to formulate as stimuli-responsive on-demand vehicles. Decoupling storage from release actuation: the hydrogel primarily provides storage (macroscale depot), while the liposomes can be designed as the stimuli-responsive nanodepot for on-demand release. This decoupling becomes especially powerful in externally triggered systems because immobilized liposomes can be activated repeatedly without requiring the nanoparticles to migrate; instead, the stimulus acts where the depot is located. This logic is explicit in nanocellulose liposome systems designed for on-demand release, where liposomes are treated as drug reservoirs whose baseline leakage is minimized by the hydrogel environment, and release is activated by an external stimulus (Gangurde et al., 2025; Lem, Gangurde, et al., 2024).

In addition to the implant systems, the liposomal hydrogel systems are explored in wound healing due to their hydrating, mechanically supportive nature of the hydrogel with drug loading capacity of the liposomes (Grijalvo et al., 2016; Palácio et al., 2025). A rapidly growing subset of this field uses light-activated liposomal hydrogel systems to add external, clinically controlled timing either via ROS pathways or photothermal heating, which is attractive for infected or hard-to-heal wounds (Liu et al., 2020; Moorcroft et al., 2020; Xing et al., 2024). It is well documented in the literature that red light irradiation can accelerate wound healing by promoting angiogenesis, cell proliferation and migration, and collagen synthesis in the affected area (F. Deng et al., 2024). Xing et al. developed a photocured, biodegradable liposome encapsulating tetrahydrocurcumin and hepatocyte growth factor, which was loaded into a gelatin methacrylate hydrogel for anti-inflammatory, scarless wound healing. Drug-loaded liposomes were cross-linked with hydrogel via UV photo cross-linking to form a photocurable hydrogel. The synergistic effect of active molecules in addition to light exposure helps in ROS scavenging, inflammation reduction, scarring inhibition, and promotion of angiogenesis together leading to effective wound healing (D. Xing et al., 2024). There are some mechanistic implications that need to be considered to achieve effective on demand controlled release such as minimum passive leakage: amount of the encapsulated dose (due to low encapsulation efficiency of the liposomes, depth penetration of stimuli (depending on the application area the intensity of stimuli might affect the stimuli signal), stimuli signal loss due to diffraction and absorption of the light stimuli in the hydrogel.

Much more research is needed to evaluate how liposomal hydrogel systems can be translated from laboratory research to industrial development. Key considerations include controlling liposome leakage, ensuring formulation and storage stability, assessing cytotoxicity, establishing robust sterilization strategies, achieving batch-to-batch consistency, and developing scalable manufacturing workflows. Although liposomal hydrogel systems have shown clear promise in both in vitro and in vivo studies, they have not yet progressed into clinical trials. This limited clinical translation is often attributed to stability challenges, practical constraints such as the need for implantation, and high production costs. Collectively, these factors may continue to hinder broader clinical adoption and large-scale manufacturing of liposomal hydrogel systems.

2.6 On-demand biocatalysis of cellulose hydrogel with encapsulated enzymes

Despite their exceptional biocompatibility and water-rich environment, aCNF hydrogels are reported not to degrade in the human body or under standard in vivo culture conditions due to the lack of the necessary enzymes for degradation. In tissue engineering and local drug delivery, this is crucial because a non-degradable hydrogel can obstruct cell infiltration and necessitate surgical removal after therapeutic release is complete. In this context, controlled enzymatic degradation of the hydrogel presents a practical way to remove hydrogel scaffolds without interfering with mammalian biochemical pathways (Bastard et al., 2025).

From a mechanistic standpoint, “biocatalysis” here refers to enzymatic hydrolysis of β(1→4) glycosidic bonds within cellulose nanofibrils, which converts the fibrillar network into shorter fragments and soluble sugars, progressively weakening the hydrogel network and increasing porosity. The enzymatic degradation products of cellulose are characterized as non-toxic sugars, in contrast to some synthetic hydrogel degradation chemistries that generate non-native fragments, thereby making this material safer for in vivo applications. Cellulase is a multi-component enzyme complex often sourced from fungi such as *Trichoderma reesei*. containing endoglucanase (EG), exoglucanase or cellobiohydrolase (CBH), and β-glucosidase (BG), which act together to hydrolyze cellulose to cellobiose and glucose. The functional mechanism is that EG introduces internal cuts on easily accessible regions in fibers, CBH processively releases soluble cellobiose from chain ends, and BG relieves product inhibition by converting cellobiose to glucose. (Shi et al., 2023; Srivastava et al., 2018; Xu et al., 2023) Synergy among these activities is a well-established feature of efficient cellulose depolymerization. For CNF hydrogel networks built from high-aspect-ratio fibrils, complete conversion to glucose is not

always required to achieve functional degradation. Even partial chain scission and fibril fragmentation can be sufficient to collapse the hydrogel network, reduce viscosity, and form macro pores, which is often the practical goal in scaffolds and depots.

Bastard et al. developed cellulase enzyme-loaded casein microparticles to degrade nanocellulose hydrogels over 21 days, thereby supporting 3D cell growth. The casein macroparticle provided large pores to encapsulate the cellulase molecules while delaying the controlled degradation of the cellulose films by slowly releasing the active enzymes for over 21 days, eventually generating more space for cell proliferation and increasing the cell growth (Bastard et al., 2025). In a second, conceptually related application, cellulase-encapsulated chitosan–caseinate nanoparticles are incorporated as nanocarriers into 3D-printed chitosan hydrogel scaffolds filled with cellulose nanofibers for in vitro tissue engineering. The encapsulation of enzymes in nanoparticles preserved enzyme activity as compared to free enzymes, while sustaining their release up to 14 days, which contributes to a higher amount of the enzyme available for cellulose biodegradation for longer application times (Tamo et al., 2022). Taken together, these studies position cellulase not only as a degrading agent but as a process-enabling trigger that converts an otherwise stable nanocellulose network into a dynamic, tunable biomaterial. Liposomes offer a more flexible option for encapsulating cellulase enzymes, as they are smaller and more compositionally tunable than microparticles. They can be engineered for triggered release to modulate the on-demand release and have been well studied for preserving protein function (Chaize et al., 2004; Colletier et al., 2002). As a result, liposome-encapsulated cellulases represent a strategy for localized, slowed, or on-demand biocatalysis of nanocellulose depots into dynamically remodelable biomaterials, when and where the application requires it. This is explained in more detail in the results and discussion section of this thesis.

3 Aims of the study

The aim of this study was to develop and optimize robust light-responsive liposomes that enable cargo release upon light exposure. Further, we combine these liposomes with nanocellulose hydrogel, forming a liposomal hydrogel nanodepot system for spatiotemporal release of the cargo molecule. We also studied the release of cellulase enzymes, proving on-demand biocatalysis of cellulose-based hydrogels upon light activation.

The specific aims were:

1. **Develop the thermoresponsive and ROS-sensitive light-activated liposomes for on-demand drug delivery.** (I, II, III)
   To formulate thermosensitive, ROS-sensitive light-activated liposomes with optimized lipid membrane composition and photosensitizers, high stability at physiological temperature, and rapid triggered release upon light activation. Different aspects of preparing liposomes with minimum passive leakage and optimum surface charge while facilitating cargo release after exposure to light were studied. To study and visualize real-time degradation kinetics of the ROS- sensitive lipid film using HS-AFM.

2. **Studying the on-demand release of the cargo molecules from the liposomal hydrogel nanodepot system.** (II, III)
   To develop a nanodepot system by immobilizing liposomes in the nanocellulose hydrogel matrices, facilitating long-term retention and controlled release after light activation. Liposome and nanocellulose interactions and mobility were also quantified to evaluate the stability of the system.

3. **Demonstrate on-demand biocatalysis of cellulose-based hydrogels using cellulase enzymes encapsulated in ROS-sensitive liposomes**. (III)
   To encapsulate cellulase enzyme in light-responsive liposomes to facilitate the degradation of cellulose hydrogel while maintaining its activity. The factors affecting cellulase enzyme activity were studied carefully to finalize the protocol for liposome preparation to preserve enzyme activity.

4 Materials and methods

4.1 Preparation of Light-Activated Liposomes (I, II, III)

Light-activated liposomes were prepared using the thin-film hydration method. Lipids were first dissolved in chloroform to prepare stock solutions. The required volumes of each lipid stock, according to the compositions in Table 3, were pipetted into a glass tube. Chloroform was removed using a vacuum rotary evaporator in a 63 °C water bath for 1 h to form a thin lipid film.

Table 3 List of liposome compositions

	Lipid composition	Lipid molar ratio	Hydration solution and photosensitizer	Publication
1.	DPPC:DSPC:DOTAP: Lyso-PC: DSPE	75:5:10:10:4	Calcein (60mM, 280 mOsm, pH 7.4) and 0.62 mg/mL ICG in HEPES buffer	I
2.	DPPC:DSPC:DOTAP: Lyso-PC:DSPE-PEG 2000	75:5:10:10:4	Calcein (60mM, 280 mOsm, pH 7.4) and 0.62 mg/mL ICG in HEPES buffer	I
3.	DPPC:DSPC:DOTAP: Cholesterol: DSPE-PEG 2000	75:15:10:10:4	Calcein (60mM, 280 mOsm, pH 7.4) and 0.62 mg/mL ICG in HEPES buffer	I
4.	DPPC:DSPC:DPTAP: Lyso-PC:DSPE-PEG 2000	75:15:10:10:4	Calcein (60mM, 280 mOsm, pH 7.4) and 0.62 mg/mL ICG in HEPES buffer	I, II
5.	DPPC: DSPC: Lyso-PC: DSPE-PEG 2000	75:15:10:4	Calcein (60mM, 280 mOsm, pH 7.4) and 0.62 mg/mL ICG in HEPES buffer	I, II
6.	DOPC:Cholesterol: DPPC:DSPE-PEG 2000	50:25: 20:5 (60mM)	Cellulase enzyme (5 mg/mL) and ZnPC II was dissolved in chloroform and added during thin film preparation (0.3 mg/mL)	III

The film was then hydrated with the required components for the formulation listed in Table 3, using a heated water bath at either 63 °C or 48 °C, depending on the formulation. During hydration, the lipid solution was mixed every 10 min until the lipid film had fully disappeared. The resulting liposome suspension was extruded 11 times through polycarbonate membranes (100 nm or 800 nm) using a mini extruder (Avanti Polar Lipids, Inc., Alabaster, USA). Samples were then rapidly cooled and stored at 2-8 °C. Unencapsulated molecules were removed by size-exclusion chromatography (SEC) using Sephadex® G-50.

For cellulase-encapsulated liposomes, the lipid film was hydrated at 48 °C, followed by 10 freeze–thaw cycles. The suspension was then extruded through an 800 nm filter at the same temperature as hydration and purified using µPulse® Tangential flow filtration (TFF).

4.2 Preparation of liposomal hydrogel system

To prepare the liposomal hydrogel system, the required amounts of hydrogels and liposomes (Table 4) were mixed to form a homogeneous mixture.

Table 4 List of liposomal hydrogel systems

Liposomal hydrogel system	Composition	Publication
aCNF hydrogel with Calcein loaded liposomes	For 1 g, 260 µL of liposome solution was mixed with 740 mg of 2.7% aCNF to achieve final concentration of 2% w/w using syringe mixing method.	II
aCNF hydrogel with cellulase enzyme loaded liposomes	For 200 mg of 1% w/w aCNF liposomal hydrogel, 86.6 mg of 2.3% w/w stock aCNF was mixed with 113.4 µL of purified cellulase liposomes using Gilson capillary piston tips.	III
Interpenetrating polymer network (IPN) hydrogels with cellulase enzyme loaded liposomes	For 200 mg of a 0.4% w/w IPN liposomal hydrogel, 134 mg of a 0.6% w/w stock IPN hydrogel (composed of 0.3% w/w MLG and 0.3% w/w aCNF) was mixed with 66 µL of cellulase liposomes using Gilson capillary piston tips.	III

4.3 Characterization of Liposomes

The hydrodynamic diameter of the liposomes was measured with a dynamic light scattering (DLS) automated plate sampler (Zetasizer APS, Malvern Instruments, Malvern, United Kingdom). The size distributions were reported by polydispersity index (PdI). Zeta potential was determined using a Zetasizer ZS (Malvern Instruments, Malvern, United Kingdom) using a DTS1070 Zetasizer measurement cell. For both size and zeta measurements, 10 µL of sample was diluted 1000 times with 20 mM and 10 mM HEPES buffers, respectively.

Differential Scanning Calorimetry: 20 µL of the unpurified liposome sample was pipetted onto aluminium pan and sealed with aluminium lid. The sample and reference pan, each containing the same amount of water, were heated under a nitrogen atmosphere using a linear temperature gradient from 25 to 80 °C. The phase transitions were detected as negative, endothermic peaks in the baseline-corrected thermograms after analysis using TRIOS software.

4.4 Stability of liposomes and liposomal hydrogel systems (I, II)

Temperature-induced calcein release from liposomes: The temperature-induced release of calcein from liposomes was studied using the self-quenching behavior of calcein. The calcein release was measured over a temperature range of 33–55 °C. Initially, 490 µL of HEPES buffer was heated to the desired temperature in an Eppendorf ThermoMixer (Eppendorf AG, Hamburg, Germany). Once the target temperature was achieved, 10 µL of the purified liposome solution was added to the prewarmed buffer, and the mixture was mixed for 10 min at 300 rpm using an Eppendorf ThermoMixer (Eppendorf AG, Hamburg, Germany). The sample was then quickly cooled in an ice bath. The cold control sample was prepared by mixing 490 µL of buffer and 10 µL of liposomes which was kept in the refrigerator (2–8 °C) until the measurement. 100 µL of each sample was pipetted into a black 96-well plate with an opaque bottom to measure calcein fluorescence (excitation 493 nm, emission 518 nm) using a Varioskan LUX (Thermo Fisher Scientific Inc., Waltham). The calcein release was expressed as a percentage using equation 1

$$\mathrm{CR} = \frac{(F - F0)}{(F100 - F0)} X100 \qquad (1)$$

Temperature-Induced Calcein Release from liposomal hydrogel system:
1 g of 2% w/w liposomal hydrogels prepared as described in Table 4 was placed in a 24-well plate. The hydrogel surface was smoothed, and the plate was placed in the fridge for 3-4 h to settle. To study the temperature-induced cargo release, the plate containing LHS was heated to 50 °C using a ThermoMixer (Eppendorf AG, Hamburg, Germany) for 20 min. After heating, 1 mL of HEPES buffer was added to each well, and the plate was transferred to a 37 °C incubator. 100 µL samples were collected into a black 96-well plate with an opaque bottom at predetermined time points, and the same volume of fresh buffer was added after each sampling. The fluorescence of calcein in the samples was measured using Varioskan LUX, and the percentage release was calculated using equation 1.

Stability of liposomal hydrogel system: Liposomal hydrogel samples (1 g, 2% w/w) were placed in a 24-well plate, and the surface of the hydrogel was smoothed with a spatula. After this, the well plate was kept in the fridge to allow the hydrogel to settle well for 3–4 h. The well plate was brought to room temperature before adding HEPES buffer on top of each hydrogel (1 mL). Afterward, the well plate was kept in an incubator at 37 °C under shaking at 300 rpm for 90 days. 100 µL of samples were collected in an opaque-bottom black 96-well plate at predetermined time intervals,

and the same volume was replaced with fresh buffer after each sampling. The fluorescence of the samples (excitation 493 nm, emission 518 nm) was measured using Varioskan LUX (Thermo Fisher Scientific Inc., Waltham, MA, USA) before and after adding 10% Triton-X 100 solution.

4.5 Light-activated release from liposomes and liposomal hydrogel systems (I, II, III)

Light-activated release from liposomes: Calcein release from liposomes after light activation was studied using the ML8500 Modulight instrument (ML8500, Modulight Inc., Tampere, Finland). The liposomes were diluted 1:10 (v/v) with HEPES buffer in a clear-bottom, black 96-well plate (Thermo Fisher Scientific Inc., Waltham, MA) and incubated at 37 °C. After a 10 min incubation period, the sample was exposed to an 808 nm laser for 5–120 s with an intensity of 1 W/cm^2. The control sample on the same plate was protected from light exposure. After laser irradiation, the plate was immediately cooled in an ice bath. Then, the calcein fluorescence (excitation 493 nm, emission 518 nm) was measured with a Varioskan LUX, and % calcein release was calculated by using equation 1.

Light- Activated Release from liposomal hydrogel system: For light activation, a 24-well plate filled with 1 g of 2% w/w liposomal hydrogel was exposed to 1 W/cm^2 808 nm light for 80 s using an automatic biomedical illumination instrument (ML8500, Modulight Inc., Tampere, Finland). Following light exposure, 1 mL of HEPES buffer was pipetted onto the liposomal hydrogel, and the plate was transferred to the incubator to monitor calcein release over time after light activation. A control sample was not exposed to any conditions and was also transferred to the incubator after adding 1 mL of buffer on top of the hydrogel. 100 µL samples were collected at predetermined time points in a black opaque 96-well plate. The extracted volume was replaced with fresh buffer after each sampling. The fluorescence of the calcein was measured using Varioskan LUX (Thermo Fisher Scientific Inc., Waltham, MA, USA). Calcein release was expressed as a percentage using equation 1.

Influence of thickness: To study the effect of hydrogel thickness on light-activated release, two setups were prepared in 24-well plates with liposomal hydrogel systems of 0.2 cm and 0.5 cm thickness. Liposome concentration was kept the same in both systems. The well plates were exposed to the same light intensity (1 W/cm^2) and dose (80 J/cm^2). After light exposure, 1 mL of HEPES buffer was pipetted into each well, and the plate was transferred to the incubator to evaluate calcein release over time following light activation. The collected samples were analyzed as mentioned in light-activated release from LHS.

Influence of dose of light: The liposomal hydrogel system was exposed to three different doses of light, 20, 40, and 80 J/cm², respectively, while keeping the light intensity constant (1 W/cm²). Sample preparation, collection, and analysis were otherwise the same as those described in the light-activated release from LHS.

4.6 Degradation of liposomal hydrogel system after enzyme release upon light-activation

Preparation of cellulase enzyme encapsulated liposomes: Liposomes protect fragile enzymes from inactivation, shield them from premature interactions with the surrounding matrix, and release them on demand in response to external stimuli. Reliable enzyme activity after release is critically dependent on liposome preparation parameters. Therefore, we first optimized liposomal encapsulation of cellulase by investigating factors such as freeze-thaw cycles, sonication, lipid concentration, processing temperature, and light intensity. Our goal was to maximize encapsulation efficiency while preserving enzymatic activity after encapsulation and illumination. Figure 7 illustrates the optimized steps for preparing cellulase liposomes and the protocol used to study the degradation of LHS after cellulase release upon light activation.

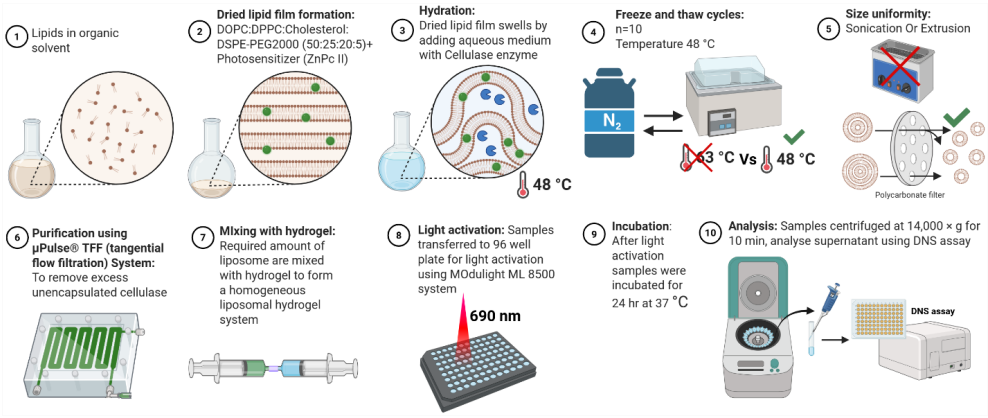

Figure 7 Illustrating the process of cellulase encapsulating liposome and liposomal hydrogel preparation and analysis. To preserve cellulase activity during liposome preparation, the protocol was modified by changing the liposome composition (DSPC replaced by DPPC), lowering the hydration temperature from 63 to 48 °C, and replacing the sonication step with extrusion. Created with Biorender.com

Reducing sugar assay: The amount of sugar in hydrogels after degradation, after light-activated release of cellulases, was measured using 3,5-dinitrosalicylic acid (DNS) reducing assay (Ribeiro et al., 2010). For calibration, a standard curve was generated using D-glucose solutions (0–20 mg/mL) prepared from a stock D-glucose solution (Merck). Following light activation, aCNF and IPN liposomal hydrogel samples were incubated for 24 h at 37 °C and then centrifuged at 14,000 × g for 10 min to separate the supernatant from the undigested cellulose mass. An aliquot of 2 µL supernatant collected from the reaction was mixed with 171 µL DNS reagent (sample:DNS = 1:20) in a transparent 96-well plate. The plate was incubated at 100 °C for 10 min, and the absorbance was measured at 580 nm using a microplate reader. The quantity of reducing sugars was calculated using the equation obtained from the standard curve and the percentage of relative amount of reducing sugar generated upon light-activated release of cellulase enzyme was quantified by using equation 2

$$\text{Relative amount of reducing sugars (\%)} = \frac{RS\ Sample - RS\ NC}{RS\ PC - RS\ NC} X100 \quad \text{.....(2)}$$

Where RS Sample, is reducing sugars detected in sample, RS NC, is reducing sugars detected in negative control sample containing hydrogel with buffer and RS PC, is reducing sugars detected in positive control sample containing hydrogel and cellulase enzyme.

4.7 High Speed-Atomic Force Microscopy

Sample preparation: ROS-sensitive liposomes without a photosensitizer and the cellulase enzyme were prepared with the composition shown in Table 2 (6). The liposomes were diluted to a lipid concentration of 0.1 mg/mL in milliQ water, then subjected to tip sonication (NR-50M, Microtech, Japan) for 5 s to break the liposomes. 2 mM MgCl2 was added to the sample before pipetting onto the mica sample stage to improve attachment of the lipid film.

HS-AFM imaging: HS-AFM images were recorded using a laboratory-built system in tapping mode (Ando et al., 2001; Uchihashi & Ganser, 2020). HS-AFM cantilevers (AppNano, BioLever- Silicon Nitride Cantilever, Cantilever length- 10 µm, Width- 2 µm) with a spring constant typically between 0.1 N m^{-1} and 0.2 N m^{-1}, and a resonance frequency of approximately ~0.5 MHz in solution was used. At the very end of the cantilever, a carbon tip was manufactured by electron-beam deposition using a dedicated FE-SEM instrument, with a typical length of 100-300 nm. These tips were etched using argon plasma to achieve a tip radius of <5 nm.
Immediately before HS-AFM imaging, 2 µL of the sonicated liposome sample was pipetted onto a freshly cleaved mica and incubated at room temperature for 10 min

under a humid hood. After incubation, the sample surface was thoroughly rinsed with ultrapure water and immersed in a well filled with 80 µL of milliQ water and imaged using Igor Pro 9 application. After imaging the lipid bilayer (a lipid raft with 3-6 nm in height), 10 µL of 0.3% hydrogen peroxide (H_2O_2) was added to the chambers in two separate additions (final H_2O_2 concentration 0.03% after 1st addition and 0.06% after 2nd addition) while imaging, causing disturbance to the images. The scanning speed was 300 ms/frame. The images were analyzed using a custom-made tool based on pyNuD v1.5.0 (E. H.-L. Chen et al., 2023).

4.8 Other characterizations

Method	Purpose	Publication
Surface plasmon resonance (SPR)	Surface interactions between liposomes and aCNF hydrogel	II
Fluorescence recovery after photobleaching (FRAP)	To study the movement of liposomes inside the liposomal hydrogel system	II, III
Scanning electron microscopy (SEM)	To view and study the surface of cellulose-based hydrogels (aCNF and IPN) before and after cellulase enzyme interaction	III
Sewlling ratio	To evaluate the swelling of the aCNF hydrogel in buffer.	II
Confocal laser microscopy	To study the distribution of liposomes in cellulose-based hydrogel matrix	II, III

5 Results and Discussion

5.1 Release from light-activated liposomes (I)

While developing thermosensitive light-activated liposomes, optimization is done at three stages: composition, stability, and responsiveness to stimuli. The key factors to consider are that the formulation must remain stable at body temperature while rapidly switching to a high-permeability state upon light activation, releasing the cargo molecule, with a reproducible release profile across batches. The key variables to observe when designing such a system are the thermal response window of the membrane and light activation. The thermal response window depends on the types of lipids used (saturated and unsaturated), which determine bilayer packing, stability, and transition temperature. Additives used to stabilize the bilayer can further shift this transition and, in turn, influence both baseline leakage and triggered release. Light activation, on the other hand, depends on the photosensitizer's concentration, type, and placement within the bilayer. These factors control how efficiently light is converted into heat or ROS and therefore directly determine the strength and reliability of the light-triggered response.

To develop a light-responsive liposomal hydrogel system for on-demand delivery, the first step was to prepare cationic light-activated thermosensitive liposomes (CLTSL) and to assess their stability at physiological temperatures and cargo release upon light activation. These liposomes were then incorporated into an anionic CNF hydrogel to obtain the final light-activated liposomal hydrogel platform. Many more formulations were tested than are presented in the following section. But to keep this discussion short, the focus is on a few key formulations and what was learned from them. The performance of the developed formulations was compared with standard anionic light-activated thermosensitive liposomes (ALTSL). The optimized formulation showed the desired combined heat- and light-triggered release profile (Figure 8, green).

To prepare cationic liposomes, we needed a positively charged lipids. DOTAP is one of the most commonly used cationic lipids for producing positively charged liposomes, especially in gene delivery applications (T. Wang et al., 2024). Therefore, DOTAP was first selected as the cationic lipid in a formulation with DPPC as the primary thermosensitive lipid, along with DSPC and DSPE. However, this initial lipid composition was not suitable for our purposes because green aggregates formed immediately upon hydration of the lipid film. According to literature, ICG is an amphiphilic molecule, and its stability within the bilayer is enhanced in the presence of a PEGylated lipid. We therefore suspected that, in the

absence of PEG, unfavorable interactions between the lipids and ICG contributed to aggregation (Lajunen et al., 2016). To address this, a second formulation with the same lipid composition was prepared by replacing DSPE with DSPE-PEG2000. This modification markedly improved the physical stability of the system. The resulting liposomes showed a size of ~103 nm and a PDI of 0.036, indicating successful liposome formation. The improved stability suggests that the PEG chains played an important role in stabilizing ICG and preventing aggregation. Although these PEGylated DOTAP-containing liposomes were physically stable after preparation, their release behavior was not suitable. The formulation $CLTSL_{DOTAP}$ was very leaky, showing substantial calcein release already at low temperatures. In the temperature-triggered release study, around 60% release was observed at 35 °C, and the release increased sharply with further heating, approaching full release by 40 °C (Figure 8A, gray), indicating that the formulation was not stable at physiological temperatures. The DSC data further supported this observation. The onset of phase transition was approximately 32 °C, which explains the early release seen below body temperature. Since DOTAP has a relatively low transition temperature, its incorporation likely reduced the overall phase transition temperature of the membrane, thereby promoting premature leakage (Danaei et al., 2018). A similar trend was observed in the light-triggered release experiment (Figure 8B, gray), where the formulation displayed a high level of release already at the earliest measured time points. Together, these results demonstrated that $CLTSL_{DOTAP}$ was too unstable for our applications.

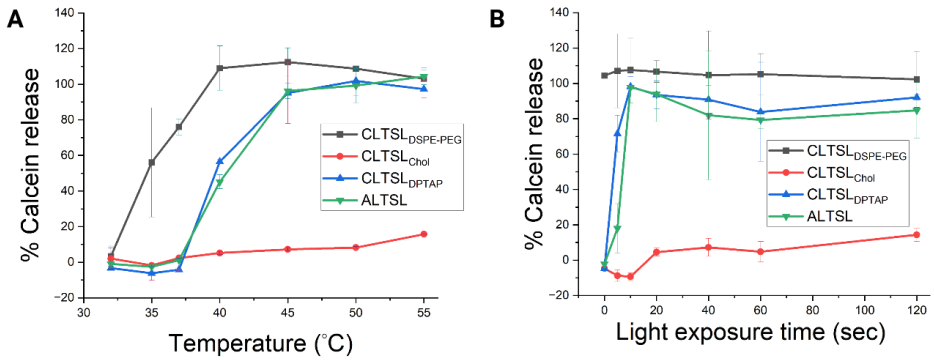

Figure 8 **A.** Temperature and **B.** Light (808nm 1 W/cm²) activated calcein release from cationic (CLTSL) and anionic (ALTSL) light activated thermosensitive liposomes. Error bars indicate the standard deviations (n = 3). Reprinted from (Gangurde et al., 2023), with permission from the American Chemical Society.

To improve membrane stability, 10 mol% cholesterol was introduced into the DOTAP-containing formulation. Cholesterol is known to reduce membrane fluidity and enhance bilayer stability by increasing lipid packing (de Meyer & Smit, 2009;

Redondo-Morata et al., 2012). As expected, the addition of cholesterol improved retention of the encapsulated cargo (Figure 8A, red). However, this increased stability came at the expense of responsiveness to triggers. The formulation $CLTSL_{chol}$ showed minimal calcein release in both the temperature- and light-triggered release studies (Figure 8A and B, red). Even under elevated temperature or light exposure, the release remained very low. These results indicate that cholesterol made the membrane too rigid, thereby suppressing the desired stimulus-responsive release.

To resolve this trade-off between stability and responsiveness, DOTAP was replaced with DPTAP. In contrast to DOTAP, DPTAP is a saturated cationic lipid with C16 acyl chains, which can promote tighter packing within the bilayer and reduce passive leakage. The resulting formulation, $CLTSL_{DPTAP}$, showed a higher T_m of 41 °C in the DSC analysis, indicating improved membrane stability compared with the DOTAP containing formulation. As shown in Figure 8A (blue), very little calcein release was observed at 32, 35, and 37 °C, indicating that the formulation remained stable at and near physiological temperatures. At 40 °C, the release increased markedly, and by 45 °C it reached nearly complete release. This profile confirms that $CLTSL_{DPTAP}$ retained strong thermosensitivity, while remaining stable under physiologically relevant conditions. A similar trend was observed in the light-triggered release experiment (Figure 8B, blue). Upon irradiation, calcein release increased rapidly within the first few seconds of light exposure and remained stable in the absence of light. These results show that $CLTSL_{DPTAP}$ achieved the most favorable balance between stability and triggered release. Compared with $CLTSL_{DOTAP}$, it was substantially more stable, and compared with $CLTSL_{chol}$, it retained clear responsiveness to both heat and light (Figure 9). Based on these results, $CLTSL_{DPTAP}$ was selected as the most suitable formulation for further incorporation into the aCNF hydrogel system.

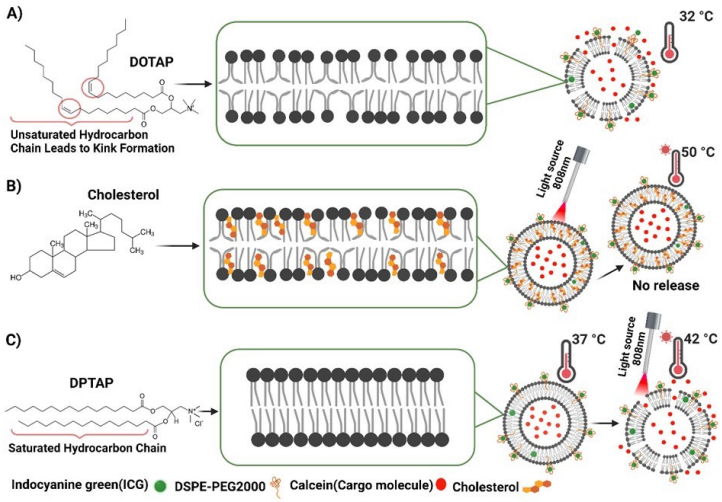

Figure 9 Schematic Illustration of lipid bilayers and their release profile based on light activation. **A.** Fluid lipid bilayer with unsaturated lipid (DOTAP), **B.** Lipid bilayer with cholesterol, **C.** Ordered lipid bilayer with saturated lipid (DPTAP). Reprinted from (Gangurde et al., 2023), with permission from American Chemical Society.

5.2 Characterization of liposomal hydrogel system (II)

5.2.1 Surface interactions between liposomes and aCNF hydrogel

As an idea to create a liposomal hydrogel system for drug delivery applications, we mixed cationic liposomes with anionic CNF hydrogel, where both electrostatic interactions, along with a 3D fibrous network of the hydrogel, hold the liposome, acting as a reservoir carrying liposomes, so that they can release cargo molecules when exposed to light. The ideal system is the one that retains liposomes for a long period with minimal passive leakage from the hydrogel. According to previous research by Auvinen et al., three main factors can directly affect liposome leakage: liposome size, liposome surface charge, and hydrogel concentration. Auvinen et al studied how the properties of the nanoparticles, such as size, shape, and charge, affect their release from aCNF hydrogels. The fiber content of the hydrogel plays an important role in release. At low concentration (1% w/w), small liposomes were released faster than large liposomes, whereas at 2% w/w concentration, only small liposomes were released, with a 3D fiber network preventing the release of large liposomes. On the other hand, liposomes with positive charge were found to show nearly zero release despite small size in both hydrogel concentrations. This can only be explained by the strong binding of the liposomes to the nanocellulose network, most likely due to electrostatic interactions (Auvinen et al., 2022; Paukkonen et al.,

2017). Owing to these results, we carefully selected an appropriate hydrogel concentration, size, and liposome surface charge.

Surface plasmon resonance technique was used to evaluate how liposomes interact with aCNF surface. With the help of SPR sonogram, we compared the interaction of cationic (73±6 nm) and anionic liposomes (112±2 nm) with aCNF hydrogel (2% w/w). The findings showed a high affinity between cationic liposomes and aCNF, giving a strong signal (Figure 10A, black), while anionic liposomes displayed minimal interaction with aCNF (Figure 10A, red). Non-covalent interactions, such as hydrogen bonds and electrostatic interactions, are the main driving forces in the interactions of biomolecules with carbohydrates (Malik et al., 2019). The cationic and anionic liposomes used in this study have exactly the same composition except for the presence/absence of cationic lipid DPTAP, resulting in surface charges of + 14±0.7 and - 22.5 ± 0.58 mV, respectively. The interaction of these liposomes with aCNF with a surface charge of around -39 mV can be attributed to the strong electrostatic interaction of positively charged lipid DPTAP with negatively charged CNF.

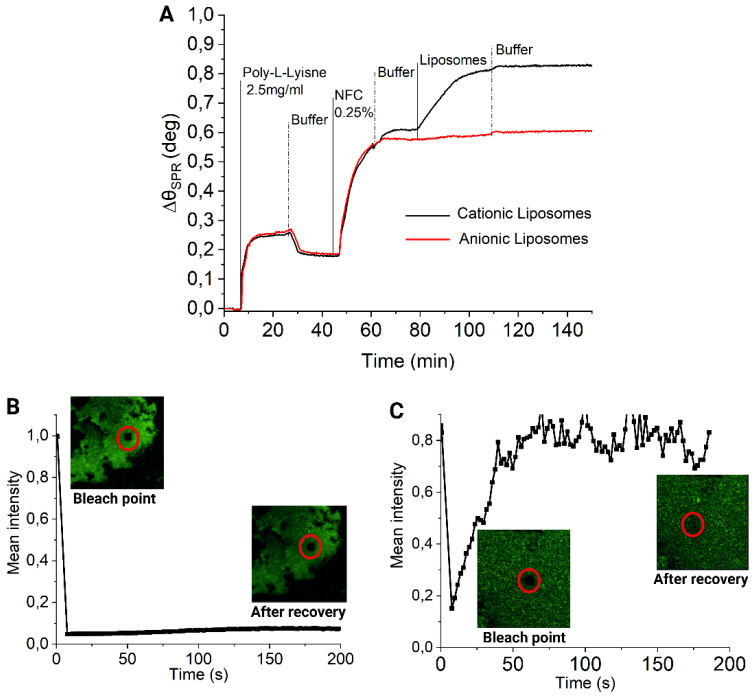

Figure 10 **A**. SPR sensogram of cationic and anionic liposome interaction with aCNF cellulose nanofiber film, **B and C**: FRAP analysis of aCNF hydrogel interaction with cationic liposomes. **B.** Showing low fluorescent recovery after photobleaching in dense areas of aCNF, **C.** Showing almost complete recovery after photobleaching in less dense areas of hydrogel. Reprinted from (Gangurde et al., 2025), with permission from Elsevier.

We observed the liposome hydrogel system under confocal microscopy and performed Z-stack imaging to evaluate liposome distribution within the aCNF hydrogel. Surprisingly, we found that the liposomes are not homogeneously distributed in the hydrogel; they tend to concentrate in the denser fibrillar network, while a smaller amount is found in the looser network. This is due to the heterogeneous nature of the nanocellulose hydrogel, which contains a mixed fibrillar network that forms both loose and dense networks. This was further confirmed by fluorescence recovery after photobleaching (FRAP) testing, in which we labeled the cationic liposomes with the fluorescent NBD lipid and tracked their movement/recovery in random areas within the liposomal hydrogel system. The FRAP measurement in some areas showed complete recovery of the liposomes in the bleached spots within few minutes (Figure 10C), representing higher mobility of the liposomes and suggesting a less dense hydrogel network area. In contrast, some areas showed almost no recovery, close to zero, even after 10 min of measurement, reflecting limited movement of the liposomes due to trapping within the denser hydrogel network (Figure 10B). These results suggest that the liposomal hydrogel system is structurally non-uniform. This is likely caused by an uneven distribution of nanocellulose fibers throughout the hydrogel. In regions where the nanocellulose network is denser, liposomes appear to become more strongly trapped, which limits their mobility.

5.2.2 Stability of liposomal hydrogel system

The practical use of the liposomal hydrogel system in long-term implantable applications depends on two main factors: the stability of the liposomes, which we discussed at the start of this section, and how well the hydrogel can encapsulate the liposomes over the long term. The passive release behavior of the liposomal hydrogel system was evaluated by monitoring the release of cationic liposomes into the surrounding buffer over 90 days at 37 °C, without light activation, in order to assess the long-term stability of the depot system. To examine the effect of liposome surface charge on hydrogel retention, the release of cationic and anionic liposomes from 2% w/w aCNF was compared (Figure 11A).

Liposome release was quantified using calcein fluorescence, based on the increase in fluorescence observed after liposome disruption and dilution of calcein in the buffer. The release profiles showed a clear charge-dependent difference: cationic liposomes showed very slow passive release, remaining below 5% during the first 20 days and reaching only about 7% after 90 days (Figure 11A, open square), whereas anionic liposomes showed a rapid initial burst release of nearly 20% within 20 days, followed by a steady increase to about 40% by day 90 (Figure 11A, open circle). These results indicate that cationic liposomes were retained much more

effectively within the aCNF hydrogel, most likely due to favorable electrostatic interactions, while anionic liposomes were released more readily because of electrostatic repulsion. Although FRAP and confocal imaging suggested a non-uniform distribution of cationic liposomes within the hydrogel, this did not substantially affect their overall passive release profile. Thompson et al. studied the release of saturated and unsaturated liposomes from agar hydrogel and found that the liposomes made from saturated lipids are more sturdy and do not move out of the hydrogel, while the liposomes made from unsaturated lipids were flexible and could squeeze through the loose networks in the hydrogel (Thompson et al., 2020). The small, gradual leakage observed for cationic liposomes may be related to liposomes located in the less dense upper regions of the hydrogel, where trapping is weaker and release into the buffer is easier. Overall, these findings show that surface charge strongly influences liposome retention and release behavior, and that cationic liposomes form a more stable depot system suitable for on-demand drug delivery applications.

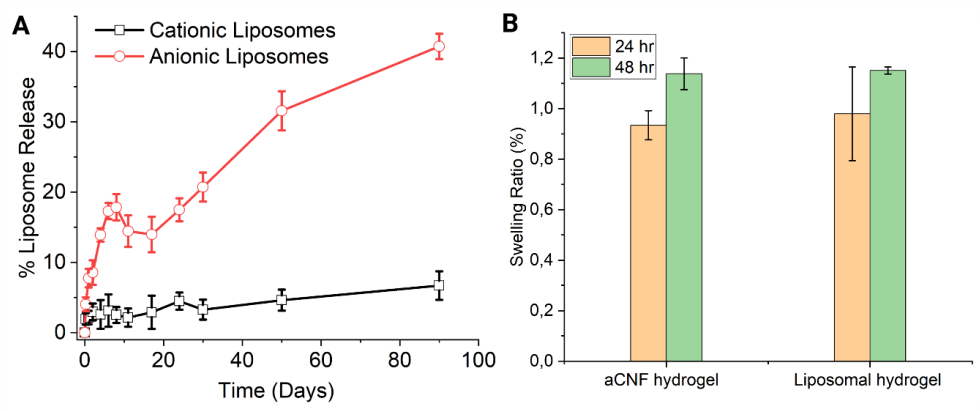

Figure 11 **A**. Passive release of liposome from liposomal hydrogel system over 90 days at 37 °C, **B**. Swelling ratio of aCNF and hydrogel liposomal hydrogel system with 2 % w/w solid content. Reprinted from (Gangurde et al., 2025), with permission from Elsevier.

The swelling of hydrogel is crucial to the stability of liposome containing hydrogel systems, acting as a mediator that affects both structural integrity and premature drug release. To evaluate the overall stability of the system, the swelling ratio was measured gravimetrically by comparing the weight of the hydrogel before and after swelling. As shown in Figure 11B, both the aCNF hydrogel and the liposomal hydrogel system showed very low swelling over 48 h. The liposomal hydrogel showed swelling ratios of approximately 1.0 after 24 h and 1.15 after 48 h, while the pure aCNF hydrogel showed comparable values of about 0.93 and 1.13 at the same time points. Although there was a small increase in swelling over time, the overall swelling remained minimal in both systems. According to the literature, hydrogels

with a swelling ratio below 1.5 are generally considered non-swelling hydrogels (R. Wang et al., 2024), indicating that the liposomal hydrogel remained non-swollen in the buffer used for the release studies. This low swelling supports the passive release results and suggests that the system maintains its structural stability under the tested conditions. Importantly, the similar swelling behavior of the two hydrogels indicates that incorporation of liposomes does not significantly alter the integrity of the aCNF hydrogel.

5.3 Release from liposomal hydrogel system (II)

5.3.1 Heat and light-activated release from LHS

To evaluate whether the developed liposomal hydrogel system is suitable for on-demand release, its response to external stimuli was assessed by monitoring calcein release and comparing unstimulated control samples at 37 °C with samples exposed to either heat (50 °C) or NIR light (808 nm). As shown in Figure 12A (solid square), raising the temperature above the phase transition temperature of the liposomes triggered calcein release, confirming that the embedded thermosensitive liposomes remained responsive even after incorporation into the hydrogel. The release was not immediate but sustained, with about half of the encapsulated calcein being released within the first few hours and approximately 80% released after 24 h. This indicated that the nanocellulose hydrogel acted as a rate-limiting matrix for the diffusion of this small hydrophilic molecule.

A very similar release profile was observed after light activation (Figure 12A, open circle), where samples were irradiated with 808 nm NIR light at 1 W/cm^2 for 80 s while otherwise maintained at 37 °C, demonstrating that ICG-containing liposomes were able to efficiently convert light into heat, raising the membrane temperature above its phase transition and inducing calcein release. However, compared to liposomes dispersed in buffer, which required shorter exposure times to trigger release in earlier studies (Gangurde et al., 2023; Lajunen et al., 2016, 2018), a longer irradiation time was required in the hydrogel system. The hydrogel network likely caused light scattering, reducing light intensity.

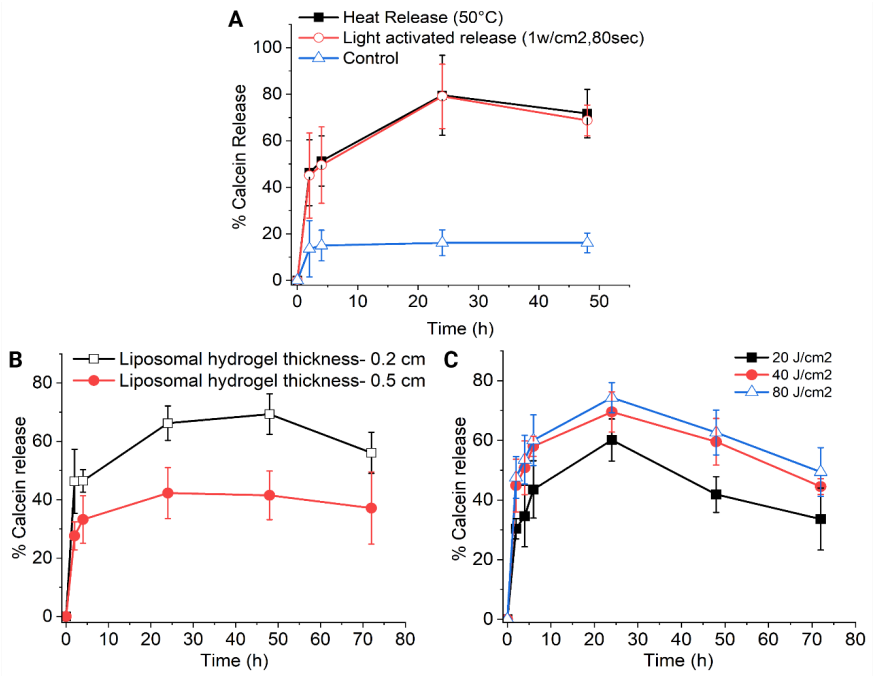

Figure 12 **A**. Heat and light-activated calcein release from liposomal hydrogel samples. **B**. Calcein release after light activation (808 nm, 1 W/cm²) in 0.2 cm (gray) and 0.5 cm (red) liposomal hydrogel thicknesses **C**. Calcein release after exposure to different light doses at (808 nm, 1 W/cm²). Reprinted from (Gangurde et al., 2025), with permission from Elsevier.

Infrared thermal imaging showed that the aCNF hydrogel containing ICG-loaded liposomes reached about 50.6 °C after 80 s of irradiation, whereas the hydrogel without ICG liposomes increased only to about 38.2 °C, confirming that the photothermal effect originated from liposomal ICG and that light could effectively penetrate the hydrogel. In contrast, the control sample showed only limited calcein release, remaining at about 14-15% over the measurement period and thus, highlighting the system's stability in the absence of external stimulation (Figure 12A, open triangle). It is worth noting that the release plateaued below complete release, at ~80%, suggesting that the generated heat was not uniformly distributed throughout the hydrogel and not all liposomes were equally exposed to the stimulus, leading us to study additional factors affecting the release from the liposomal hydrogel system.

5.3.2 Factors influencing the release from LHS upon light activation (II)

To examine whether the release can be tuned by the physical dimensions of the depot, the influence of liposomal hydrogel thickness was evaluated under NIR irradiation. LHS of two different thicknesses were prepared using the same liposome concentration, producing hydrogels with thicknesses of 0.2 cm (2 mm) and 0.5 cm (5 mm). Both samples were exposed to the same light activation (808 nm, 1 W/cm^2, 80 s), and calcein release was monitored over time. As shown in Figure 12B, the thinner hydrogel showed clearly higher release than the thicker one throughout the experiment. In detail, the 0.2 cm gel showed rapid release after irradiation, reaching around 60% release, whereas the 0.5 cm gel released only about 40% under the same conditions. This result demonstrates that hydrogel thickness has a strong influence on the efficiency of light-activated release in the liposomal hydrogel system. The lower release observed in the thicker hydrogel is most likely due to loss of light intensity as it travels through the material. Although aCNF contains more than 90% water and water transmits 808 nm NIR light relatively well, the hydrogel is not fully transparent (Yew et al., 2024). In thicker samples, light scattering within the nanocellulose network reduces the effective intensity reaching liposomes located deeper in the hydrogel. This limits photothermal heating and, consequently, reduces the extent of calcein release.

In addition, the liposomes contain ICG in the lipid bilayer, which strongly absorbs NIR light. As light penetrates the liposomal hydrogel, progressive absorption by ICG can further reduce the amount of light penetrating into deeper regions. This interpretation is consistent with the previous findings that ICG concentration strongly affects NIR light absorption (Lajunen et al., 2018). Therefore, not only hydrogel thickness but also the optical properties of the medium and the ICG loading of the liposomes are important factors affecting release via LHS. The concentration (solid content) of the nanocellulose is also likely to contribute to this behavior. At 2% w/w, aCNF is only semi-transparent and somewhat hazy, which can scatter incident light and reduce the energy available for photothermal conversion in the deeper layers of the hydrogel. Previous studies have also shown that the fibrillar structure of CNF plays an important role in light scattering, with smaller fibers causing greater scattering (Jacucci et al., 2021; Toivonen et al., 2018). Even so, the thicker 5 mm gel still showed a calcein release profile, indicating that NIR-triggered release remains feasible even in larger hydrogel depots, although with reduced efficiency.

For light-activated drug delivery applications, understanding the relationship between light dose and release behavior is essential. Since tissue exposure at 808 nm is generally considered safe at intensities below 1 W/cm^2 (Hudson et al., 2013),

this thesis studied the effect of light dose by varying the exposure time while keeping the light intensity constant at 1 W/cm² in liposomal hydrogels of similar thickness (5 mm). Under these conditions, light doses of 20, 40, and 80 J/cm² corresponded to exposure times of 20, 40, and 80 s, respectively. As shown in Figure 12C, increasing the light dose increased calcein release, with the highest release observed at 80 J/cm², reaching about 75% at 24 h, followed by approximately 70% at 40 J/cm² and 60% at 20 J/cm². Notably, even the lowest dose of 20 J/cm² released a significant amount of calcein, indicating that ICG incorporated in the liposomal bilayer absorbs NIR light efficiently even after short exposure.

All three groups showed a similar overall release pattern, with maximum release occurring within the first 24 h, followed by a decrease, thereafter, suggesting that once calcein is released from the liposomes into the hydrogel, the hydrogel matrix further modulates its diffusion over time. The dose-dependent increase in release may also be related to progressive photothermal activation throughout the hydrogel, where longer irradiation allows the effect of light to extend deeper into the system. These findings show that calcein release can be tuned simply by adjusting light exposure time, while also demonstrating that the developed liposomal hydrogel is highly responsive, achieving substantial cargo release with irradiation times as short as 20-80 s, which is considerably shorter than the exposure times commonly used (2-10 min) in many light-triggered drug delivery systems (Y. Xing et al., 2022). Overall, these results show that hydrogel thickness and light dose are important design parameters for modulating light-activated release, while also highlighting a practical limitation of NIR-based activation in thicker materials and, potentially, in deeper-tissue applications.

5.4 On-demand enzymatic degradation of cellulose hydrogels (III)

Despite their exceptional biocompatibility, the limited biodegradability of nanocellulose-based hydrogels in humans under physiological conditions restricts their use in many biomedical applications, including implants for drug delivery, tissue engineering, and wound healing (Ai et al., 2023; Bacakova et al., 2019; Heise et al., 2021). Enzyme-triggered hydrogel degradation represents a promising strategy to overcome this limitation. By introducing exogenous cellulase, β-1,4-glycosidic bonds in cellulose can be cleaved, generating glucose and oligosaccharides as degradation products (Figure 13A). This enzymatic hydrolysis reduces the nanocellulose hydrogel's viscosity and mechanical integrity by converting the cellulosic hydrogel into soluble sugars. The measurement of generated soluble sugars (glucose) provides a direct and quantitative readout of the degradation kinetics of the cellulose hydrogel (Al Talebi et al., 2022). In this thesis,

we encapsulated the cellulase enzyme in liposomes to preserve its activity and presented a proof-of-concept study demonstrating the necessary formulation optimization and light-activation parameters for on-demand, enzyme-mediated degradation of nanocellulose hydrogels (Figure 13A). We used two types of polysaccharide-based hydrogels with different solid contents to demonstrate the effective loss of hydrogel structure due to the degradation of nanocellulose fibers by cellulase enzymes. aCNF hydrogels (2% w/w), similar to those used for the light-activated release, and interpenetrating polymer network (IPN) hydrogel (0.4% w/w) prepared by crosslinking mixed-linkage β-glucan (MLG) with aCNF to form hydrogels were used. In IPN hydrogels, aCNF provides mechanical strength, while MLG polymer mediates crosslinking between aCNF networks, enabling formation of the hydrogel while maintaining its ultra-low solid content. These polysaccharide-based aCNF and IPN hydrogels act as reservoirs for light-sensitive cellulase encapsulating liposomes; the degradation of aCNF and IPN hydrogels was quantified via DNS assay upon light-activated cellulase release.

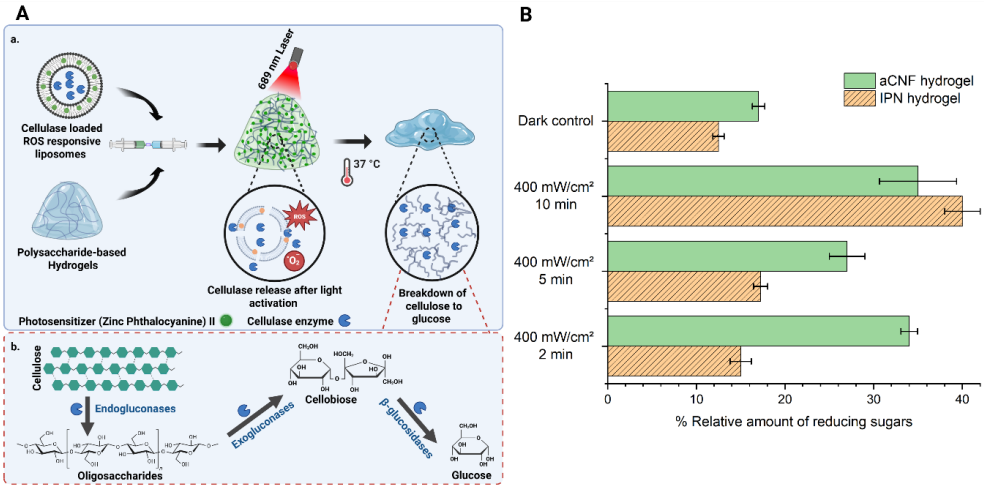

Figure 13 **A**. Schematic illustration of polysaccharide-based hydrogel breakdown after release of cellulase enzymes from liposomes upon light activation. **B**. Relative amount of reducing sugars generated after degradation of polysaccharide-based aCNF and interpenetrating polymer network hydrogels upon light activation.

Optimized cellulase-loaded liposomes were subsequently incorporated into polysaccharide-based aCNF and IPN hydrogels, and the degradation of the hydrogels following light activation was evaluated as a percentage of the relative amount of reducing sugar generated in samples exposed to light (690 nm, 400 mW/cm²) or in dark control, as compared to negative control containing hydrogel and buffer (0%) and positive control containing hydrogel and cellulase enzyme (100%). To obtain a clear picture of the release profile and to study the effect of light

dose (J/cm^2) on cellulase enzyme release, the liposomal hydrogel systems were exposed to different doses of light, 48 (2 min), 120 (5 min), and 240 (10 min) J/cm^2. A clear dependence on light exposure was observed, with longer red-light illumination yielding higher reducing sugar concentrations in both hydrogels. Upon light activation with the highest dose of light, followed by 24 hours of incubation under physiological conditions, enzymatic hydrolysis reached up to 34% for aCNF and 40% for IPN liposomal hydrogels, indicating a light-dose-dependent enzymatic degradation of the cellulose matrix in both hydrogels (Figure 13B).

Interestingly, the non-illuminated (dark control) samples released a moderate amount of reducing sugars, although less than the light-activated samples. Dark control aCNF liposomal hydrogel produced around ~15%, and IPN liposomal hydrogels produced about ~12% of reducing sugars (Figure 13B). This baseline release was slightly higher than expected; there could be two possible reasons for this. One: a small fraction of cellulase leaked from the ROS-sensitive liposomes without photo-triggering (possibly due to minor liposome instability or diffusion). Second, some cellulase enzymes may be adsorbed onto the lipid membrane during liposome preparation without affecting their active sites, so after mixing with hydrogels, the adsorbed enzymes react with the substrate during incubation. However, the reducing sugar output from dark samples remained significantly lower than that of the 10 min illuminated samples in both hydrogel types, confirming that light activation can release the encapsulated enzyme from ROS-sensitive liposomes. Future optimization steps could include formulating ROS-sensitive liposomes that generate larger pores and eliminating the activity of the cellulase enzyme adsorbed on the liposome surface to minimize activity in dark control samples.

Overall, light-activated release showed that red light triggered the release of cellulase from ROS-sensitive liposomes, thereby enhancing cellulose hydrolysis. The IPN hydrogel provided a more favorable environment for light-activated degradation due to lower substrate content, whereas the aCNF hydrogel's higher substrate content generated overall less reducing sugar compared to the positive control. These findings highlight the successful implementation of a light-responsive enzymatic system, in which light illumination controls the timing and extent of cellulose breakdown across different hydrogel matrices. The strong correlation between light dose and reducing sugar release, coupled with lower activity in dark control (~15% in both hydrogels), underscores the specificity and utility of the photo-triggered release mechanism for on-demand polysaccharide-based hydrogel degradation.

5.5 Studying ROS-sensitive lipid film degradation using high-speed atomic force microscopy (III)

In this thesis, we used two types of liposomes and mechanisms to induce light-triggered release: thermosensitive and ROS-activated liposomes. Using DSC measurements, we studied bilayer destabilization in thermosensitive liposomes, but we could not apply the same technique to ROS-activated liposomes. To understand liposome degradation following ROS generation, we investigated ROS-sensitive supported lipid bilayers (SLBs) using high-speed atomic force microscopy (HS-AFM) with a ROS-sensitive lipid mixture matching the composition of this study (DOPC: DPPC: Cholesterol: DSPE-PEG-2k) and compared them with a control film composed of 100% DOPC. Reactive oxygen species were generated in situ by adding hydrogen peroxide (H_2O_2) instead of using a photosensitizer, as light activation of the photosensitizer using an external laser could interfere with the laser used to track the tip in HS-AFM. The generated ROS reacts with the unsaturated acyl chains of DOPC, leading to oxidative modification and destabilization of the bilayer. ROS radicals react with unsaturated chains in lipids, resulting in the formation of primary oxidation products like lipid hydroperoxides. These hydroperoxides contribute to lipid membrane contraction, which destabilizes the membrane. The primary products are then further oxidized into secondary oxidation products, such as water-soluble short-chain aldehydes, which further destabilize the lipid membrane (Grebenteuch et al., 2021; Lem, Kekki, et al., 2024). A total of 0.09% H_2O_2 was added in three steps (0.03% each), with 5–10 min incubation after each addition; the second dose was added only after minimal additional degradation was observed following the first incubation.

Prior to H_2O_2 addition, the ROS-sensitive lipid mixture formed a compact patch (Figure 14a) with a relatively uniform height (Figure 14a1). The line profile shows an apparent SLB thickness of ~5–6 nm and a length of ~200 nm along the measured cross-section (patch area ~1.5×10^4 nm^2). After H_2O_2 addition, the same SLB patch markedly decreased in lateral size to ~ 100 nm (patch area ~1×10^4 nm^2) (Figure 14b, b1) while maintaining a comparable height (~5–6 nm). No pore generation was observed in the patch; we hypothesize that this may be due to degradation proceeding via non-localized oxidative scission and removal/dissolution of lipids from the perimeter. This indicates that oxidative degradation primarily occurs at the edges of lipid patches, where unsaturated lipids are more vulnerable and thus more readily available for degradation than those embedded in the lipid bilayer, thereby maintaining the bilayer height throughout the experiment.

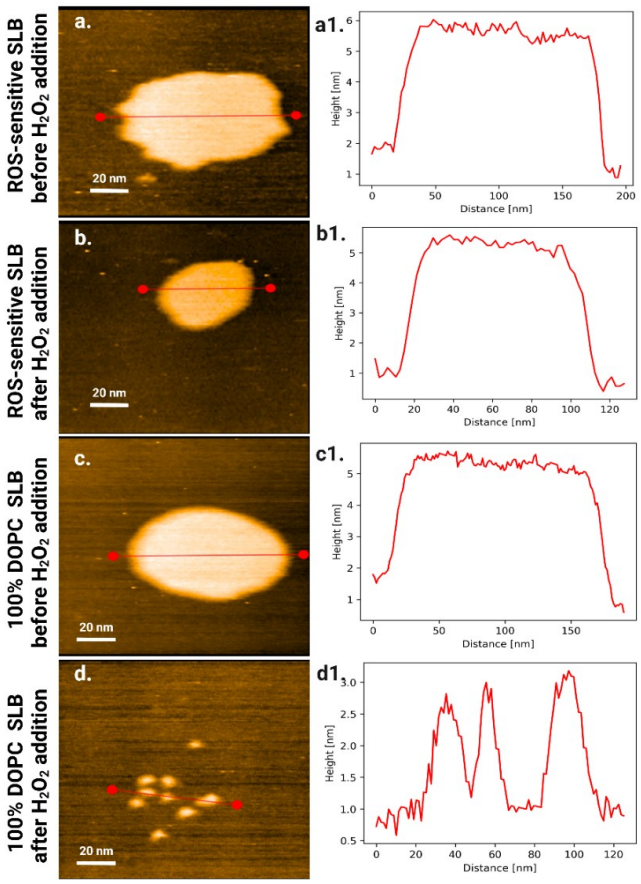

Figure 14 HS-AFM visualization of supported lipid bilayer before and after H_2O_2 induced ROS generation. **a.** AFM image of a ROS-sensitive supported lipid bilayer (SLB) patch (DOPC: Cholesterol: DPPC: DSPE-PEG-2k) before H_2O_2 addition, **a1.** corresponding height, distance line profile taken along the red line, **b.** Same mixed SLB patch after H_2O_2 additions and 20 min of incubation, **b1.** corresponding height distance profile. **c.** AFM image of 100% DOPC SLB patch before H_2O_2 addition, **c1.** corresponding height distance profile. **d.** Pure DOPC SLB after 3 H_2O_2 additions and 10 min of incubation, **d1.** corresponding height distance profile. Scale bars 20 nm.

In contrast, the 100% DOPC SLB initially showed a similarly continuous patch with an apparent thickness of ~3–4 nm (Figure 14c, c1) and a length of 180 nm, but following H_2O_2 exposure, it underwent near-complete degradation (Figure 14d, d1). We repeated the experiments multiple times and found that the SLB thickness ranged from 3 to 6 nm in both lipid films. The post-treatment image shows remaining lipid bilayer fragments rather than a continuous SLB, and the height profile no longer shows a continuous plateau; instead, discontinuous peaks (up to ~2–3 nm) indicate residual lipid rafts and substantial loss of the intact bilayer.

A possible explanation for the slower or incomplete degradation of the lipid mixture bilayer compared to 100% DOPC is compositional stabilization. This can be

attributed to several factors: (i) DPPC contains saturated fatty acid chains, which are inherently less susceptible to oxidative chain reactions than unsaturated lipids (Bőcskei-Antal et al., 2019) (ii) Cholesterol can enhance membrane order and packing, thereby reducing permeability (Kaddah et al., 2018); and (iii) DSPE-PEG-2k may offer steric stabilization and affect interactions (Lajunen et al., 2018). Together, these components can reduce the effective rate of oxidative disruption in the bilayer. This could also be one reason for the incomplete or reduced release of cellulase enzymes from the liposomes after light activation (Figure 13B), as complete degradation of the lipid film is not possible due to the lipid composition.

The time-resolved plot of lipid patch size (nm^2) shown in Figure 15 gives a clearer view of the degradation kinetics of the lipid bilayers. At the start of the measurement, before the addition of H_2O_2, both films had comparable patch areas (approximately 1.5×10^4 nm^2). After the addition of H_2O_2, the DOPC film (Figure 15, red line, points of H_2O_2 additions are marked with arrows) showed a rapid area loss and steep initial decrease within the first ~100–150 s, followed by continued decline to a few thousand nm^2 by ~300–350 s, and then an approach toward near zero patch area by 400–450 s. Whereas the ROS-sensitive lipid mixture (Figure 15, gray line) shows significantly slower, more gradual area reduction, declining from ~1.5×10^4 nm^2 to roughly 1.0×10^4 nm^2 over time. The graph is comparatively shallow and does not exhibit the abrupt collapse observed in DOPC film, indicating a more stable lipid film.

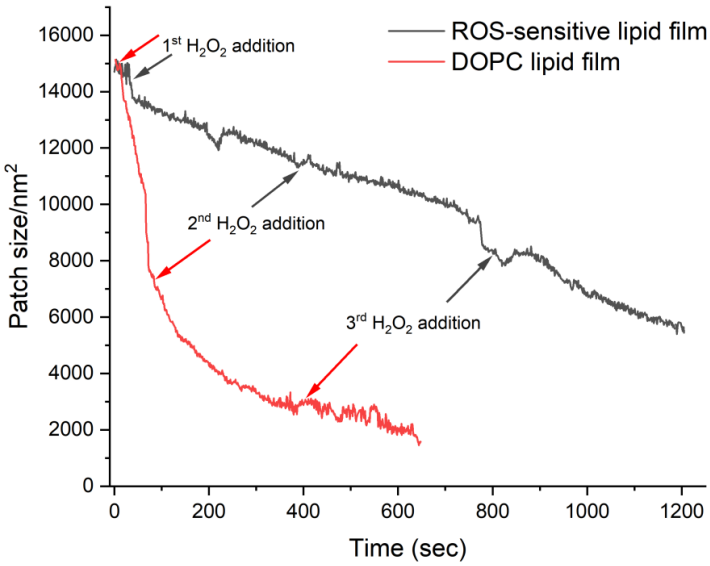

Figure 15 Time resolved reduction in the supported lipid bilayer patch area of the 100% DOPC (red) and ROS-sensitive lipid film (gray; DOPC: DPPC: Cholesterol: DSPE-PEG-2k) over time during H_2O_2 treatment measured using HS-AFM.

By calculating the rate of film degradation through the measurement of the slope (change in area per change in time) during each phase of H_2O_2 addition, we can gain insight into how the speed of lipid film degradation varies throughout the experiment. For the ROS-sensitive lipid film, the slope in the first phase was -7.5 (0-300 s), which then decreased to -6 (350-800 s), indicating a slowdown in degradation. Toward the end of the experiment, the slope increased slightly to -8 (800-1200 s) after the third addition of H_2O_2, showing a steady decrease in surface area over time. In contrast, the changes in slope for the DOPC lipid film were more significant. The slope was -96.5 (0-100 s) in the first phase of addition, then decreased to -13.30 (150-400 s) in the second phase, and further dropped to -4 (400-650 s) in the final phase. This pattern indicates an initial sharp decline in area after the first addition of H_2O_2, followed by a gradual slowing over time. This observation would support our hypothesis regarding the solubilization of lipids from the perimeter. Lipids on the outer edges dissolve more rapidly (with a steeper slope), ultimately leading to a slower rate of change in surface area.

6 Future directions

In this thesis, we studied the development of light-sensitive liposomal hydrogel and how light can be used to modulate drug release. Light stimulation offers several controllable parameters, making it an attractive choice for on-demand drug delivery. However, despite its advantages, limited light penetration remains a major challenge for drug delivery to deeper parts of the body. Future research must pay close attention to the penetration of light for treatment in deeper parts of the body. One possible approach is the use of implantable light sources placed close to the drug reservoir. In recent years, biocompatible implantable light sources have been used in neuroscience research, particularly in optogenetic studies in animal models (S. M. Won et al., 2021; Yang et al., 2021). Building on this idea, as a continuation of this thesis work, we have begun exploring an implantable system that combines a battery-powered, programmable, wireless, remotely controlled light source with a liposomal hydrogel drug reservoir (Figure 16).

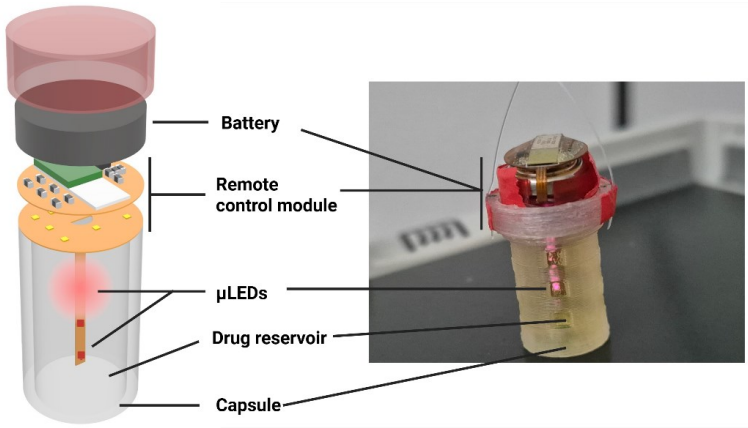

Figure 16 Illustration of a remotely controlled implant with battery-powered µLED probe and liposomal hydrogel in 3D printed capsule.

The current concept uses a probe with six µLEDs, operating at 808 nm or 690 nm depending on the application, connected to a battery module and wirelessly controlled via a mobile phone interface. In this system, the dose of light can be adjusted by varying both the light intensity and the duration of illumination, providing a practical way to study externally programmed release from an implanted reservoir. At present, we are testing the prototype of the implantable device for early-stage feasibility by conducting stability studies and evaluating connection reliability and operating time in in vitro settings. Several important issues still need to be resolved before meaningful drug-release studies can be

conducted, including long-term stability, battery recharging, waterproofing, and the overall robustness of the system under conditions relevant to implantation. More broadly, the future development of such devices will depend on progress in miniaturization, biocompatibility, reproducibility, long-term power supply, and reliable wireless communication. These are well-recognized challenges in implantable bioelectronic and active drug delivery systems and represent a substantial engineering barrier to translation.

Overall, the findings of this thesis support the potential of the light-triggered liposomal hydrogel system, but they also highlight that the major drawback is not only formulation design, but also the practical delivery of light to the intended site. For this reason, future work should proceed in a stepwise manner, with equal attention to formulation performance and device engineering. Although the idea of a remotely controlled implantable light-triggered drug delivery system is promising, its application will depend on whether these fundamental technical challenges can be solved in a safe and reproducible way.

7 Conclusion

In this thesis, plant-based anionic nanocellulose hydrogel was used as a natural, sustainable, and biocompatible reservoir for light-activated liposomes, making the system suitable for long-term use and cargo release.

This work demonstrated that lipid structure, including chain saturation, phase transition temperature, and additive effects, controls membrane stability in liposomes, thereby affecting leakage and activation efficiency. These findings provide a basis for composition-to-function design in developing light-triggerable liposomes. A stable cationic NIR light-activated liposomal formulation was developed, which showed rapid release under NIR exposure with minimal passive leakage **(I)**.

We further showed how these liposomes can be translated from a nanoparticle concept into a depot-like delivery system by embedding them in aCNF hydrogel. Cationic liposomes were strongly retained within the aCNF hydrogel matrix via electrostatic interactions, forming a stable liposomal hydrogel reservoir capable of localized, sustained performance. Importantly, cargo release was not only light-triggered but also tunable within the system, as hydrogel thickness and applied light dose influenced the release. By combining hydrogel retention with liposomal triggerability, this system offers a strategy for localized drug delivery in which the depot remains stable until release is triggered when needed **(II)**.

Finally, we extended the work toward light-responsive liposomes designed for on-demand release of cellulases. This part addressed a practical limitation of poor biodegradability of cellulose-based hydrogels under physiological conditions. Although complete and effective biodegradation was not achieved, light-activated release of cellulase from ROS-sensitive liposomes was demonstrated in both aCNF and IPN liposomal hydrogels, with light dose-dependent increase in reducing sugars and corresponding hydrogel degradation. HS-AFM monitoring of lipid bilayers provided mechanistic insight for future formulation optimization aimed at improving enzyme release **(III)**.

In conclusion, this thesis advances on-demand drug delivery from the conventional release concept toward a triggered and more programmable framework in which i) formulation stability, ii) trigger responsiveness, iii) depot retention, and iv) enzymatic function are considered as interdependent design variables rather than separate factors.

References

Abdul Khalil, H. P. S., Davoudpour, Y., Islam, Md. N., Mustapha, A., Sudesh, K., Dungani, R., & Jawaid, M. (2014). Production and modification of nanofibrillated cellulose using various mechanical processes: A review. *Carbohydrate Polymers*, *99*, 649–665. https://doi.org/10.1016/j.carbpol.2013.08.069

Adepu, S., & Ramakrishna, S. (2021). Controlled Drug Delivery Systems: Current Status and Future Directions. *Molecules*, *26*(19), 5905. https://doi.org/10.3390/molecules26195905

Agiba, A. M., Arreola-Ramírez, J. L., Carbajal, V., & Segura-Medina, P. (2024). Light-Responsive and Dual-Targeting Liposomes: From Mechanisms to Targeting Strategies. *Molecules*, *29*(3), 636. https://doi.org/10.3390/molecules29030636

Ai, Y., Lin, Z., Zhao, W., Cui, M., Qi, W., Huang, R., & Su, R. (2023). Nanocellulose-based hydrogels for drug delivery. *Journal of Materials Chemistry B*, *11*(30), 7004–7023. https://doi.org/10.1039/D3TB00478C

Akbarzadeh, A., Rezaei-Sadabady, R., Davaran, S., Joo, S. W., Zarghami, N., Hanifehpour, Y., Samiei, M., Kouhi, M., & Nejati-Koshki, K. (2013). Liposome: classification, preparation, and applications. *Nanoscale Research Letters*, *8*(1), 102. https://doi.org/10.1186/1556-276X-8-102

Al Talebi, Z. A., Al-Kawaz, H. S., Mahdi, R. K., Al-Hassnawi, A. T., Alta'ee, A. H., Hadwan, A. M., khudhair, D. A., & Hadwan, M. H. (2022). An optimized protocol for estimating cellulase activity in biological samples. *Analytical Biochemistry*, *655*, 114860. https://doi.org/10.1016/j.ab.2022.114860

Alkahtani, M. E., Elbadawi, M., Chapman, C. A. R., Green, R. A., Gaisford, S., Orlu, M., & Basit, A. W. (2024). Electroactive Polymers for On-Demand Drug Release. *Advanced Healthcare Materials*, *13*(3). https://doi.org/10.1002/adhm.202301759

Alvarez-Lorenzo, C., Bromberg, L., & Concheiro, A. (2009). Light-sensitive Intelligent Drug Delivery Systems †. *Photochemistry and Photobiology*, *85*(4), 848–860. https://doi.org/10.1111/j.1751-1097.2008.00530.x

Angilè, F. E., Vargo, K. B., Sehgal, C. M., Hammer, D. A., & Lee, D. (2014). Recombinant Protein-Stabilized Monodisperse Microbubbles with Tunable Size Using a Valve-Based Microfluidic Device. *Langmuir*, *30*(42), 12610–12618. https://doi.org/10.1021/la502610c

Ansari, M. J., Rajendran, R. R., Mohanto, S., Agarwal, U., Panda, K., Dhotre, K., Manne, R., Deepak, A., Zafar, A., Yasir, M., & Pramanik, S. (2022). Poly(N-isopropylacrylamide)-Based Hydrogels for Biomedical Applications: A Review of the State-of-the-Art. *Gels*, *8*(7), 454. https://doi.org/10.3390/gels8070454

Antoniou, A. I., Giofrè, S., Seneci, P., Passarella, D., & Pellegrino, S. (2021). Stimulus-responsive liposomes for biomedical applications. *Drug Discovery Today*, *26*(8), 1794–1824. https://doi.org/10.1016/j.drudis.2021.05.010

Ashrafizadeh, M., Delfi, M., Zarrabi, A., Bigham, A., Sharifi, E., Rabiee, N., Paiva-Santos, A. C., Kumar, A. P., Tan, S. C., Hushmandi, K., Ren, J., Zare, E. N., & Makvandi, P. (2022). Stimuli-responsive liposomal nanoformulations in cancer therapy: Pre-clinical & clinical approaches. *Journal of Controlled Release*, *351*, 50–80. https://doi.org/10.1016/j.jconrel.2022.08.001

Atila, D., Dalgic, A. D., Krzemińska, A., Pietrasik, J., Gendaszewska-Darmach, E., Bociaga, D., Lipinska, M., Laoutid, F., Passion, J., & Kumaravel, V. (2024). Injectable Liposome-Loaded Hydrogel Formulations with Controlled Release of Curcumin and *α* -Tocopherol for Dental Tissue Engineering. *Advanced Healthcare Materials*, *13*(23). https://doi.org/10.1002/adhm.202400966

Auvinen, V.-V., Laurén, P., Shen, B., Isokuortti, J., Durandin, N., Lajunen, T., Linko, V., & Laaksonen, T. (2022). Nanoparticle release from anionic nanocellulose hydrogel matrix. *Cellulose*, *29*(18), 9707–9717. https://doi.org/10.1007/s10570-022-04875-1

Bacakova, L., Pajorova, J., Bacakova, M., Skogberg, A., Kallio, P., Kolarova, K., & Svorcik, V. (2019). Versatile Application of Nanocellulose: From Industry to Skin Tissue Engineering and Wound Healing. *Nanomaterials*, *9*(2), 164. https://doi.org/10.3390/nano9020164

Bacellar, I. O. L., & Baptista, M. S. (2019). Mechanisms of Photosensitized Lipid Oxidation and Membrane Permeabilization. *ACS Omega*, *4*(26), 21636–21646. https://doi.org/10.1021/acsomega.9b03244

Bangham, A. D., Standish, M. M., & Weissmann, G. (1965). The action of steroids and streptolysin S on the permeability of phospholipid structures to cations. *Journal of Molecular Biology*, *13*(1), 253-IN28. https://doi.org/10.1016/S0022-2836(65)80094-8

Barbora, A., Bohar, O., Sivan, A. A., Magory, E., Nause, A., & Minnes, R. (2021). Higher pulse frequency of near-infrared laser irradiation increases penetration depth for novel biomedical applications. *PLOS ONE*, *16*(1), e0245350. https://doi.org/10.1371/journal.pone.0245350

Bastard, C., Schulte, J. C.-T., Asaduzzaman, M., Hohn, C., Kittel, Y., De Laporte, L., & Gebhardt, R. (2025). Casein microparticles filled with cellulase to enzymatically degrade nanocellulose for cell growth. *Biomaterials Science*, *13*(9), 2435–2443. https://doi.org/10.1039/D4BM01508H

Binder, H., & Gawrisch, K. (2001). Effect of Unsaturated Lipid Chains on Dimensions, Molecular Order and Hydration of Membranes. *The Journal of Physical Chemistry B*, *105*(49), 12378–12390. https://doi.org/10.1021/jp010118h

Bőcskei-Antal, B., Zolcsák, Á., Kósa, N., Voszka, I., Csík, G., Tóth, K., & Herenyi, L. (2019). Comparison of light-induced formation of reactive oxygen species and the membrane destruction of two mesoporphyrin derivatives in liposomes. *Scientific Reports*, *9*(1), 11312. https://doi.org/10.1038/s41598-019-47841-x

Brahmankar DM, J. SB. (2009). *Biopharmaceutics and Pharmacokinetics: Pharmacokinetics* (2nd ed.). Vallabh Prakashan.

Brudno, Y., & Mooney, D. J. (2015). On-demand drug delivery from local depots. *Journal of Controlled Release*, *219*, 8–17. https://doi.org/10.1016/j.jconrel.2015.09.011

Cai, Y., Chai, T., Nguyen, W., Liu, J., Xiao, E., Ran, X., Ran, Y., Du, D., Chen, W., & Chen, X. (2025). Phototherapy in cancer treatment: strategies and challenges. *Signal Transduction and Targeted Therapy*, *10*(1), 115. https://doi.org/10.1038/s41392-025-02140-y

Cai, Y., Zhang, L., Cheng, W., Xu, W., Yuan, K., Xiong, R., & Huang, C. (2025). On-demand release of insulin using glucose-responsive chitosan-based three-compartment microspheres. *International Journal of Biological*

Macromolecules, *293*, 139351. https://doi.org/10.1016/j.ijbiomac.2024.139351

Carovac, A., Smajlovic, F., & Junuzovic, D. (2011). Application of Ultrasound in Medicine. *Acta Informatica Medica*, *19*(3), 168. https://doi.org/10.5455/aim.2011.19.168-171

Carter, K. A., Shao, S., Hoopes, M. I., Luo, D., Ahsan, B., Grigoryants, V. M., Song, W., Huang, H., Zhang, G., Pandey, R. K., Geng, J., Pfeifer, B. A., Scholes, C. P., Ortega, J., Karttunen, M., & Lovell, J. F. (2014). Porphyrin–phospholipid liposomes permeabilized by near-infrared light. *Nature Communications*, *5*(1), 3546. https://doi.org/10.1038/ncomms4546

Chaize, B., Colletier, J.-P., Winterhalter, M., & Fournier, D. (2004). Encapsulation of Enzymes in Liposomes: High Encapsulation Efficiency and Control of Substrate Permeability. *Artificial Cells, Blood Substitutes, and Biotechnology*, *32*(1), 67–75. https://doi.org/10.1081/BIO-120028669

Chander, N., Morstein, J., Bolten, J. S., Shemet, A., Cullis, P. R., Trauner, D., & Witzigmann, D. (2021). Optimized Photoactivatable Lipid Nanoparticles Enable Red Light Triggered Drug Release. *Small*, *17*(21). https://doi.org/10.1002/smll.202008198

Chelliah, R., Rubab, M., Vijayalakshmi, S., Karuvelan, M., Barathikannan, K., & Oh, D.-H. (2025). Liposomes for drug delivery: Classification, therapeutic applications, and limitations. *Next Nanotechnology*, *8*, 100209. https://doi.org/10.1016/j.nxnano.2025.100209

Chen, E. H.-L., Wang, C.-H., Liao, Y.-T., Chan, F.-Y., Kanaoka, Y., Uchihashi, T., Kato, K., Lai, L., Chang, Y.-W., Ho, M.-C., & Chen, R. P.-Y. (2023). Visualizing the membrane disruption action of antimicrobial peptides by cryo-electron tomography. *Nature Communications*, *14*(1), 5464. https://doi.org/10.1038/s41467-023-41156-2

Chen, Q., Yang, Z., Liu, H., Man, J., Oladejo, A. O., Ibrahim, S., Wang, S., & Hao, B. (2024). Novel Drug Delivery Systems: An Important Direction for Drug Innovation Research and Development. *Pharmaceutics*, *16*(5), 674. https://doi.org/10.3390/pharmaceutics16050674

Chen, W., Xie, W., Zhao, G., & Shuai, Q. (2023). Efficient pH-Responsive Nano-Drug Delivery System Based on Dynamic Boronic Acid/Ester Transformation. *Molecules*, *28*(11), 4461. https://doi.org/10.3390/molecules28114461

Chen, Y., Sun, H., Li, Y., Han, X., Yang, Y., Chen, Z., Zhao, X., Qian, Y., Liu, X., Zhou, F., Bai, J., & Qiao, Y. (2025). Magnetic nanomaterials for hyperthermia-based therapy and controlled drug delivery. *Bioactive Materials*, *53*, 591–629. https://doi.org/10.1016/j.bioactmat.2025.07.033

Chi, T., Sang, T., Wang, Y., & Ye, Z. (2024). Cleavage and Noncleavage Chemistry in Reactive Oxygen Species (ROS)-Responsive Materials for Smart Drug Delivery. *Bioconjugate Chemistry*, *35*(1), 1–21. https://doi.org/10.1021/acs.bioconjchem.3c00476

Chiu, M., & Prenner, E. (2011). Differential scanning calorimetry: An invaluable tool for a detailed thermodynamic characterization of macromolecules and their interactions. *Journal of Pharmacy And Bioallied Sciences*, *3*(1), 39. https://doi.org/10.4103/0975-7406.76463

Colletier, J.-P., Chaize, B., Winterhalter, M., & Fournier, D. (2002). Protein encapsulation in liposomes: efficiency depends on interactions between protein and phospholipid bilayer. *BMC Biotechnology*, *2*(1), 9. https://doi.org/10.1186/1472-6750-2-9

Comiskey, S. J., & Heath, T. D. (1990). Serum-induced leakage of negatively-charged liposomes at nanomolar lipid concentrations. *Biochemistry*, *29*(15), 3626–3631. https://doi.org/10.1021/bi00467a006

Cook, A. B., & Decuzzi, P. (2021). Harnessing Endogenous Stimuli for Responsive Materials in Theranostics. *ACS Nano*, *15*(2), 2068–2098. https://doi.org/10.1021/acsnano.0c09115

Correa, S., Grosskopf, A. K., Klich, J. H., Lopez Hernandez, H., & Appel, E. A. (2022). Injectable liposome-based supramolecular hydrogels for the programmable release of multiple protein drugs. *Matter*, *5*(6), 1816–1838. https://doi.org/10.1016/j.matt.2022.03.001

Correia, J. H., Rodrigues, J. A., Pimenta, S., Dong, T., & Yang, Z. (2021). Photodynamic Therapy Review: Principles, Photosensitizers, Applications, and Future Directions. *Pharmaceutics*, *13*(9), 1332. https://doi.org/10.3390/pharmaceutics13091332

Danaei, M., Kalantari, M., Raji, M., Samareh Fekri, H., Saber, R., Asnani, G. P., Mortazavi, S. M., Mozafari, M. R., Rasti, B., & Taheriazam, A. (2018). Probing nanoliposomes using single particle analytical techniques: effect of excipients, solvents, phase transition and zeta potential. *Heliyon*, *4*(12), e01088. https://doi.org/10.1016/j.heliyon.2018.e01088

Davoodi, P., Lee, L. Y., Xu, Q., Sunil, V., Sun, Y., Soh, S., & Wang, C.-H. (2018). Drug delivery systems for programmed and on-demand release. *Advanced Drug Delivery Reviews*, *132*, 104–138. https://doi.org/10.1016/j.addr.2018.07.002

de Meyer, F., & Smit, B. (2009). Effect of cholesterol on the structure of a phospholipid bilayer. *Proceedings of the National Academy of Sciences*, *106*(10), 3654–3658. https://doi.org/10.1073/pnas.0809959106

Deng, F., Yang, R., Yang, Y., Li, X., Hou, J., Liu, Y., Lu, J., Huangfu, S., Meng, Y., Wu, S., & Zhang, L. (2024). Visible light accelerates skin wound healing and alleviates scar formation in mice by adjusting STAT3 signaling. *Communications Biology*, *7*(1), 1266. https://doi.org/10.1038/s42003-024-06973-1

Deng, X., Shao, Z., & Zhao, Y. (2021). Solutions to the Drawbacks of Photothermal and Photodynamic Cancer Therapy. *Advanced Science*, *8*(3). https://doi.org/10.1002/advs.202002504

Deng, Z., Zhen, Z., Hu, X., Wu, S., Xu, Z., & Chu, P. K. (2011). Hollow chitosan–silica nanospheres as pH-sensitive targeted delivery carriers in breast cancer therapy. *Biomaterials*, *32*(21), 4976–4986. https://doi.org/10.1016/j.biomaterials.2011.03.050

Ding, H., Tan, P., Fu, S., Tian, X., Zhang, H., Ma, X., Gu, Z., & Luo, K. (2022). Preparation and application of pH-responsive drug delivery systems. *Journal of Controlled Release*, *348*, 206–238. https://doi.org/10.1016/j.jconrel.2022.05.056

El-Husseiny, H. M., Mady, E. A., Hamabe, L., Abugomaa, A., Shimada, K., Yoshida, T., Tanaka, T., Yokoi, A., Elbadawy, M., & Tanaka, R. (2022). Smart/stimuli-responsive hydrogels: Cutting-edge platforms for tissue engineering and other biomedical applications. *Materials Today Bio*, *13*, 100186. https://doi.org/10.1016/j.mtbio.2021.100186

Fang, H., Xu, S., Wang, Y., Yang, H., & Su, D. (2023). Endogenous stimuli-responsive drug delivery nanoplatforms for kidney disease therapy. *Colloids and Surfaces B: Biointerfaces*, *232*, 113598. https://doi.org/10.1016/j.colsurfb.2023.113598

Fatima, H., Shukrullah, S., Hussain, H., Aslam, H., & Naz, M. Y. (2023). Utility of various drug delivery systems and their advantages and disadvantages. In *Nanotechnology for Drug Delivery and Pharmaceuticals* (pp. 235–258). Elsevier. https://doi.org/10.1016/B978-0-323-95325-2.00015-8

Gangurde, P., Gounani, Z., Zini, J., Polez, R. T., Österberg, M., Lauren, P., Lajunen, T., & Laaksonen, T. (2025). Harnessing liposomal nanocellulose hydrogel for NIR-light driven on-demand drug delivery. *Carbohydrate Polymer Technologies and Applications*, *10*, 100787. https://doi.org/10.1016/j.carpta.2025.100787

Gangurde, P., Mahmoudzadeh, M., Gounani, Z., Koivuniemi, A., Laurén, P., Lajunen, T., & Laaksonen, T. (2023). Development of Robust Cationic Light-Activated Thermosensitive Liposomes: Choosing the Right Lipids. *Molecular Pharmaceutics*, *20*(11), 5728–5738. https://doi.org/10.1021/acs.molpharmaceut.3c00602

Gao, J., Xu, Y., Zheng, Y., Wang, X., Li, S., Yan, G., Wang, J., & Tang, R. (2019). pH-sensitive carboxymethyl chitosan hydrogels via acid-labile ortho ester linkage as an implantable drug delivery system. *Carbohydrate Polymers*, *225*, 115237. https://doi.org/10.1016/j.carbpol.2019.115237

Grebenteuch, S., Kroh, L. W., Drusch, S., & Rohn, S. (2021). Formation of Secondary and Tertiary Volatile Compounds Resulting from the Lipid Oxidation of Rapeseed Oil. *Foods*, *10*(10), 2417. https://doi.org/10.3390/foods10102417

Grijalvo, S., Mayr, J., Eritja, R., & Díaz, D. D. (2016). Biodegradable liposome-encapsulated hydrogels for biomedical applications: a marriage of convenience. *Biomaterials Science*, *4*(4), 555–574. https://doi.org/10.1039/C5BM00481K

Gu, Z., Dang, T. T., Ma, M., Tang, B. C., Cheng, H., Jiang, S., Dong, Y., Zhang, Y., & Anderson, D. G. (2013). Glucose-Responsive Microgels Integrated with

Enzyme Nanocapsules for Closed-Loop Insulin Delivery. *ACS Nano*, *7*(8), 6758–6766. https://doi.org/10.1021/nn401617u

Guo, F., Du, Y., Wang, Y., Wang, M., Wang, L., Yu, N., Luo, S., Wu, F., & Yang, G. (2024). Targeted drug delivery systems for matrix metalloproteinase-responsive anoparticles in tumor cells: A review. *International Journal of Biological Macromolecules*, *257*, 128658. https://doi.org/10.1016/j.ijbiomac.2023.128658

Guo, X., Cheng, Y., Zhao, X., Luo, Y., Chen, J., & Yuan, W.-E. (2018). Advances in redox-responsive drug delivery systems of tumor microenvironment. *Journal of Nanobiotechnology*, *16*(1), 74. https://doi.org/10.1186/s12951-018-0398-2

Gupta, M. K., Lee, S. H., Crowder, S. W., Wang, X., Hofmeister, L. H., Nelson, C. E., Bellan, L. M., Duvall, C. L., & Sung, H.-J. (2015). Oligoproline-derived nanocarrier for dual stimuli-responsive gene delivery. *Journal of Materials Chemistry B*, *3*(36), 7271–7280. https://doi.org/10.1039/C5TB00988J

Han, S., Yang, H., Ni, X., Deng, Y., Li, Z., Xing, X., & Du, M. (2023). Programmed release of vascular endothelial growth factor and exosome from injectable chitosan nanofibrous microsphere-based PLGA-PEG-PLGA hydrogel for enhanced bone regeneration. *International Journal of Biological Macromolecules*, *253*, 126721. https://doi.org/10.1016/j.ijbiomac.2023.126721

Heise, K., Kontturi, E., Allahverdiyeva, Y., Tammelin, T., Linder, M. B., Nonappa, & Ikkala, O. (2021). Nanocellulose: Recent Fundamental Advances and Emerging Biological and Biomimicking Applications. *Advanced Materials*, *33*(3). https://doi.org/10.1002/adma.202004349

Hoffman, A. S. (2012). Hydrogels for biomedical applications. *Advanced Drug Delivery Reviews*, *64*, 18–23. https://doi.org/10.1016/j.addr.2012.09.010

Hooshmand, S. E., Jahanpeimay Sabet, M., Hasanzadeh, A., Kamrani Mousavi, S. M., Haeri Moghaddam, N., Hooshmand, S. A., Rabiee, N., Liu, Y., Hamblin, M. R., & Karimi, M. (2022). Histidine-enhanced gene delivery systems: The state of the art. *The Journal of Gene Medicine*, *24*(5). https://doi.org/10.1002/jgm.3415

Hu, H., Busa, P., Zhao, Y., & Zhao, C. (2024). Externally triggered drug delivery systems. *Smart Materials in Medicine*, *5*(3), 386–408. https://doi.org/10.1016/j.smaim.2024.08.004

Hudson, D. E., Hudson, D. O., Wininger, J. M., & Richardson, B. D. (2013). Penetration of Laser Light at 808 and 980 nm in Bovine Tissue Samples. *Photomedicine and Laser Surgery*, *31*(4), 163–168. https://doi.org/10.1089/pho.2012.3284

Huebsch, N., Kearney, C. J., Zhao, X., Kim, J., Cezar, C. A., Suo, Z., & Mooney, D. J. (2014). Ultrasound-triggered disruption and self-healing of reversibly cross-linked hydrogels for drug delivery and enhanced chemotherapy. *Proceedings of the National Academy of Sciences*, *111*(27), 9762–9767. https://doi.org/10.1073/pnas.1405469111

Isogai, A., Saito, T., & Fukuzumi, H. (2011). TEMPO-oxidized cellulose nanofibers. *Nanoscale*, *3*(1), 71–85. https://doi.org/10.1039/C0NR00583E

Jacucci, G., Schertel, L., Zhang, Y., Yang, H., & Vignolini, S. (2021). Light Management with Natural Materials: From Whiteness to Transparency. *Advanced Materials*, *33*(28). https://doi.org/10.1002/adma.202001215

Jeong, Y., Shim, Y. S., Jo, Y. K., & Cha, H. J. (2025). Redox-activatable inhalable mucoadhesive proteinic nanotherapeutics for targeted treatment of lung cancer. *Biomaterials*, *316*, 123004. https://doi.org/10.1016/j.biomaterials.2024.123004

Jobdeedamrong, A., & Crespy, D. (2025). Redox-Responsive Polyprodrugs: Recent Innovations in Reduction- and Oxidation-Responsive Drug Delivery Systems. *Chemistry of Materials*, *37*(6), 2073–2086. https://doi.org/10.1021/acs.chemmater.4c03181

Jowkarderis, L., & van de Ven, T. G. M. (2015). Mesh size analysis of cellulose nanofibril hydrogels using solute exclusion and PFG-NMR spectroscopy. *Soft Matter*, *11*(47), 9201–9210. https://doi.org/10.1039/C5SM01752A

Kaddah, S., Khreich, N., Kaddah, F., Charcosset, C., & Greige-Gerges, H. (2018). Cholesterol modulates the liposome membrane fluidity and permeability for a hydrophilic molecule. *Food and Chemical Toxicology*, *113*, 40–48. https://doi.org/10.1016/j.fct.2018.01.017

Kaya, M. (2024). Characterization of TEMPO-Oxidized Cellulose Nanofiber From Biowaste and Its Influence on Molecular Behavior of Fluorescent Rhodamine B Dye in Aqueous Suspensions. *Journal of Fluorescence*, *35*(6), 4053–4063. https://doi.org/10.1007/s10895-024-03824-4

Khandelwal, M., & Windle, A. H. (2013). Hierarchical Organisation in the Most Abundant Biopolymer –Cellulose. *MRS Proceedings*, *1504*, mrsf12-1504-v02-03. https://doi.org/10.1557/opl.2013.379

Kim, G., Wu, Q., Chu, J. L., Smith, E. J., Oelze, M. L., Moore, J. S., & Li, K. C. (2022). Ultrasound controlled mechanophore activation in hydrogels for cancer therapy. *Proceedings of the National Academy of Sciences*, *119*(4). https://doi.org/10.1073/pnas.2109791119

Kim, M. M., & Darafsheh, A. (2020). Light Sources and Dosimetry Techniques for Photodynamic Therapy. *Photochemistry and Photobiology*, *96*(2), 280–294. https://doi.org/10.1111/php.13219

Kost, J., & Langer, R. (1992). Responsive polymer systems for controlled delivery of therapeutics. *Trends in Biotechnology*, *10*, 127–131. https://doi.org/10.1016/0167-7799(92)90194-Z

Kubota, T., Kurashina, Y., Zhao, J., Ando, K., & Onoe, H. (2021). Ultrasound-triggered on-demand drug delivery using hydrogel microbeads with release enhancer. *Materials & Design*, *203*, 109580. https://doi.org/10.1016/j.matdes.2021.109580

Kwon, J., Kim, J., Park, S., Khang, G., Kang, P. M., & Lee, D. (2013). Inflammation-Responsive Antioxidant Nanoparticles Based on a Polymeric Prodrug of Vanillin. *Biomacromolecules*, *14*(5), 1618–1626. https://doi.org/10.1021/bm400256h

Lajunen, T., Kontturi, L.-S., Viitala, L., Manna, M., Cramariuc, O., Róg, T., Bunker, A., Laaksonen, T., Viitala, T., Murtomäki, L., & Urtti, A. (2016). Indocyanine Green-Loaded Liposomes for Light-Triggered Drug Release. *Molecular Pharmaceutics*, *13*(6), 2095–2107. https://doi.org/10.1021/acs.molpharmaceut.6b00207

Lajunen, T., Nurmi, R., Wilbie, D., Ruoslahti, T., Johansson, N. G., Korhonen, O., Rog, T., Bunker, A., Ruponen, M., & Urtti, A. (2018). The effect of light sensitizer localization on the stability of indocyanine green liposomes.

Journal of Controlled Release, *284*, 213–223. https://doi.org/10.1016/j.jconrel.2018.06.029

Larrañeta, E., & Domínguez-Robles, J. (2025). Long-acting drug delivery systems: Current landscape and future prospects. *Drug Discovery Today*, *30*(9), 104447. https://doi.org/10.1016/j.drudis.2025.104447

Le-Deygen, I. M., Vlasova, K. Yu., Kutsenok, E. O., Usvaliev, A. D., Efremova, M. V., Zhigachev, A. O., Rudakovskaya, P. G., Golovin, D. Yu., Gribanovsky, S. L., Kudryashova, E. V., Majouga, A. G., Golovin, Y. I., Kabanov, A. V., & Klyachko, N. L. (2019). Magnetic nanorods for remote disruption of lipid membranes by non-heating low frequency magnetic field. *Nanomedicine: Nanotechnology, Biology and Medicine*, *21*, 102065. https://doi.org/10.1016/j.nano.2019.102065

Lee, S. H., Kim, C. R., Cho, Y. C., Kim, S.-N., Kim, B. H., Lee, C., Ji, H. B., Han, J. H., Park, C. G., Hong, H., & Choy, Y. Bin. (2022). Magnetically actuating implantable pump for the on-demand and needle-free administration of human growth hormone. *International Journal of Pharmaceutics*, *618*, 121664. https://doi.org/10.1016/j.ijpharm.2022.121664

Lem, O., Gangurde, P., Koivuniemi, A., Keskinen, A., Efimov, A., Durandin, N., & Laaksonen, T. (2024). Far-red light-triggered cargo release from liposomes bound to a photosensitizer-cellulose nanofiber hydrogel. *Carbohydrate Polymers*, *336*, 122134. https://doi.org/10.1016/j.carbpol.2024.122134

Lem, O., Kekki, R., Koivuniemi, A., Efimov, A., Laaksonen, T., & Durandin, N. (2024). The role of lipid oxidation pathway in reactive oxygen species-mediated cargo release from liposomes. *Materials Advances*, *5*(22), 8878–8888. https://doi.org/10.1039/D4MA00535J

Leung, S. J., & Romanowski, M. (2012). Light-Activated Content Release from Liposomes. *Theranostics*, *2*(10), 1020–1036. https://doi.org/10.7150/thno.4847

Levingstone, T., Ali, B., Kearney, C., & Dunne, N. (2021). Hydroxyapatite sonosensitization of ultrasound-triggered, thermally responsive hydrogels: An on-demand delivery system for bone repair applications. *Journal of Biomedical Materials Research Part B: Applied Biomaterials*, *109*(10), 1622–1633. https://doi.org/10.1002/jbm.b.34820

Li, J., Yu, J., Song, J., Zhang, Y., Li, N., Wang, Z., Qin, M., Zhao, M., Zhang, B., Huang, R., Zhou, S., Liu, Y., He, Z., Liu, H., Dan Liu, & Wang, Y. (2025). Galloylated liposomes enable targeted drug delivery by overcoming protein corona shielding. *Nature Communications*, *16*(1), 7926. https://doi.org/10.1038/s41467-025-63198-4

Li, X., Fu, M., Wu, J., Zhang, C., Deng, X., Dhinakar, A., Huang, W., Qian, H., & Ge, L. (2017). pH-sensitive peptide hydrogel for glucose-responsive insulin delivery. *Acta Biomaterialia*, *51*, 294–303. https://doi.org/10.1016/j.actbio.2017.01.016

Li, X., Shang, H., Wu, W., Li, S., Lin, Z., Duan, J., Xu, L., & Li, J. (2016). Glucose-Responsive Micelles for Controlled Insulin Release Based on Transformation from Amphiphilic to Double Hydrophilic. *Journal of Nanoscience and Nanotechnology*, *16*(6), 5457–5463. https://doi.org/10.1166/jnn.2016.11655

Li, Y., Xiao, K., Luo, J., Xiao, W., Lee, J. S., Gonik, A. M., Kato, J., Dong, T. A., & Lam, K. S. (2011). Well-defined, reversible disulfide cross-linked micelles for on-demand paclitaxel delivery. *Biomaterials*, *32*(27), 6633–6645. https://doi.org/10.1016/j.biomaterials.2011.05.050

Liang, Y., Li, Z., Huang, Y., Yu, R., & Guo, B. (2021). Dual-Dynamic-Bond Cross-Linked Antibacterial Adhesive Hydrogel Sealants with On-Demand Removability for Post-Wound-Closure and Infected Wound Healing. *ACS Nano*, *15*(4), 7078–7093. https://doi.org/10.1021/acsnano.1c00204

Lipicky, R. J. (1994). Trough: peak ratio: the rationale behind the United States Food and Drug Administration recommendations. *Journal of Hypertension. Supplement : Official Journal of the International Society of Hypertension*, *12*(8), S17-8; discussion S18-9.

Liu, J. F., Jang, B., Issadore, D., & Tsourkas, A. (2019). Use of magnetic fields and nanoparticles to trigger drug release and improve tumor targeting. *WIREs Nanomedicine and Nanobiotechnology*, *11*(6). https://doi.org/10.1002/wnan.1571

Liu, Y., Fan, Q., Huo, Y., Liu, C., Li, B., & Li, Y. (2020). Construction of a Mesoporous Polydopamine@GO/Cellulose Nanofibril Composite Hydrogel with an Encapsulation Structure for Controllable Drug Release and Toxicity

Shielding. *ACS Applied Materials & Interfaces*, *12*(51), 57410–57420. https://doi.org/10.1021/acsami.0c15465

Long, K., Yang, Y., Lv, W., Jiang, K., Li, Y., Lo, A. C. Y., Lam, W. C., Zhan, C., & Wang, W. (2021). Green Light-Triggered Intraocular Drug Release for Intravenous Chemotherapy of Retinoblastoma. *Advanced Science*, *8*(20). https://doi.org/10.1002/advs.202101754

Luo, D., Li, N., Carter, K. A., Lin, C., Geng, J., Shao, S., Huang, W., Qin, Y., Atilla-Gokcumen, G. E., & Lovell, J. F. (2016). Rapid Light-Triggered Drug Release in Liposomes Containing Small Amounts of Unsaturated and Porphyrin–Phospholipids. *Small*, *12*(22), 3039–3047. https://doi.org/10.1002/smll.201503966

Lv, S., Wu, Y., Cai, K., He, H., Li, Y., Lan, M., Chen, X., Cheng, J., & Yin, L. (2018). High Drug Loading and Sub-Quantitative Loading Efficiency of Polymeric Micelles Driven by Donor–Receptor Coordination Interactions. *Journal of the American Chemical Society*, *140*(4), 1235–1238. https://doi.org/10.1021/jacs.7b12776

Malik, A., Baig, M. H., & Manavalan, B. (2019). Protein-Carbohydrate Interactions. In *Encyclopedia of Bioinformatics and Computational Biology* (pp. 666–677). Elsevier. https://doi.org/10.1016/B978-0-12-809633-8.20661-4

Miranda, D., & Lovell, J. F. (2016). Mechanisms of light-induced liposome permeabilization. *Bioengineering & Translational Medicine*, *1*(3), 267–276. https://doi.org/10.1002/btm2.10032

Mirshafiee, V., Mahmoudi, M., Lou, K., Cheng, J., & Kraft, M. L. (2013). Protein corona significantly reduces active targeting yield. *Chemical Communications*, *49*(25), 2557. https://doi.org/10.1039/c3cc37307j

Mirvakili, S. M., & Langer, R. (2021). Wireless on-demand drug delivery. *Nature Electronics*, *4*(7), 464–477. https://doi.org/10.1038/s41928-021-00614-9

Mo, Y., Cheng, M. H. Y., D'Elia, A., Doran, K., Ding, L., Chen, J., Cullis, P. R., & Zheng, G. (2023). Light-Activated siRNA Endosomal Release (LASER) by Porphyrin Lipid Nanoparticles. *ACS Nano*, *17*(5), 4688–4703. https://doi.org/10.1021/acsnano.2c10936

Moorcroft, S. C. T., Roach, L., Jayne, D. G., Ong, Z. Y., & Evans, S. D. (2020). Nanoparticle-Loaded Hydrogel for the Light-Activated Release and Photothermal Enhancement of Antimicrobial Peptides. *ACS Applied Materials & Interfaces*, *12*(22), 24544–24554. https://doi.org/10.1021/acsami.9b22587

Mou, Y., Zhang, P., Lai, W.-F., & Zhang, D. (2022). Design and applications of liposome-in-gel as carriers for cancer therapy. *Drug Delivery*, *29*(1), 3245–3255. https://doi.org/10.1080/10717544.2022.2139021

Muhammad, F., Wang, A., Guo, M., Zhao, J., Qi, W., Yingjie, G., Gu, J., & Zhu, G. (2013). pH Dictates the Release of Hydrophobic Drug Cocktail from Mesoporous Nanoarchitecture. *ACS Applied Materials & Interfaces*, *5*(22), 11828–11835. https://doi.org/10.1021/am4035027

Needham, D., Park, J.-Y., Wright, A. M., & Tong, J. (2013). Materials characterization of the low temperature sensitive liposome (LTSL): effects of the lipid composition (lysolipid and DSPE–PEG2000) on the thermal transition and release of doxorubicin. *Faraday Discuss.*, *161*, 515–534. https://doi.org/10.1039/C2FD20111A

Olson, F., Hunt, C. A., Szoka, F. C., Vail, W. J., & Papahadjopoulos, D. (1979). Preparation of liposomes of defined size distribution by extrusion through polycarbonate membranes. *Biochimica et Biophysica Acta (BBA) - Biomembranes*, *557*(1), 9–23. https://doi.org/10.1016/0005-2736(79)90085-3

Özbek, B., & Ülgen, K. Ö. (2000). The stability of enzymes after sonication. *Process Biochemistry*, *35*(9), 1037–1043. https://doi.org/10.1016/S0032-9592(00)00141-2

Palácio, S. B., Dias, M. E. de S., Macêdo, D. C. dos S., Ferraz-Carvalho, R. de S., Almeida, F. J. F., Campos, L. A. de A., Lima, K. F. A., Santos, N. P. da S., Aguiar Junior, F. C. de A., Aguiar, J. L. de A., Cavalcanti, I. M. F., & Santos-Magalhães, N. S. (2025). Wound healing effects of β-lapachone-loaded liposomal hydrogel based on bacterial cellulose and hydroxyethylcellulose. *Next Research*, *2*(3), 100651. https://doi.org/10.1016/j.nexres.2025.100651

Park, K. (2014). Controlled drug delivery systems: Past forward and future back. *Journal of Controlled Release*, *190*, 3–8. https://doi.org/10.1016/j.jconrel.2014.03.054

Pashkovskaya, A., Kotova, E., Zorlu, Y., Dumoulin, F., Ahsen, V., Agapov, I., & Antonenko, Y. (2010). Light-Triggered Liposomal Release: Membrane Permeabilization by Photodynamic Action. *Langmuir*, *26*(8), 5726–5733. https://doi.org/10.1021/la903867a

Paukkonen, H., Kunnari, M., Laurén, P., Hakkarainen, T., Auvinen, V.-V., Oksanen, T., Koivuniemi, R., Yliperttula, M., & Laaksonen, T. (2017). Nanofibrillar cellulose hydrogels and reconstructed hydrogels as matrices for controlled drug release. *International Journal of Pharmaceutics*, *532*(1), 269–280. https://doi.org/10.1016/j.ijpharm.2017.09.002

Phanthong, P., Reubroycharoen, P., Hao, X., Xu, G., Abudula, A., & Guan, G. (2018). Nanocellulose: Extraction and application. *Carbon Resources Conversion*, *1*(1), 32–43. https://doi.org/10.1016/j.crcon.2018.05.004

Piech, D. K., Johnson, B. C., Shen, K., Ghanbari, M. M., Li, K. Y., Neely, R. M., Kay, J. E., Carmena, J. M., Maharbiz, M. M., & Muller, R. (2020). A wireless millimetre-scale implantable neural stimulator with ultrasonically powered bidirectional communication. *Nature Biomedical Engineering*, *4*(2), 207–222. https://doi.org/10.1038/s41551-020-0518-9

Poulose, A., Parameswaranpillai, J., George, J. J., Gopi, J. A., Krishnasamy, S., Dominic C. D., M., Hameed, N., Salim, N. V., Radoor, S., & Sienkiewicz, N. (2022). Nanocellulose: A Fundamental Material for Science and Technology Applications. *Molecules*, *27*(22), 8032. https://doi.org/10.3390/molecules27228032

Qing, G., Zhao, X., Gong, N., Chen, J., Li, X., Gan, Y., Wang, Y., Zhang, Z., Zhang, Y., Guo, W., Luo, Y., & Liang, X.-J. (2019). Thermo-responsive triple-function nanotransporter for efficient chemo-photothermal therapy of multidrug-resistant bacterial infection. *Nature Communications*, *10*(1), 4336. https://doi.org/10.1038/s41467-019-12313-3

Rapp, T. L., & DeForest, C. A. (2021). Targeting drug delivery with light: A highly focused approach. *Advanced Drug Delivery Reviews*, *171*, 94–107. https://doi.org/10.1016/j.addr.2021.01.009

Raza, A., Hayat, U., Rasheed, T., Bilal, M., & Iqbal, H. M. N. (2019). “Smart” materials-based near-infrared light-responsive drug delivery systems for cancer treatment: A review. *Journal of Materials Research and Technology*, *8*(1), 1497–1509. https://doi.org/10.1016/j.jmrt.2018.03.007

Redondo-Morata, L., Giannotti, M. I., & Sanz, F. (2012). Influence of Cholesterol on the Phase Transition of Lipid Bilayers: A Temperature-Controlled Force Spectroscopy Study. *Langmuir*, *28*(35), 12851–12860. https://doi.org/10.1021/la302620t

Regan, D., Williams, J., Borri, P., & Langbein, W. (2019). Lipid Bilayer Thickness Measured by Quantitative DIC Reveals Phase Transitions and Effects of Substrate Hydrophilicity. *Langmuir*, *35*(43), 13805–13814. https://doi.org/10.1021/acs.langmuir.9b02538

Ribeiro, O., Wiebe, M., Ilmén, M., Domingues, L., & Penttilä, M. (2010). Expression of Trichoderma reesei cellulases CBHI and EGI in Ashbya gossypii. *Applied Microbiology and Biotechnology*, *87*(4), 1437–1446. https://doi.org/10.1007/s00253-010-2610-7

Rinaldi, A., Caraffi, R., Grazioli, M. V., Oddone, N., Giardino, L., Tosi, G., Vandelli, M. A., Calzà, L., Ruozi, B., & Duskey, J. T. (2022). Applications of the ROS-Responsive Thioketal Linker for the Production of Smart Nanomedicines. *Polymers*, *14*(4), 687. https://doi.org/10.3390/polym14040687

Sadhukhan, P., Kundu, M., Chatterjee, S., Ghosh, N., Manna, P., Das, J., & Sil, P. C. (2019). Targeted delivery of quercetin via pH-responsive zinc oxide nanoparticles for breast cancer therapy. *Materials Science and Engineering: C*, *100*, 129–140. https://doi.org/10.1016/j.msec.2019.02.096

Saito, T., Kimura, S., Nishiyama, Y., & Isogai, A. (2007). Cellulose Nanofibers Prepared by TEMPO-Mediated Oxidation of Native Cellulose. *Biomacromolecules*, *8*(8), 2485–2491. https://doi.org/10.1021/bm0703970

Salehpour, F., Cassano, P., Rouhi, N., Hamblin, M. R., De Taboada, L., Farajdokht, F., & Mahmoudi, J. (2019). Penetration Profiles of Visible and Near-Infrared Lasers and Light-Emitting Diode Light Through the Head Tissues in Animal and Human Species: A Review of Literature. *Photobiomodulation, Photomedicine, and Laser Surgery*, *37*(10), 581–595. https://doi.org/10.1089/photob.2019.4676

Salvati, A., Pitek, A. S., Monopoli, M. P., Prapainop, K., Bombelli, F. B., Hristov, D. R., Kelly, P. M., Åberg, C., Mahon, E., & Dawson, K. A. (2013). Transferrin-functionalized nanoparticles lose their targeting capabilities when a biomolecule corona adsorbs on the surface. *Nature Nanotechnology*, *8*(2), 137–143. https://doi.org/10.1038/nnano.2012.237

Sanati, M., & Amin Yavari, S. (2024). Liposome-integrated hydrogel hybrids: Promising platforms for cancer therapy and tissue regeneration. *Journal of Controlled Release*, *368*, 703–727. https://doi.org/10.1016/j.jconrel.2024.03.008

Savari, M.-N. (2024). Fe3O4@Chitosan@ZIF-8@RVG29, an anti-glioma nanoplatform guided by fixed and activated by alternating magnetic field. *Scientific Reports*, *14*(1), 7000. https://doi.org/10.1038/s41598-024-57565-2

Schönfeldová, T., Piller, P., Kovacik, F., Pabst, G., Okur, H. I., & Roke, S. (2021). Lipid Melting Transitions Involve Structural Redistribution of Interfacial Water. *The Journal of Physical Chemistry B*, *125*(45), 12457–12465. https://doi.org/10.1021/acs.jpcb.1c06868

Semple, S. C., Chonn, A., & Cullis, P. R. (1998). Interactions of liposomes and lipid-based carrier systems with blood proteins: Relation to clearance behaviour in vivo. *Advanced Drug Delivery Reviews*, *32*(1–2), 3–17. https://doi.org/10.1016/S0169-409X(97)00128-2

Shah, R. M., Jadhav, S. R., Bryant, G., Kaur, I. P., & Harding, I. H. (2025). On the formation and stability mechanisms of diverse lipid-based nanostructures for drug delivery. *Advances in Colloid and Interface Science*, *338*, 103402. https://doi.org/10.1016/j.cis.2025.103402

Shah, V. M., Nguyen, D. X., Patel, P., Cote, B., Al-Fatease, A., Pham, Y., Huynh, M. G., Woo, Y., & Alani, A. W. (2019). Liposomes produced by microfluidics and extrusion: A comparison for scale-up purposes. *Nanomedicine: Nanotechnology, Biology and Medicine*, *18*, 146–156. https://doi.org/10.1016/j.nano.2019.02.019

Shapiro, B., Kulkarni, S., Nacev, A., Muro, S., Stepanov, P. Y., & Weinberg, I. N. (2015). Open challenges in magnetic drug targeting. *WIREs Nanomedicine and Nanobiotechnology*, *7*(3), 446–457. https://doi.org/10.1002/wnan.1311

Shi, Q., Abdel-Hamid, A. M., Sun, Z., Cheng, Y., Tu, T., Cann, I., Yao, B., & Zhu, W. (2023). Carbohydrate-binding modules facilitate the enzymatic hydrolysis of lignocellulosic biomass: Releasing reducing sugars and dissociative lignin available for producing biofuels and chemicals. *Biotechnology Advances*, *65*, 108126. https://doi.org/10.1016/j.biotechadv.2023.108126

Sobczak, M. (2022). Enzyme-Responsive Hydrogels as Potential Drug Delivery Systems—State of Knowledge and Future Prospects. *International Journal of Molecular Sciences*, *23*(8), 4421. https://doi.org/10.3390/ijms23084421

Sokolov, V. S., Batishchev, O. V., Akimov, S. A., Galimzyanov, T. R., Konstantinova, A. N., Malingriaux, E., Gorbunova, Y. G., Knyazev, D. G., & Pohl, P. (2018). Residence time of singlet oxygen in membranes. *Scientific Reports*, *8*(1), 14000. https://doi.org/10.1038/s41598-018-31901-9

Srivastava, N., Srivastava, M., Mishra, P. K., Gupta, V. K., Molina, G., Rodriguez-Couto, S., Manikanta, A., & Ramteke, P. W. (2018). Applications of fungal cellulases in biofuel production: Advances and limitations. *Renewable and Sustainable Energy Reviews*, *82*, 2379–2386. https://doi.org/10.1016/j.rser.2017.08.074

Sun, M., Hao Pontius, M. H., Yang, S., Pendekanti, T., Raghunathan, S., Shavit, J. A., & Sen Gupta, A. (2023). Direct delivery of plasmin using clot-anchoring thrombin-responsive nanoparticles for targeted fibrinolytic therapy. *Journal of Thrombosis and Haemostasis*, *21*(4), 983–994. https://doi.org/10.1016/j.jtha.2022.11.037

Sun, X., Setrerrahmane, S., Li, C., Hu, J., & Xu, H. (2024). Nucleic acid drugs: recent progress and future perspectives. *Signal Transduction and Targeted Therapy*, *9*(1), 316. https://doi.org/10.1038/s41392-024-02035-4

Szoka, F., & Papahadjopoulos, D. (1978). Procedure for preparation of liposomes with large internal aqueous space and high capture by reverse-phase evaporation. *Proceedings of the National Academy of Sciences*, *75*(9), 4194–4198. https://doi.org/10.1073/pnas.75.9.4194

Tamo, A. K., Tran, T. A., Doench, I., Jahangir, S., Lall, A., David, L., Peniche-Covas, C., Walther, A., & Osorio-Madrazo, A. (2022). 3D Printing of Cellulase-Laden Cellulose Nanofiber/Chitosan Hydrogel Composites: Towards Tissue Engineering Functional Biomaterials with Enzyme-Mediated

Biodegradation. *Materials*, *15*(17), 6039. https://doi.org/10.3390/ma15176039

Tao, Y., Chan, H. F., Shi, B., Li, M., & Leong, K. W. (2020). Light: A Magical Tool for Controlled Drug Delivery. *Advanced Functional Materials*, *30*(49). https://doi.org/10.1002/adfm.202005029

Teixeira do Nascimento, A., Stoddart, P. R., Goris, T., Kael, M., Manasseh, R., Alt, K., Tashkandi, J., Kim, B. C., & Moulton, S. E. (2025). Stimuli-Responsive Materials for Biomedical Applications. *Advanced Materials*, *37*(36). https://doi.org/10.1002/adma.202507559

Thanou, M., & Gedroyc, W. (2013). MRI-Guided Focused Ultrasound as a New Method of Drug Delivery. *Journal of Drug Delivery*, *2013*, 1–12. https://doi.org/10.1155/2013/616197

Thompson, B. R., Zarket, B. C., Lauten, E. H., Amin, S., Muthukrishnan, S., & Raghavan, S. R. (2020). Liposomes Entrapped in Biopolymer Hydrogels Can Spontaneously Release into the External Solution. *Langmuir*, *36*(26), 7268–7276. https://doi.org/10.1021/acs.langmuir.0c00596

Timko, B. P., & Kohane, D. S. (2014). Prospects for near-infrared technology in remotely triggered drug delivery. *Expert Opinion on Drug Delivery*, *11*(11), 1681–1685. https://doi.org/10.1517/17425247.2014.930435

Toivonen, M. S., Onelli, O. D., Jacucci, G., Lovikka, V., Rojas, O. J., Ikkala, O., & Vignolini, S. (2018). Anomalous-Diffusion-Assisted Brightness in White Cellulose Nanofibril Membranes. *Advanced Materials*, *30*(16). https://doi.org/10.1002/adma.201704050

Trache, D., Tarchoun, A. F., Derradji, M., Hamidon, T. S., Masruchin, N., Brosse, N., & Hussin, M. H. (2020). Nanocellulose: From Fundamentals to Advanced Applications. *Frontiers in Chemistry*, *8*. https://doi.org/10.3389/fchem.2020.00392

Wang, M., Gao, B., Wang, X., Li, W., & Feng, Y. (2022). Enzyme-responsive strategy as a prospective cue to construct intelligent biomaterials for disease diagnosis and therapy. *Biomaterials Science*, *10*(8), 1883–1903. https://doi.org/10.1039/D2BM00067A

Wang, R., Cheng, C., Wang, H., & Wang, D. (2024). Swollen hydrogel nanotechnology: Advanced applications of the rudimentary swelling

properties of hydrogels. *ChemPhysMater*, *3*(4), 357–375. https://doi.org/10.1016/j.chphma.2024.07.006

Wang, T., Tang, Y., Tao, Y., Zhou, H., & Ding, D. (2024). Nucleic acid drug and delivery techniques for disease therapy: Present situation and future prospect. *Interdisciplinary Medicine*, *2*(1). https://doi.org/10.1002/INMD.20230041

Wang, T.-Y., Wilson, K., Machtaler, S., & Willmann, J. (2014). Ultrasound and Microbubble Guided Drug Delivery: Mechanistic Understanding and Clinical Implications. *Current Pharmaceutical Biotechnology*, *14*(8), 743–752. https://doi.org/10.2174/1389201014666131226114611

Wang, Y., Boero, G., Zhang, X., & Brugger, J. (2022). Nanopore Generation in Biodegradable Silk/Magnetic Nanoparticle Membranes by an External Magnetic Field for Implantable Drug Delivery. *ACS Applied Materials & Interfaces*, *14*(35), 40418–40426. https://doi.org/10.1021/acsami.2c10603

Wang, Z., Ju, Y., Ali, Z., Yin, H., Sheng, F., Lin, J., Wang, B., & Hou, Y. (2019). Near-infrared light and tumor microenvironment dual responsive size-switchable nanocapsules for multimodal tumor theranostics. *Nature Communications*, *10*(1), 4418. https://doi.org/10.1038/s41467-019-12142-4

Weiner, N., Martin, F., & Riaz, M. (1989). Liposomes as a Drug Delivery System. *Drug Development and Industrial Pharmacy*, *15*(10), 1523–1554. https://doi.org/10.3109/03639048909052502

Weiser, J. R., & Saltzman, W. M. (2014). Controlled release for local delivery of drugs: barriers and models. *Journal of Controlled Release*, *190*, 664–673. https://doi.org/10.1016/j.jconrel.2014.04.048

Wilson, D. S., Dalmasso, G., Wang, L., Sitaraman, S. V., Merlin, D., & Murthy, N. (2010). Orally delivered thioketal nanoparticles loaded with TNF-α–siRNA target inflammation and inhibit gene expression in the intestines. *Nature Materials*, *9*(11), 923–928. https://doi.org/10.1038/nmat2859

Won, S. M., Cai, L., Gutruf, P., & Rogers, J. A. (2021). Wireless and battery-free technologies for neuroengineering. *Nature Biomedical Engineering*, *7*(4), 405–423. https://doi.org/10.1038/s41551-021-00683-3

Won, T., Goh, M., Lim, C., Moon, J., Lee, K., Park, J., Chung, K., Kim, Y., Lee, S., Hong, H. J., & Gwon, K. (2025). Recent Progress in Cellulose Nanofibril

Hydrogels for Biomedical Applications. *Polymers*, *17*(17), 2272. https://doi.org/10.3390/polym17172272

Wu, J., Xu, Y., Zhang, Y., Zhen, Y., & Guo, X. (2026). Light-Gated ZIF-90 Nanoplatform via Azobenzene Photoisomerization for Spatiotemporally Precise Antibacterial Delivery. *ACS Applied Materials & Interfaces*, *18*(12), 18101–18110. https://doi.org/10.1021/acsami.5c25959

Wu, T., Wilhelm, M. J., Ma, J., Li, Y., Wu, Y., & Dai, H. (2022). Influence of Phase Transitions on Diffusive Molecular Transport Across Biological Membranes. *Angewandte Chemie International Edition*, *61*(42). https://doi.org/10.1002/anie.202205608

Wu, Y., Wang, Y., Long, L., Hu, C., Kong, Q., & Wang, Y. (2022). A spatiotemporal release platform based on pH/ROS stimuli-responsive hydrogel in wound repairing. *Journal of Controlled Release*, *341*, 147–165. https://doi.org/10.1016/j.jconrel.2021.11.027

Xing, D., Xia, G., Tang, X., Zhuang, Z., Shan, J., Fang, X., Qiu, L., Zha, X., & Chen, X. (2024). A Multifunctional Nanocomposite Hydrogel Delivery System Based on Dual-Loaded Liposomes for Scarless Wound Healing. *Advanced Healthcare Materials*, *13*(28). https://doi.org/10.1002/adhm.202401619

Xing, Y., Zeng, B., & Yang, W. (2022). Light responsive hydrogels for controlled drug delivery. *Frontiers in Bioengineering and Biotechnology*, *10*. https://doi.org/10.3389/fbioe.2022.1075670

Xu, C., Tong, S., Sun, L., & Gu, X. (2023). Cellulase immobilization to enhance enzymatic hydrolysis of lignocellulosic biomass: An all-inclusive review. *Carbohydrate Polymers*, *321*, 121319. https://doi.org/10.1016/j.carbpol.2023.121319

Yang, Y., Long, K., Chu, Y., Lu, H., Wang, W., & Zhan, C. (2024). Photoresponsive Drug Delivery Systems: Challenges and Progress. *Advanced Functional Materials*, *34*(38). https://doi.org/10.1002/adfm.202402975

Yang, Y., Wu, M., Vázquez-Guardado, A., Wegener, A. J., Grajales-Reyes, J. G., Deng, Y., Wang, T., Avila, R., Moreno, J. A., Minkowicz, S., Dumrongprechachan, V., Lee, J., Zhang, S., Legaria, A. A., Ma, Y., Mehta, S., Franklin, D., Hartman, L., Bai, W., … Rogers, J. A. (2021). Wireless multilateral devices for optogenetic studies of individual and social behaviors.

Nature Neuroscience, *24*(7), 1035–1045. https://doi.org/10.1038/s41593-021-00849-x

Yavlovich, A., Smith, B., Gupta, K., Blumenthal, R., & Puri, A. (2010). Light-sensitive lipid-based nanoparticles for drug delivery: design principles and future considerations for biological applications. *Molecular Membrane Biology*, *27*(7), 364–381. https://doi.org/10.3109/09687688.2010.507788

Yeingst, T. J., Arrizabalaga, J. H., & Hayes, D. J. (2022). Ultrasound-Induced Drug Release from Stimuli-Responsive Hydrogels. *Gels*, *8*(9), 554. https://doi.org/10.3390/gels8090554

Yew, P. Y. M., Chee, P. L., Lin, Q., Owh, C., Li, J., Dou, Q. Q., Loh, X. J., Kai, D., & Zhang, Y. (2024). Hydrogel for light delivery in biomedical applications. *Bioactive Materials*, *37*, 407–423. https://doi.org/10.1016/j.bioactmat.2024.03.031

Yi, Y., Wang, L., Chen, L., Lin, Y., Luo, Z., Chen, Z., Li, T., Wu, J., & Zhong, Z. (2020). Farnesal-loaded pH-sensitive polymeric micelles provided effective prevention and treatment on dental caries. *Journal of Nanobiotechnology*, *18*(1), 89. https://doi.org/10.1186/s12951-020-00633-2

Yoo, M. K., Sung, Y. K., Lee, Y. M., & Cho, C. S. (2000). Effect of polyelectrolyte on the lower critical solution temperature of poly(N-isopropyl acrylamide) in the poly(NIPAAm-co-acrylic acid) hydrogel. *Polymer*, *41*(15), 5713–5719. https://doi.org/10.1016/S0032-3861(99)00779-X

Yoshida, T., Lai, T. C., Kwon, G. S., & Sako, K. (2013). pH- and ion-sensitive polymers for drug delivery. *Expert Opinion on Drug Delivery*, *10*(11), 1497–1513. https://doi.org/10.1517/17425247.2013.821978

Yudina, A., & Moonen, C. (2012). Ultrasound-induced cell permeabilisation and hyperthermia: Strategies for local delivery of compounds with intracellular mode of action. *International Journal of Hyperthermia*, *28*(4), 311–319. https://doi.org/10.3109/02656736.2012.664307

Zeng, L., Ding, N., Chen, Z., Zheng, X., Liu, X., Zhang, H., Lv, X., Wang, Y., Chen, Y., Hu, M., & Kang, Y. (2026). Redox Dual-Responsive Drug Delivery System with Cascade of Reactive Oxygen Species Self-Generation for Enhanced Cancer Chemotherapy. *Advanced Healthcare Materials*. https://doi.org/10.1002/adhm.71002

Zhang, C., An, T., Wang, D., Wan, G., Zhang, M., Wang, H., Zhang, S., Li, R., Yang, X., & Wang, Y. (2016). Stepwise pH-responsive nanoparticles containing charge-reversible pullulan-based shells and poly(β-amino ester)/poly(lactic-co-glycolic acid) cores as carriers of anticancer drugs for combination therapy on hepatocellular carcinoma. *Journal of Controlled Release*, *226*, 193–204. https://doi.org/10.1016/j.jconrel.2016.02.030

Zhang, L., Zhang, S., Xu, J., Li, Y., He, J., Yang, Y., Huynh, T., Ni, P., Duan, G., Yang, Z., & Zhou, R. (2020). Low-Dose X-ray-Responsive Diselenide Nanocarriers for Effective Delivery of Anticancer Agents. *ACS Applied Materials & Interfaces*, *12*(39), 43398–43407. https://doi.org/10.1021/acsami.0c11627

Zhang, M., Hu, W., Cai, C., Wu, Y., Li, J., & Dong, S. (2022). Advanced application of stimuli-responsive drug delivery system for inflammatory arthritis treatment. *Materials Today Bio*, *14*, 100223. https://doi.org/10.1016/j.mtbio.2022.100223

Zhang, M., Yu, T., Li, J., Yan, H., Lyu, L., Yu, Y., Yang, G., Zhang, T., Zhou, Y., Wang, X., & Liu, D. (2024). Matrix Metalloproteinase-Responsive Hydrogel with On-Demand Release of Phosphatidylserine Promotes Bone Regeneration Through Immunomodulation. *Advanced Science*, *11*(20). https://doi.org/10.1002/advs.202306924

Zhang, R., Nie, T., Fang, Y., Huang, H., & Wu, J. (2022). Poly(disulfide)s: From Synthesis to Drug Delivery. *Biomacromolecules*, *23*(1), 1–19. https://doi.org/10.1021/acs.biomac.1c01210

Zhang, Y., Yang, C., Wang, W., Liu, J., Liu, Q., Huang, F., Chu, L., Gao, H., Li, C., Kong, D., Liu, Q., & Liu, J. (2016). Co-delivery of doxorubicin and curcumin by pH-sensitive prodrug nanoparticle for combination therapy of cancer. *Scientific Reports*, *6*(1), 21225. https://doi.org/10.1038/srep21225

Zhao, L., Wang, L., Zhang, Y., Xiao, S., Bi, F., Zhao, J., Gai, G., & Ding, J. (2017). Glucose Oxidase-Based Glucose-Sensitive Drug Delivery for Diabetes Treatment. *Polymers*, *9*(7), 255. https://doi.org/10.3390/polym9070255

Zhao, Q., Liu, J., Liu, S., Han, J., Chen, Y., Shen, J., Zhu, K., & Ma, X. (2022). Multipronged Micelles–Hydrogel for Targeted and Prolonged Drug Delivery

in Chronic Wound Infections. *ACS Applied Materials & Interfaces*, *14*(41), 46224–46238. https://doi.org/10.1021/acsami.2c12530

Zheng, Y., Zheng, G., Li, Y. Y., Gong, X., Chen, Z., Zhu, L., Xu, Y., Xie, X., Wu, S., & Jiang, L. (2023). Implantable magnetically-actuated capsule for on-demand delivery. *Journal of Controlled Release*, *364*, 576–588. https://doi.org/10.1016/j.jconrel.2023.11.009

Zhu, T. C., Pogue, B. W., Dimofte, A., Finlay, J. C., Lilge, L., Sunar, U., Simone, C. B., & van Veen, R. L. P. (2025). AAPM Task Group Report 274: Fluence rate dosimetry for photodynamic therapy (PDT). *Medical Physics*, *52*(3), 1354–1371. https://doi.org/10.1002/mp.17613